From Research Center Borstel

Leibniz Lung Center

Director: Prof. Dr. Ulrich Schaible

“T helper cytokines in systemic sclerosis: Clinical and experimental perspectives on pulmonary involvement”

Dissertation
for the Fulfillment of
Requirements
for the Doctoral Degree
of the University of Lübeck

from the Department of Natural Sciences

Submitted by

Afsaneh Mehrpouyan

from Karaj, Iran

Lübeck 2025

First referee: PD Dr. rer. nat. Xinhua Yu

Second referee: Prof. Dr. med. Peter König

Date of oral examination: 23.02.2026

Approved for printing: Lübeck, 24.02.2026

Table of contents

Tables

Figures

Zusammenfassung

Hintergrund und Zielsetzung: Systemische Sklerose (SSc) ist eine chronische Autoimmunerkrankung, die durch Entzündungen, Vaskulopathie und fortschreitende Fibrose der Haut und innerer Organe gekennzeichnet ist. Zentrale Faktoren in der Pathogenese sind eine Fehlregulation der Immunantwort und ein Dysfunktion des Endothels. So wurde eine Verschiebung der Immunbalance zugunsten von T-Helferzell-Zytokinen des Typs 2 (Th2) wurde mit systemischer Sklerose in Verbindung gebracht, was auf eine Th2-assoziierte Erkrankung hindeutet. Ziel dieser Studie war es, die Rolle von T-Helfer-Zytokinen bei Patienten mit SSc sowie in einem experimentellen Modell der SSc-assoziierten pulmonal-arteriellen Hypertonie (PAH) zu untersuchen.

Methoden: Für eine klinische Studie wurden insgesamt 128 Patienten mit SSc aus der Klinik für Rheumatologie und Klinische Immunologie der Universität zu Lübeck und 69 gesunde Individuen am Forschungszentrum Borstel rekrutiert. Das experimentelle Modell der SSc-PAH wurde durch Immunisierung von IL-13-transgenen (IL-13tg) Mäusen mit Membranextrakten von CHO-Zellen, die den humanen Angiotensin-II-Typ-1-Rezeptor (AT1R) überexprimieren, induziert. Um das therapeutische Potenzial einer IL-6-Signalinhibition zu bestimmen, wurden IL-13tg-Mäuse entweder mit AT1R-immunisiert oder naiv belassen und nachfolgend mit neutralisierenden monoklonalen Antikörpern (mAk) gegen murines IL-6 oder den IL-6-Rezeptor (IL-6R) sowie mit entsprechenden Isotypkontrollen behandelt. Die Lungenpathologie wurde histologisch mittels Hämatoxylin-Eosin (H&E)-Färbung analysiert. Die Spiegel humaner und muriner T-Helfer-Zytokine wurden im Serum und/oder in bronchoalveolärer Lavageflüssigkeit (BAL) mittels LEGENDplex™ Multi-Analyte Flow Assay Kit bestimmt. Die Lungen-Transkriptome wurden unter Verwendung von Agilent Mouse GE 4x44K v2 Mikroarrays analysiert.

Ergebnisse: Patienten mit SSc wiesen im Vergleich zu gesunden Kontrollen signifikant erhöhte Serumspiegel mehrerer T-Helfer-Zytokine, darunter IL-2, IL-4, IL-6, IL-10, IFN-γ und TNF-α auf. Der IL-6-Serumspiegel korrelierte positiv mit dem Vorliegen einer interstitiellen Lungenerkrankung (ILD) sowie einer PAH. Entgegen der Erwartung konnte jedoch im

Tiermodell die Behandlung mit anti-IL-6 oder anti-IL-6R die Entwicklung einer experimentellen okklusiven Vaskulopathie bei AT1R-immunisierten IL-13tg-Mäusen nicht verhindern. Überraschenderweise konnte hier sogar ein gegenteiliger Effekt beobachtet werden. Nach Behandlung mit den blockierenden Antikörpern wiesen die Tiere einen tendenziell schwereren Krankheitsverlauf als die unbehandelten Kontrollen auf. Darüber hinaus war bereits die Behandlung mit anti-IL-6 allen ausreichend, um in nicht-immunisierten IL-13tg-Mäusen eine pulmonale okklusive Vaskulopathie auszulösen. Die Analyse des Transkriptoms der Lungen dieser Tiere zeigte, dass die Behandlung mit anti-IL-6 bereits in nicht-immunisierten IL-13tg-Mäusen zu einer massiven Dysregulation von immunrelevanten Genen führt.

Schlussfolgerung: Obwohl für IL-6 bei vielen Erkrankungen eine proinfammatorische Rolle nachgewiesen wurde, konnte diese Funktion in der vorliegenden Studie nicht bestätigt werden. Weiterhin legen meine Ergebnisse nahe, dass bei einer experimentellen pulmonalen Vaskulopathie im Kontext der SSc, IL-6 als protektiver Regulator auftritt. Diese Ergebnisse vermitteln neue Erkenntnisse zur pro- wie auch antiinflammatorischen Rolle von IL-6 in der Pathogenese der SSc und sind von Relevanz zur Beurteilung dieses Zytokins als potentielle Zielstruktur in der Behandlung der SSc-assozierten PAH.

Abstract

Background and Objectives: Systemic sclerosis (SSc) is a chronic autoimmune disease characterized by inflammation, vasculopathy, and progressive fibrosis affecting the skin and internal organs. Immune dysregulation and endothelial dysfunction are essential players in the development of SSc. A bias toward T helper 2 (Th2) cytokines has been demonstrated to be associated with SSc, implicating SSc as a Th2-associated disease. This study aimed to investigate the role of T helper cytokines in patients with SSc and in an experimental model of SSc-associated pulmonary arterial hypertension (PAH).

Methods: A total of 128 patients with SSc were recruited from the Department of Rheumatology and Clinical Immunology, University of Lübeck. 69 healthy individuals served as controls and were enrolled at the Research Center Borstel. The experimental model of SSc-PAH was induced in IL-13 transgenic (IL-13tg) mice via immunization with membrane extracts of CHO cells overexpressing human angiotensin II type 1 receptor (AT1R). To assess therapeutic potential of targeting IL-6 signaling, IL-13tg mice, either naïve or AT1R-immunized, were treated with neutralizing monoclonal antibodies (mAbs) against murine IL-6 or IL-6 receptor (IL-6R), or with corresponding isotype control antibodies. Lung pathology was evaluated by histological analysis using hematoxylin and eosin (H&E) staining. The levels of human and murine T helper cytokines were measured in serum and/or bronchoalveolar lavage (BAL) fluid using LEGENDplex™ Multi-Analyte Flow Assay Kit. Lung transcriptomes were analyzed using Agilent Mouse GE 4x44K v2 microarrays.

Results: Patients with SSc exhibited significantly elevated serum levels of multiple T helper cytokines compared to healthy controls, including IL-2, IL-4, IL-6, IL-10, IFN-γ, and TNF-α. Among these cytokines, serum IL-6 levels were positively correlated with as the presence of both interstitial lung disease (ILD) and PAH. In the experimental model, treatment with anti-IL6 or anti-IL-6R did not prevent the development of experimental occlusive vasculopathy in AT1R-immunized IL-13tg mice. By contrast, a trend toward a more severe vascular pathology was observed in AT1R-immunized IL-13tg mice treated with IL-6 or IL-6R-neutralizing mAbs compared to isotype-treated controls, although the differences were not statistically significant. Furthermore, treatment with anti-IL-6 mAb alone was sufficient to induce pulmonary occlusive vasculopathy in non-immunized IL-13tg mice. Transcriptomic analysis revealed that anti-IL-6

mAb treatment dysregulated the expression of immune-related genes in the lungs of unimmunized IL-13tg mice.

Conclusion: Although IL-6 has been shown to exert a proinflammatory role in many diseases, this function could not be confirmed in the present study. Moreover, my findings suggest that, in an experimental model of pulmonary vasculopathy in the context of systemic sclerosis, IL-6 may act as a protective regulator. These results provide new insights into both the pro- and anti-inflammatory roles of IL-6 in the pathogenesis of systemic sclerosis and highlight the importance of carefully reconsidering this cytokine as a potential therapeutic target for SSc-associated PAH.

Appendix

List of abbreviations

ACA: Anti-centromere antibody

ACE: Angiotensin converting enzyme

ANA: Anti-nuclear antibody

Ang II: Angiotensin II

Anti-topo I: Anti–DNA topoisomerase I

AT1R: Angiotensin II type 1 receptor

ATA: anti-topoisomerase I antibody

bFGF: Basic fibroblast growth factor

BLM: Bleomycin

CFA: Complete Freund's adjuvant

CYC: Cyclophosphamide

dcSSc: Diffused cutaneous systemic sclerosis

ETAR: Endothelin-1 type A receptors

FDA: Food and Drug Administration

FGF: Fibroblast growth factor

Fli1: Friend leukemia virus integration 1

Fra2: Fos-related antigen 2

GI: Gastrointestinal

HOCl: Hypochlorous acid

i.p.: Intraperitoneal injection

IFA: Incomplete Freund's adjuvant

IFN-γ: Interferon-γ

IgG: Immunoglobulin G

IL-1: Interlukin-1

IL-2: Interlukin-2

IL-4: Interlukin-4

IL-5: Interlukin-5

IL-6: Interlukin-6

IL-8: Interlukin-8

IL-9: Interlukin-9

IL-10: Interlukin-10

IL-13: Interlukin-13

IL-13tg mice: Interlukin-13 transgenic mice

IL-17A: Interlukin-17A

IL-17F: Interlukin-17F

IL-21: Interlukin-21

IL-22: Interlukin-22

ILD: Interstitial lung disease

Klf5: Krüppel-like factor 5

lcSSc: Limited cutaneous systemic sclerosis

mAbs: Monoclonal antibodies

MCP: Metacarpophalangeal

MMF: Mycophenolate mofetil

mRSS: Modified Rodnan skin score

MSC: Mesenchymal stromal cell

NET: neutrophil extracellular trap

NF-κB: Nuclear factor kappa-light-chain-enhancer of activated B cells

PAH: Pulmonary arterial hypertension

PAMP: pathogen-associated molecular patterns

PBMCs: Peripheral blood mononuclear cells

PDGF: Platelet-derived growth factor

PEx: Plasma exchange

PRR: pattern recognition receptors

p-STAT3: Phosphorylated Signal transducer and activator of transcription 3

PTEN: Phosphatase and tensin

ROS: Reactive oxygen species

RT: Room temperature

s.c.: Subcutaneous injection

SIRT3: Sirtuin 3

SLE: Systemic lupus erythematosus

SRC: Scleroderma renal crisis

SSc: Systemic sclerosis

SSc-ILD: SSc-associated ILD

STAT3: Signal transducer and activator of transcription 3

TGF-β: Transforming growth factor β

Th1: T helper 1 cells

Th2: T helper 2 cells

Th17: T helper 17 cells

TNF: Tumor necrosis factor

Topo I: DNA topoisomerase I

Treg: Regulatory T cells

Tsk: Tight skin

uPAR: Urokinase-type plasminogen activator receptor

VEGF: Vascular endothelial growth factor

1. Introduction

1.1. Systemic Sclerosis (SSc)

Systemic sclerosis (SSc), also referred to as scleroderma, is a chronic autoimmune connective tissue disease characterized by chronic inflammation, widespread fibrosis, and progressive vasculopathy affecting multiple organ systems. Among rheumatoid diseases, SSc is associated with the highest mortality, with a 10-year survival rate of only 62.5% (1,2). Although the precise etiology of SSc is incompletely understood, it is believed to result from a complex interplay of genetic predisposition, epigenetic factors, environmental triggers, and hormonal influences (3). These factors contribute to the considerable heterogeneity in clinical manifestations and disease course observed among affected individuals (4,5). The clinical spectrum of SSc is highly diverse, with potential involvement of the skin, lungs, heart, kidneys, muscles, and gastrointestinal tract, leading to significant morbidity and mortality (6,7).

1.1.1. Classification and diagnosis of SSc

Accurate classification of SSc is essential for early diagnosis, clinical management, and standardized inclusion in clinical trials. The first formal classification system was proposed in 1980 by the American Rheumatism Association (ARA), focusing primarily on cutaneous involvement and internal organ manifestations. However, these criteria demonstrated limited sensitivity, especially in patients with early-stage disease or limited skin involvement, resulting in the underdiagnosis of individuals presenting with incomplete disease features (8,9).

To improve diagnostic accuracy and better capture the disease's heterogeneity, the American College of Rheumatology (ACR) and the European League Against Rheumatism (EULAR) jointly developed revised classification criteria in 2013 (10). These criteria incorporate a weighted scoring system based on both clinical features and serological markers (10). A cumulative score of 9 or higher is considered a diagnosis for SSc. These updated criteria more accurately reflect the heterogeneous nature of SSc and facilitate earlier recognition and diagnosis of the disease.

The most heavily weighted item in this system is skin thickening of the fingers extending proximally to the metacarpophalangeal joints (MCPs), which alone is sufficient for classification. In the absence of this major criterion, seven additional features are considered: limited skin thickening of fingers (sclerodactyly or puffy fingers), fingertip lesions (digital ulcers or pitting scars), telangiectasia, nailfold capillary abnormalities, pulmonary involvement (interstitial lung disease or pulmonary arterial hypertension), Raynaud's phenomenon, and SSc-related autoantibodies. Each of these features is assigned a score based on its diagnostic specificity.

The 2013 ACR/EULAR classification criteria demonstrated a sensitivity of 91% and a specificity of 92%, representing a substantial improvement over the 1980 ACR criteria and enabling the identification of patients with limited or early disease presentations (10). Consequently, these updated criteria have become the current standard for both research and clinical settings in the assessment of SSc (Table 1) (10).

Table 1. The 2013 ACR/EULAR Classification Criteria for Systemic Sclerosis

Item	**Sub-item**	**Score***
Skin thickening of the fingers	Proximal to the metacarpophalangeal joints (sufficient alone for diagnosis)	9
	Sclerodactyly (distal to MCPs)	4
	Puffy fingers	2
Fingertip lesions	Digital tip ulcers	2
	Fingertip pitting scars	3
Telangiectasia	-	2
Abnormal nailfold capillaries	Capillary dilation and/or loss, megacapillaries	2
Pulmonary involvement	Interstitial lung disease (ILD) and/or pulmonary arterial hypertension (PAH)	2
Raynaud's phenomenon	-	3
SSc-related autoantibodies	Anticentromere, anti-topoisomerase I (Scl-70), or anti-RNA polymerase III	3

* A total score of ≥9 is considered as diagnosis for systemic sclerosis. MCP, metacarpophalangeal.

Based on the extent of skin involvement, SSc is classified into three main subsets: limited cutaneous SSc (lcSSc), diffuse cutaneous SSc (dcSSc), and sine scleroderma SSc (ssSSc). In lcSSc, skin thickening is typically confined to distal extremities and face, and internal organ involvement generally presents in a milder form. In contrast, dcSSc is characterized by more extensive skin involvement, often affecting the trunk and proximal limbs, and is associated with early and severe visceral organ complications, including pulmonary and renal manifestations (4,5). The ssSSc subset represents a rare clinical phenotype marked by the absence of cutaneous fibrosis, despite the presence of internal organ involvement and immunological abnormalities (11).

A key immunological hallmark of SSc is the presence of disease-specific autoantibodies, which serve as critical biomarkers for both diagnosis and prognosis. Among these, antinuclear antibodies (ANA) are the most frequently detected, occurring in over 90% of patients (12). Three of the most clinically relevant autoantibodies are anticentromere antibodies (ACA), anti-topoisomerase I antibodies (ATA or anti-Scl-70), and anti-RNA polymerase III antibodies (4,13). ACA targets centromeric proteins and is primarily associated with lcSSc. The prevalence of ACAs in SSc patients has been reported to range from 20% to 57.8%, with a sensitivity of 33% and specificity of 93% for the diagnosis of SSc (14). In contrast, ATA is directed against DNA topoisomerase I and is closely related to dcSSc. The prevalence of ATAs in SSc patients ranges from 14% to 71%, with a diagnostic sensitivity of 24% and exceptionally high specificity of 99.6% (14,15). Anti-RNA polymerase III (anti-RNAP III) antibodies are another important subset of disease-specific autoantibodies in SSc. They are particularly associated with dcSSc, with a prevalence ranging from 4% to 25%, and exhibit high specificity for SSc, exceeding 90% (12,14). The detection of these autoantibodies not only supports early and accurate diagnosis but also aids in risk stratification and prognosis assessment, thereby informing clinical decision-making (14).

1.1.2. Organ involvement in systemic sclerosis

As previously noted, SSc is a systemic autoimmune disease that can affect multiple organs, including the skin, lungs, heart, kidneys, liver, gastrointestinal tract, and musculoskeletal system (16). The pattern and severity of organ involvement vary significantly among patients,

contributing to the heterogeneous nature of the disease and influencing both disease progression and clinical outcomes. A detailed understanding of organ-specific manifestations not only enhances prognostic accuracy but also supports the development of individualized therapeutic strategies tailored to each patient's clinical profile (17).

1.1.2.1. Skin involvement in SSc

Skin involvement is a hallmark feature of SSc and often represents the earliest and most readily observable clinical manifestation. Cutaneous changes are instrumental in the diagnosis and subclassification of SSc and reflect the underlying pathological processes of inflammation, microvascular dysfunction, and progressive fibrosis that characterize the disease. Typically, skin fibrosis begins in the distal extremities and advances proximally. The extent and distribution of skin fibrosis form the basis for the clinical subclassification into dcSSc, lcSSc, and ssSSc (10,12).

The progression of skin involvement often follows a defined sequence, beginning with edema and inflammatory cell infiltration, progressing to dermal induration, and culminating in atrophy. Histopathological features include perivascular mononuclear infiltrates, endothelial cell damage, and an excessive deposition of extracellular matrix components, particularly type I collagen, leading to skin thickening and tightening. These changes contribute to impaired joint mobility, reduced facial expression, and the development of digital ulcers, which result in functional disability and reduced quality of life (1,18).

The modified Rodnan skin score (mRSS) is a validated clinical too widely used to assess the extent and severity of skin involvement in SSc (1,10). Elevated mRSS values are associated with more aggressive disease and worse prognosis. Particularly, in dcSSc, high and rapidly increasing mRSS values often correlate with the development of interstitial lung disease (ILD) and renal crisis (16).

1.1.2.2. Pulmonary involvement in SSc

Pulmonary involvement represents one of the most serious and life-threatening complications of SSc, significantly contributing to disease severity and mortality. Pulmonary manifestations

often arise early in the disease course, with studies reporting that up to 25% of patients develop clinically significant lung involvement requiring hospitalization within three years of diagnosis. Given the prognostic implications, early recognition and timely intervention are critical to improving clinical outcomes and quality of life in affected individuals (13,19). The two features of pulmonary complications in SSc are ILD and pulmonary arterial hypertension (PAH), both of which are leading causes of SSc-related death (1,13,20). ILD is characterized by inflammation and progressive fibrosis of the lung parenchyma, presenting clinically with symptoms such as dyspnea, cough and reduced exercise tolerance. The prevalence of ILD in SSc ranges from 35% to 52%, varying depending on diagnosis criteria and imaging techniques used (21). Notably, approximately 25% to 30% of SS patients with ILD may progress to a more severe, rapidly advanced form, termed progressive fibrosing ILD, which is associated with worse prognosis (21–23).

PAH, another severe complication of SSc, is observed in approximately 10% to 15% of patients, with higher incidence in a specific subset and with increased disease duration (24). PAH is driven by proliferative vasculopathy, including hyperplasia of pulmonary arterial smooth muscle cells and structural remodeling of the pulmonary vasculature, ultimately leading to increased pulmonary vascular resistance and elevated pulmonary artery pressures (25). If left untreated, PAH can progress to right ventricular dysfunction and heart failure, underscoring the importance of early detection and targeted management (13,20).

1.1.2.3. Other organ involvements in SSc

In addition to cutaneous and pulmonary manifestations, SSc can affect several other internal organ systems, each contributing to the disease heterogeneity and overall burden. Among these, gastrointestinal involvement is the most prevalent extracutaneous manifestation, affecting up to 90% of patients. The esophagus is most commonly involved, leading to gastroesophageal reflux, dysphagia, and esophageal dysmotility, which significantly impact nutritional status and quality of life (26).

Cardiac involvement is observed in more than one-third of SSc patients. Although often subclinical, it represents a major contributor to mortality and morbidity. Cardiac manifestations include myocardial fibrosis, pericardial effusion, arrhythmias, and both systolic and diastolic

dysfunction. Heart failure in SSC may result from PAH, renal impairment, or primary myocardial involvement (27).

Renal involvement occurs in approximately 50% of SSc patients and is closely associated with poor outcomes. The most severe renal complication is scleroderma renal crisis (SRC), which presents with abrupt-onset hypertension, rapid progressive renal failure, and frequently microangiopathic hemolytic anemia. The introduction of angiotensin-converting enzyme inhibitors has significantly improved prognosis in patients with SRC (28).

Musculoskeletal manifestations are also common and include joint stiffness, inflammatory arthritis, tendon sheath involvement, joint contractures, and proximal muscle weakness. These symptoms may mimic other connective tissue diseases and can overlap with inflammatory myopathies, further complicating the clinical picture (29).

Collectively, the multi-organ nature of SSc, compounded by immune dysregulation and widespread vascular pathology, emphasizes the systemic character of the disease. Early identification and organ-specific management are critical to improving long-term outcomes and minimizing irreversible organ damage (30).

1.1.3. Treatment for systemic sclerosis

Currently, treatments for SSc aim to slow disease progression, manage organ-specific manifestations, and enhance patients' quality of life. Therapeutic strategies can generally be classified into pharmacological and biological treatments, targeting underlying pathomechanisms of immune dysregulation, fibrosis, and vasculopathy (23,31,32).

1.1.3.1. Pharmacological Treatments for SSc

Pharmacological interventions for SSc primarily consist of small-molecule drugs and immunosuppressants that modulate inflammation, fibrosis, and vascular dysfunction.

Mycophenolate mofetil (MMF) is widely regarded as the first-line therapy for SSc-associated ILD (SSc-ILD). It functions by inhibiting inosine monophosphate dehydrogenase, thereby suppressing T and B lymphocyte proliferation and autoantibody production (33,34). Cyclophosphamide (CYC), a DNA-alkylating agent, is another immunosuppressant option for

progressive ILD. It targets rapidly proliferating immune cells and has shown efficacy in improving pulmonary function and reducing skin thickening (33,35).

Phosphodiesterase-5 (PDE-5) inhibitors such as sildenafil and tadalafil are used in the management of Raynaud's phenomenon and PAH. Sildenafil has been shown to reduce proinflammatory cytokines like IL-6 and IL-8 by inhibiting oxidative stress-mediated STAT3 and NF-κB pathways (36). Tadalafil enhances cyclic GMP signaling, facilitating vasodilation and improving pulmonary hemodynamics (37,38).

ACE inhibitors are essential for the management of SRC, significantly reducing mortality by controlling blood pressure and preventing renal failure (31). Since their introduction in 1980's, SRC has ceased to be the leading cause of SSc-related death (39).

Nintedanib, a multi-tyrosine kinase inhibitor targeting vascular endothelial growth factor receptor (VEGFR), platelet-derived growth factor receptor (PDGFR), and fibroblast growth factor receptor (FGFR), has been approved for SSc-ILD. By inhibiting fibroblast proliferation and fibrogenic signaling, it slows the rate of pulmonary function decline. However, its therapeutic benefits appear to be largely limited to the lung, with minimal effects on extrapulmonary manifestations (40).

1.1.3.2. Biological Treatments for SSc

Biological therapies, including monoclonal antibodies and emerging cellular approaches, offer targeted modulation of key immunological pathways implicated in SSc pathogenesis (31).

Given the central role of cytokine dysregulation in SSc, several biologics target specific cytokines critical to disease development. (31,41). Romilkimab, a bispecific antibody against IL-4 and IL-13, aims to inhibit T helper 2 (Th2) cytokine-driven fibrosis. Phase II trials have shown promising improvements in mRSS and trends toward improved forced vital capacity (FVC), especially in early dcSSc (42). Tocilizumab, an anti-IL-6 receptor monoclonal antibody, has been evaluated in two large Phase III trials. Although it did not significantly affect skin fibrosis, it effectively preserved lung function in patients with early SSc-ILD, leading to its FDA

approval for this indication (41,43,44). Preclinical studies further reinforce the fibrotic and inflammatory role of IL-6, supporting its potential as a therapeutic target (45).

Rituximab, a chimeric monoclonal antibody targeting CD20, depletes B cells and has demonstrated beneficial effects on both skin fibrosis and pulmonary function in patients with SSc (46,47). A novel cellular therapy using CD19-targeted CAR T cells was recently reported in a case study of a patient with severe SSc. Building on this concept, CD19-targeted CAR T cell therapy has recently emerged as a highly potent B cell-directed strategy in cancers and autoimmune diseases (48,49). Unlike monoclonal antibodies, CAR T cells achieve deep and sustained B cell depletion, offering the potential to cure autoantibody-mediated autoimmune diseases. In a recent case report of a patient with severe refractory SSc, CD19 CAR T Cell therapy led to robust B cell depletion, a significant reduction in autoantibody titers, and substantial clinical improvement (48). This case underscores the potential of CAR T cell therapy as a transformative strategy for managing refractory form of SSc.

In addition, Mesenchymal stromal cell (MSC) therapy has demonstrated promise in early-phase trials. MSCs possess immunomodulatory and antifibrotic properties. In a phase 1/2 trial, allogeneic MSC transplantation resulted in improved mRSS and stabilization of lung function, supporting ongoing Phase III clinical investigations (31,50).

A concise summary of the current pharmacological and biological therapies, their mechanisms of action, and clinical indications is provided in Table 2. Despite these therapeutic advances, a substantial proportion of patients continue to exhibit only partial responses or experience adverse effects that limit long-term treatment. These challenges underscore the ongoing need for more effective, mechanism-based therapies that address the complex, multifactorial nature of SSc pathogenesis.

Table 2. Summary of pharmacologic and biologic treatments in SSc

Treatment	Type	Target/Mechanism	Clinical Application
Mycophenolate mofetil (MMF)	Pharmacologic	T/B cell proliferation, guanosine synthesis	SSc-ILD
Cyclophosphamide	Pharmacologic	DNA replication in immune cells	SSc-ILD, skin fibrosis
Sildenafil/Tadalafil	Pharmacologic	PDE-5 inhibition, vasodilation	PAH, Raynaud's phenomenon
ACE inhibitors	Pharmacologic	Renin-angiotensin system	Scleroderma renal crisis
Nintedanib	Pharmacologic	PDGFR, FGFR, VEGFR tyrosine kinase inhibition	SSc-ILD
Mesenchymal stromal cells	Biologic	Immunomodulation, antifibrotic activity	Early diffuse SSc, investigational
Romilkimab	Biologic	IL-4/IL-13 neutralization	Diffuse SSc, fibrosis
Tocilizumab	Biologic	IL-6 receptor blockade	SSc-ILD (lung preservation)
Rituximab	Biologic	CD20+ B cell depletion	SSc-ILD, skin fibrosis
CD19 CAR T cells	Biologic (cellular)	B cell depletion, immune reset	Refractory SSc (case study)

1.2. Immune dysregulation in systemic sclerosis

1.2.1. Immune system

Living organisms are continuously exposed to potentially harmful pathogens and foreign molecules, necessitating the evolution of sophisticated defense mechanisms collectively referred to as the immune system (51,52). This system comprises two subsystems: innate and adaptive immune systems. Both include cellular and humoral components, with unique and overlapping functions that interact intricately during immune responses (52,53). In general, innate immunity provides a rapid but nonspecific defense, whereas the adaptive immune system is characterized by high specificity and long-term immunological memory.

The innate immune system is highly conserved across the animal kingdom. It comprises physical, chemical, humoral, and cellular elements. Physical barriers include skin epithelial cells

and mucosal surfaces, which prevent pathogen entry. Chemical defenses consist of antimicrobial peptides, enzymes, and pH variations in mucosal secretions that inhibit microbial adherence and colonization (52,54). This genetic recombination capability generates diverse receptor repertoires that enable pathogen-specific responses and immunological memory, conferring enhanced protection upon subsequent exposures to the same pathogen (53). Both innate and adaptive immunity include cellular and humoral components, each system possessing unique as well as overlapping functions that interact intricately during immune responses (52,53). Among humoral components, the complement system plays a critical role. It comprises over 30 soluble and membrane-bound proteins that are activated via proteolytic cascades, leading to pathogen opsonization, immune cell recruitment, and direct microbial lysis via membrane attack complexes (55,56). Cellular components of innate immunity originate mainly from bone myeloid progenitor cells in bone marrow, including neutrophils, eosinophils, and basophils, dendritic cells (DCs), macrophages, monocytes, and mast cells. In contrast, natural killer (NK) cells arise from lymphoid progenitors (51).

As the first line of defense, the innate immune system recognizes pathogens through germline-encoded pattern recognition receptors (PRRs) (51,52). These receptors detect conserved microbial structures, known as pathogen-associated molecular patterns (PAMPs) such as polysaccharides, nucleic acids, and lipoproteins (53,57). Recognition of these PAMPs by PRRs triggers downstream signaling cascades, initiating immediate, albeit nonspecific immune responses (55).

In vertebrates, this innate immune system is complemented by an advanced adaptive immune system, which relies on genetically recombined receptors on B and T lymphocytes to achieve high specificity and memory (53). This system enables robust, antigen-specific responses and more effective protection upon re-exposure to the same pathogen (53).

Adaptive immunity plays a crucial role in both pathogen defense and maintenance of immunological tolerance. Its cellular components include multiple specialized subsets of T and B lymphocytes. These cells develop and mature within primary and secondary lymphoid organs, forming an integrated lymphatic system. During development, somatic gene rearrangement generates diverse antigen receptors on lymphocytes, enabling the recognition of virtually any pathogen (58).

Adaptive immune responses are orchestrated through precisely regulated interactions among antigen-presenting cells, T cells, and B cells. T cells are primarily divided into cytotoxic T cells ($CD8^+$) and T helper cells ($CD4^+$). Cytotoxic T cells are crucial for targeting and destroying virus-infected or cancerous cells (59,60). $CD4^+$ T helper cells are central to immune regulation. On the one hand, they differentiate into specialized subsets such as Th1, Th2, Th17, and regulatory T cells (Tregs), depending on the cytokine milieu and antigenic stimulation. These subsets secrete cytokines that guide the activation and differentiation of other immune cells, like macrophages and neutrophils. The balanced function of these T helper subsets is essential for effective immune defense and preventing autoimmune responses (61,62). On the one hand, T helper cells support B cell activation, differentiation and antibody production. Upon activation, B cells differentiate into memory B cells, which confer long-term protection, and plasma cells, which produce large quantities of antibodies; the key humoral component of the adaptive immune system.

1.2.2. Immunological tolerance in autoimmune disorders

Autoimmune disorders represent a diverse group of diseases characterized by immune system's failure to distinguish between self and non-self antigens, consequently triggering aberrant immune responses against the body's own tissues (63,64). The concept of autoimmunity dates back to Paul Ehrlich's introduction of the term "horror autotoxicus" in 1901, which emphasized the detrimental consequences of self-reactivity and underscored the intricate balance necessary for immune homeostasis (65).

A fundamental function of the immune system is immunological tolerance, which enables distinguishing self from non-self antigens, thereby preventing pathological autoimmune responses. Immunological tolerance comprises two major mechanisms: central and peripheral tolerance (66). Central tolerance occurs predominantly in primary lymphoid organs, including the thymus for T cells and the bone marrow for B cells. In the bone marrow, B cell tolerance is achieved through receptor editing and apoptosis to eliminate self-reactive B cells (66,67). In the thymus, central cell tolerance involves complex processes, including both positive and negative selection (68). During positive selection, thymic cortical epithelial cells present MHC-peptide complexes, allowing the survival of thymocytes capable of recognizing self-MHC molecules

(69,70). Negative selection subsequently occurs in the thymic medulla, where T cells with high affinity for self-antigens undergo apoptosis, therefore reducing the number of autoreactive T cells entering peripheral circulation (71).

Peripheral tolerance is established in secondary lymphoid organs such as the spleen, lymph nodes, and mucosal-associated lymphoid tissues. It serves as a secondary mechanism to control self-reactive lymphocytes that escape central tolerance. In B cells, peripheral tolerance involves anergy, a state of unresponsiveness when encountering an antigen in the absence of T helper cells, and follicular exclusion, whereby self-reactive B cells are excluded from lymphoid follicles (72). In T cells, peripheral tolerance is maintained through anergy, clonal deletion, and active suppression by regulatory T cells, which correctively inhibit the activation of and proliferation of autoreactive cells (72,73).

Failure of these tolerance mechanisms is a critical factor in the pathogenesis of autoimmune diseases. The breakdown of central and/or peripheral tolerance permits the survival and activation of autoreactive lymphocytes, ultimately leading to chronic inflammation, generation of autoantibodies, and progressive tissue damage, hallmarks of autoimmune pathology (64,66).

1.2.3. T helper 1/T helper 2 and T helper 17/ T-regulatory balance

Given the essential role of T helper cells in adaptive immunity, the balance between different T helper subsets, particularly between Th1 and Th2 cells, as well as Th17 and Treg cells, plays a critical role in the development and progression of autoimmune disorders (74).

More than three decades ago, two distinct subsets of $CD4^+$ T helper cells were identified in mice and later in humans, referred to as Th1 and Th2 cells. These subsets are characterized by their expression of lineage-defining transcription factors and secretion of distinct sets of cytokines, each mediating specific immune functions (75). Following these discoveries, a model of immunopathogenesis based on Th1/Th2 polarization was proposed to explain immune responses in various diseases, including autoimmune disorders (76).

Th1 cells secrete interferon-gamma (IFN-γ), tumor necrosis factor (TNF), and IL-2 and are essential for host defense against intracellular pathogens, including *Mycobacteria*, viruses, and certain protozoa (77,78). IFN-γ, in particular, activates macrophages, enhancing their ability to

phagocytose and kill intracellular pathogens and to release proinflammatory cytokines. These immune responses are collectively referred to as type 1 immunity (79,80). In contrast, Th2 cells produce IL-4, IL-5, and IL-13, which are central to defense against helminths and response to allergens. Th2 cytokines mediate the recruitment and activation of mast cells, basophils, and eosinophils, promote IgE class switching in B cells, and contribute to fibrosis through fibroblast activation (81). These processes define type 2 immunity (82,83).

In addition to the Th1/Th2 axis, the balance between T helper 17 (Th17) cells and regulatory T (Treg) cells represents another key immunological checkpoint in the maintenance of immune homeostasis. Th17 cells, defined by their expression of the transcription factor RORγt and secretion of IL-17A, IL-17F, and IL-22, play a central role in recruiting neutrophils and amplifying inflammatory responses at mucosal and epithelial barriers (78). These cells are particularly important for host defense against extracellular bacteria and fungi but are also implicated in the pathogenesis of various autoimmune and inflammatory conditions. In contrast, Tregs are defined by the expression of the transcription factor Foxp3 and the production of anti-inflammatory cytokines such as IL-10 and TGF-β. They function to restrain excessive immune responses and maintain peripheral tolerance, thereby preventing autoimmunity (84).

A balanced Th1/Th2 response is essential for maintaining immune homeostasis. However, in many autoimmune diseases, this balance is disrupted (Figure 1). A Th1-dominant profile has been implicated in conditions such as type 1 diabetes and multiple sclerosis, where cytotoxic immune responses are prominent. Conversely, diseases like systemic lupus erythematosus (SLE) and SSc are biased toward Th2 responses. In these contexts, Th2 cytokines promote B cell activation and class switching, leading to the production of pathogenic autoantibodies. Moreover, the anti-inflammatory properties of Th2 cytokines may paradoxically drive fibrotic processes, particularly via IL-4 and IL-13, which stimulate collagen production and fibroblast proliferation (85).

Similarly, an imbalanced Th17/Treg axis is increasingly recognized as a hallmark of immune dysregulation in various autoimmune and chronic inflammatory diseases. Excessive Th17 responses contribute to tissue inflammation through IL-17-mediated recruitment of neutrophils and the induction of other pro-inflammatory cytokines, while insufficient or dysfunctional Tregs impair immune tolerance and allow the survival and expansion of autoreactive T cells (84). As summarized in Figure 1, these balances are critical for maintaining immune homeostasis.

Therefore, concurrent dysregulation of both Th1/Th2 and Th17/Treg pathways may synergistically disrupt immune homeostasis, facilitate chronic inflammation, and ultimately drive the development of autoimmunity and tissue damage.

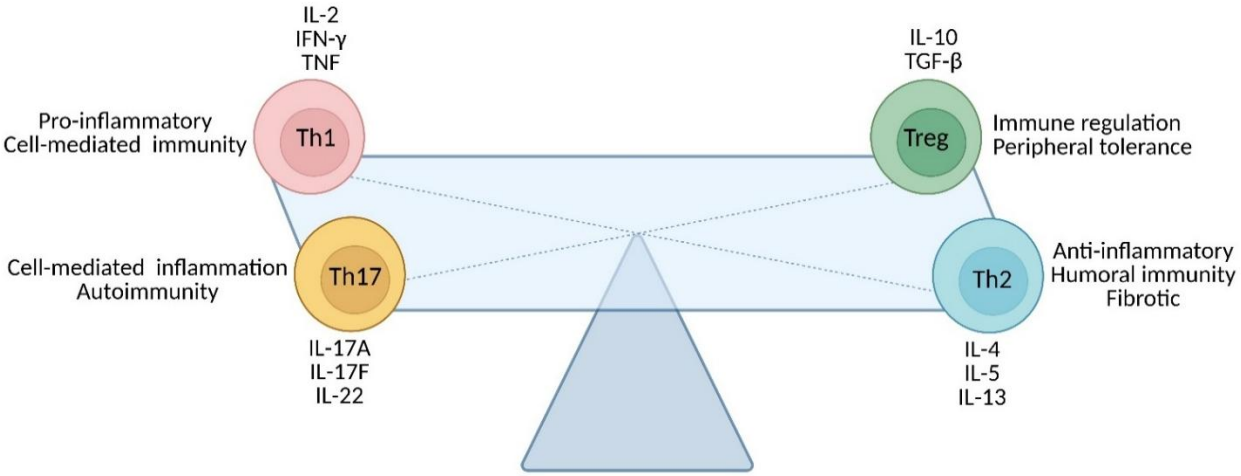

Figure 1. Overview of Th1/Th2 and Th17/Treg balances in immune regulation.

Naïve $CD4^+$ T helper (Th0) cells can differentiate into distinct effector or regulatory subsets, including Th1, Th2, Th17, and Treg cells, each characterized by unique cytokine profiles. Th1 cells primarily produce IL-2, IFN-γ, and TNF-α, while Th2 cells secrete IL-4, IL-5, IL-10, and IL-13. Th17 cells are defined by the production of IL-17A, IL-17F, and IL-22, whereas Treg cells secrete IL-10 and TGF-β. The dynamic balance among these subsets plays a central role in maintaining immune homeostasis and preventing pathological immune responses. Figure created using Biorender (https://BioRender.com).

1.2.4. Immune dysregulation in systemic sclerosis

Immune dysregulation plays a central role in the initiation and progression of SSc. In SSc, the breakdown of immunological tolerance leads to the presentation of self-antigens by antigen-presenting cells, triggering autoreactive T cell responses and the production of autoantibodies by B cells. These sustained aberrant immune responses ultimately result in chronic and systemic inflammation and drive the disease's multisystem manifestations (61,86). Although fibrosis is the most prominent clinical feature of SSc, profound immune alterations, particularly within the adaptive immune system, are evident from early disease stages. Among these, imbalances in T helper (Th) cell subsets, including Th1, Th2, Th17, and regulatory T cells (Tregs), have been implicated as key contributors to the pathogenesis of the disease (61).

A predominant Th2-skewed immune profile is consistently observed in SSc, especially in the early and active stages of the disease. Th2 cytokine, such as IL-4 and IL-13, play a pivotal role in promoting fibrosis by stimulating fibroblast proliferation and enhancing the synthesis of type I collagen, a major extracellular matrix component implicated in tissue thickening (87,88). Beyond fibrosis, Th2 cytokines contribute to immune dysregulation by promoting alternative (M2) macrophage activation and suppressing Th1-mediated inflammation, which may impair pathogen clearance and sustain chronic immune activation (87,89). Importantly, IL-13 also plays a role in the development of vasculopathy associated with SSc, contributing to endothelial dysfunction and vascular remodeling. This occurs through the enhancement of pro-angiogenic and profibrotic signaling pathways, including the upregulation of vascular endothelial growth factor (VEGF) and induction of endothelial-to-mesenchymal transition, ultimately leading to abnormal vascular structure and function (90,91). The persistence of a Th2-biased immune environment not only exacerbates fibrosis but also hinders the resolution of inflammation, thereby perpetuating the cycle of immune-mediated damage (92).

The balance between Th17 and Treg cells is another crucial axis in the immunopathology of SSc, with growing evidence indicating that its disruption contributes to loss of tolerance and chronic inflammation (93). Multiple studies have demonstrated an expansion of Th17 cells in both the blood and lesional tissues of SSc patients, accompanied by a relative reduction or dysfunction of $Foxp3^+$ Tregs, supporting a shift toward proinflammatory effector responses (93,94). IL-17A, produced by Th17 cells, has been shown to promote fibroblast growth and collagen production, thereby driving profibrotic signaling pathways (93,95). In addition, IL-17A amplifies inflammation in stromal and endothelial cells by inducing the production of cytokines and chemokines, including IL-6, CCL2, and CXCL8 (IL-8), thus connecting T cell activation to leukocyte recruitment, tissue damage, and vasculopathy (96). In contrast, Tregs in SSc show reduced suppressive capacity and phenotypic instability. Under the influence of inflammatory cytokines such as IL-6 and IL-23, Tregs can acquire Th17-like features, further shifting the balance toward inflammation (97). This Th17/Treg imbalance correlates with more severe skin involvement, vascular complications, and interstitial lung disease, highlighting its potential as a therapeutic target in SSc (93,98).

The link between the balance of T helper cell subsets and SSc has mainly been studied through the cytokines secreted by T helper cells. Multiple studies have demonstrated altered cytokine profiles in SSc patients, reflecting the complex immunopathogenesis and clinical heterogeneity (99). Elevated levels of IL-4, IL-5, and IL-13 have been detected in serum, affected tissues, and bronchoalveolar lavage fluid from SSc patients, supporting the presence of systemic and local Th2 activation (87). In addition, elevated levels of other dysregulated cytokines, including IL-6, IL-10, IFN-γ, IL-17A, have also been observed in SSc. For instance, in the study by Dantas et al. (2018), cytokine levels were significantly altered in SSc patients compared to healthy controls, with notable increases in IL-6, IL-10, and IFN-γ. These cytokines also showed distinct associations with clinical features, such as lung involvement and disease duration, highlighting their potential in disease classification (99). Similarly, in 2011 Baraut et al. reported that elevated serum levels of IL-17F and IL-13 were predictive of vascular and fibrotic complications, suggesting their potential role in prognosis and therapeutic targeting (100).

Despite these valuable insights, previous studies are characterized by two limitations. First, many studies included relatively small cohorts, limiting statistical power and reducing the generalizability of results. This limitation is particularly pronounced given the clinical heterogeneity of SSc patients in terms of disease subsets, duration, and treatment regimens. Second, most studies did not comprehensively assess T helper cytokines using broad, multiplexed panels that could simultaneously capture the spectrum of Th1, Th2, Th17, and Treg responses. Therefore, further studies involving large patient cohorts and comprehensive profiling of T helper cytokines are essential to advance our understanding of the immunopathogenesis of SSc and to identify robust immunological markers linked to disease phenotypes and clinical outcomes.

1.3. Mouse models for systemic sclerosis

Mouse models are indispensable tools for investigating human autoimmune disease development, understanding their complex pathogenesis, and evaluating novel therapeutic strategies (101,102). Broadly, mouse models for autoimmune diseases can be categorized into three groups: spontaneous models, in which disease arises due to genetic defects or manipulation without further interventions; induced models, where disease is triggered via

immunization, transfer of autoimmune elements, or exposure to environmental factors (103); and humanized mouse models, where mice are grafted with human cells or tissues or genetically engineered to express human genes (104).

To date, over 20 mouse models for SSc have been developed across these three categories. Each model mimics one or more key features of SSc, including autoimmunity, inflammation, fibrosis, and vasculopathy, but none recapitulates the full spectrum of human disease (101). A summary of the major SSc mouse models, including their classification and features, is provided in Table 3.

Table 3. Summary of mouse models for systemic sclerosis and their key features

Model	Classification	Autoimmunity	Inflammation	PAH	Fibrosis (Organ)
Tsk1$^{+/-}$ mice	Spontaneous	Yes	-	No	Skin
Tsk2$^{+/-}$ mice	Spontaneous	Yes	Yes	No	Skin
Fra-2 transgenic mice	Spontaneous	No	Yes	Yes	Skin, Lung, Heart
Relaxin KO mice	Spontaneous	No	No	No	Skin, Lung, Heart, Kidney
MRL/lpγR$^{-/-}$ mice	Spontaneous	Yes	Yes		Skin, Lung, Kidney, Liver
TβRI mice	Spontaneous	No	No	No	Skin
TβRIIΔk-fib mice	Spontaneous	No	No	No	Skin, Lung, Intestine
SIRT-3$^{+/-}$ KO mice	Spontaneous	No	No	Yes	Lung, Heart, Kidney, Liver
Caveolin 1$^{-/-}$ KO mice	Spontaneous	No	Yes	No	Skin
uPAR$^{-/-}$ KO mice	Spontaneous	No	Yes	No	Skin, Lung, Heart
PTEN KO mice (fibroblast-specific)	Spontaneous	No	No	No	Skin, Lung
Fli-1 KO Mice	Spontaneous	No	No	No	Skin
Epithelium-specific Fli-1 KO Mice	Spontaneous	Partial	Yes	No	Skin, Lung, Esophagus
KLF5$^{+/-}$/Fli1$^{+/-}$ KO mice	Spontaneous	Partial	Yes	Yes	Skin, Lung
Endothelin-1 transgenic mice	Spontaneous	No	Yes	No	Lung, Kidney
Humanized PBMC transfer model	Humanized	Yes	Minimal	No	Mild (Skin)

Skin cells-humanized model	Humanized	Yes	Yes	No	Skin
Skin-graph mouse model	Humanized	Yes	Yes	No	Skin, Lung
xenotransplant (human pDCs) mouse model	Humanized	No	Yes	No	Skin
PBMC transfer-induced mouse model (Immunodeficient mice)	Humanized	Yes	Yes	No	No
Bleomycin-induced (local/systemic)	Induced	No	Yes	No	Skin, Lung
Vinyl chloride-injected mice	Induced	No	Yes	No	Skin
VEGF tg mice	Induced	No	No	No	Skin
Topo I peptide-immunized mice	Induced	Partial	Yes	No	Skin, Lung
HOCl-induced model	Induced	Yes	Yes	No	Skin, Lung
Sclerodermatous GvHD model	Induced	Yes	Yes	No	Skin, Lung
AT1R-immunized mice	Induced	Yes	Yes	No	Skin

Some models develop SSc-like diseases due to inherent genetic mutations. The best-known examples are tight skin (Tsk) mice, including Tsk1/+ and Tsk2/+, which carry mutations in the *fibrillin-1* and *collagen* genes, respectively. These mice produce anti-topoisomerase-I autoantibodies (ATA) and develop skin fibrosis spontaneously, although they show limited vascular involvement (101). Other spontaneous models arise from targeted genetic manipulations, including gene knockout and transgene insertion. For instance, Fra-2 transgenic mice overexpress the transcription factor *Fra-2,* leading to progressive dermal and pulmonary fibrosis and PAH (102). *Fli1*$^{+/-}$ *Klf5*$^{+/-}$ mice, double heterozygous for *Fli1* and *Klf5* deletion, display skin fibrosis, vasculopathy, and pulmonary fibrosis, closely resembling SSc pathology (105). In addition to *Fli1*$^{+/-}$ *Klf5*$^{+/-}$ mice, several other gene knockout strains have been reported to develop spontaneous disease manifestations resembling SSc. These include *Fli-1* knockout and epithelium-specific *Fli-1* knockout mice, as well as mice deficient in urokinase-type plasminogen activator receptor knockout mice (*uPar*$^{+/-}$), sirtuin-3 (*Sirt3*$^{+/-}$), phosphatase and tensin homolog (*Pten*$^{+/-}$), caveolin, and relaxin (101).

In induced mouse models, SSc-like disease is triggered by exogenous stimuli, such as drugs, biological agents, or antigen immunization. The bleomycin-induced model is a classical and the

most widely used experimental system for SSc. Local or systemic administration of bleomycin induces dermal fibrosis and lung involvement resembling human SSc; however, this model lacks an autoimmune component (106). Another chemical used to induce SSc-like disease is hypochlorous acid (HOCl), a potent reactive oxygen species (ROS). Subcutaneous injection of HOCl in BALB/C mice induces multiple features of human SSc, including ATA production, skin and lung fibrosis, and renal vasculopathy and fibrosis. Sclerodermatous graft-versus-host disease (GvHD) models, generated through allogeneic hematopoietic stem cell transplantation, also replicate widespread fibrosis. However, these models show variability in the generation of autoantibodies and typically do not develop significant occlusive vasculopathy. Similarly, the topoisomerase I peptide-induced model, which involves immunization with SSc-related antigens, reproduces key features such as skin and lung fibrosis (101).

Although humans and mice share many similarities as mammals, there are still considerable differences in the immune system and microenvironment between the two species, leading to a pathophysiological gap between mouse models and human disease (103). In an effort to bridge this gap, researchers have attempted to combine elements from both species, resulting in the creation of so-called humanized mouse models (101). The first humanized mouse model for SSc was created by transplanting bioengineered skin with keratinocytes and fibroblasts isolated from patients with SSc onto the backs of immunodeficient mice. This graft leads to the development of dense collagenous dermal tissue, a feature absent in grafts from healthy donors. Furthermore, treating animals carrying healthy donor skin grafts with SSc IgG results in dermal fibrosis, suggesting that autoantibodies contribute to fibrotic initiation (107). A xenotransplant mouse model demonstrates that transplantation of human plasmacytoid dendritic cells (pDCs) significantly enhances TLR-9-induced type I interferon (IFN) responses. In addition to elevated IFN signaling, this model also exhibits markedly increased fibrotic and immune activity, thereby recapitulating key features of SSc (108). Another advancement in the humanized mouse model for SSc is the direct transplantation of skin from patients onto immunodeficient mice. While effective for studying advanced-stage skin pathology, this model is not suitable for investigating early systemic manifestations affecting internal organs (109). To overcome this limitation, a different humanized mouse model was developed by transplanting peripheral blood mononuclear cells (PBMCs) from patients with SSc into immunodeficient mice. Mice that received PBMCs from SSc patients, but not from healthy controls, produced ANA that mirrored

donor patterns and showed cellular infiltrates across multiple organs, including the lung, kidney, and liver. This model serves as a valuable platform for exploring the early disease processes, such as autoantibody production and immune cell infiltration (110).

Recently, our research group has established a novel SSc mouse model by immunizing mice with angiotensin II type-1 receptor (AT1R) (111). The AT1R is a G-protein-coupled receptor (GPCR) that plays an important role in regulating blood pressure and different cardiovascular functions. Autoantibodies against AT1R are elevated in patients with SSc and are associated with severe disease manifestations (112,113). Furthermore, in vitro studies have demonstrated that autoantibodies against AT1R are capable of stimulating fibroblasts, and the effect can be blocked by Losartan, an antagonist of AT1R (114). These findings suggest that AT1R autoantibodies are functional and may contribute to the pathogenesis of SSc. To experimentally validate this hypothesis, we immunized C57BL/6 mice with membrane extracts isolated from Chinese hamster ovary (CHO) cells overexpressing human AT1R. This immunization successfully elicited the production of functional AT1R autoantibodies and resulted in the development of hallmark SSc-like features, including skin and lung inflammation as well as dermal fibrosis (111). Thus, this in vivo experiment not only confirms the pathogenic potential of AT1R autoantibodies but also provides a novel mouse model for SSc.

However, despite reproducing several hallmark features of SSc, the AT1R immunization-induced model does not develop lung fibrosis or occlusive vasculopathy, which are two critical pulmonary manifestations of SSc. To address this limitation, we proposed a “two-hit” hypothesis for the development of pulmonary involvement in SSc (Figure 3-A). According to this model, the first hit is autoimmune activation, represented by the production of autoantibodies against AT1R, which initiates chronic local inflammation. However, a second stimulus is required to drive the development of occlusive vasculopathy and fibrosis in the lung. Given the known Th2-skewed immune profile in SSc and the pivotal role of IL-13 in promoting fibroblast activation, collagen deposition, and tissue remodeling (115,116), we hypothesized that IL-13-driven Th2 dysregulation could serve as the second hit. To test this, we immunized IL-13 transgenic (IL-13tg) mice, which specifically overexpress IL-13 in activated T cells under the promoter of hCD-2 (117). Following immunization with AT1R, IL-13tg mice developed pulmonary occlusive vasculopathy, a defining histopathological feature of PAH (Figure 3-B).

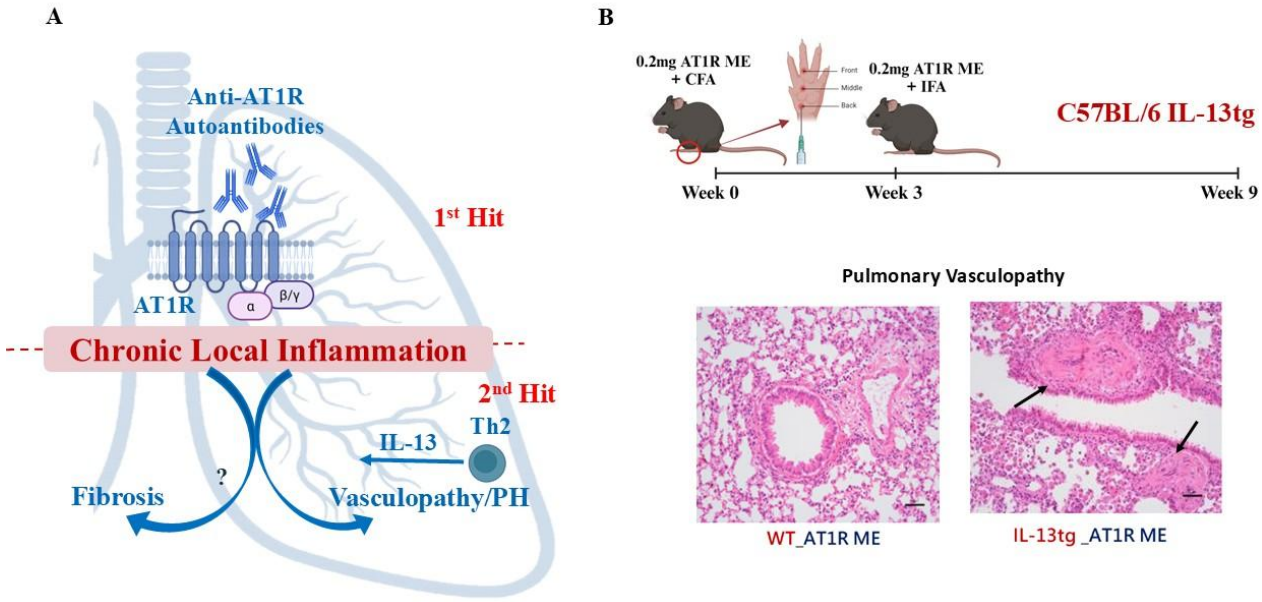

Figure 2. IL-13 as the second hit in the development of experimental pulmonary arterial hypertension (PAH) in mice.

(A) Schematic illustration of the proposed "two-hit" hypothesis underlying SSc-associated PAH and fibrosis. (B) Upper panel: Diagram of the immunization protocol using AT1R membrane extract IL-13 transgenic (IL-13tg) mice and littermate controls. Lower panel: Representative histological images of lung tissue from immunized mice. Arrows indicate occlusive vascular lesions in small pulmonary arteries. Scale bar = 50 μm. Figure created using BioRender (https://BioRender.com).

This model, which integrates autoantibody-mediated autoimmunity with Th2 cytokine dysregulation, successfully replicates key features of PAH-like vasculopathy. Thus, our AT1R-immunized IL-13tg mouse model represents a robust experimental system for SSc-associated PAH**,** providing an *in vivo* platform to study the interplay between autoimmunity, cytokine signaling, and vascular pathology, as well as to evaluate therapeutic strategies.

1.4. Aim of the study

This study aimed to investigate the role of T helper cytokines in the pathogenesis and clinical manifestations of SSc through an integrated clinical and experimental approach. In the clinical part, the goal was to identify cytokines potentially involved in the immunopathogenesis of SSc-associated pulmonary manifestations. For this purpose, a comprehensive profiling of T helper cytokines was performed in the serum of a large cohort of SSc patients and healthy controls using a multiplex bead-based immunoassay. Specifically, the study aimed to i) compare cytokine expression patterns between SSc patients and healthy individuals, ii) analyze associations between cytokine levels and key clinical manifestations, with particular emphasis on pulmonary involvement, and iii) explore immune network dysregulation in SSc by assessing cytokines correlations.

Following the identification of potential candidate cytokines, the experimental part of the study aimed to assess their functional role in the development of pulmonary vasculopathy using the previously established AT1R-immunized IL-13 transgenic (IL-13tg) mouse model. In addition, their potential as therapeutic targets for preventing or modulating vascular pathology was evaluated.

Together, this dual approach, bridging clinical observations with translational research, can be expected to enhance the understanding of immune-driven mechanisms underlying vascular pathology in SSc and to inform the development of novel cytokine-targeted therapeutic strategies (Figure 5).

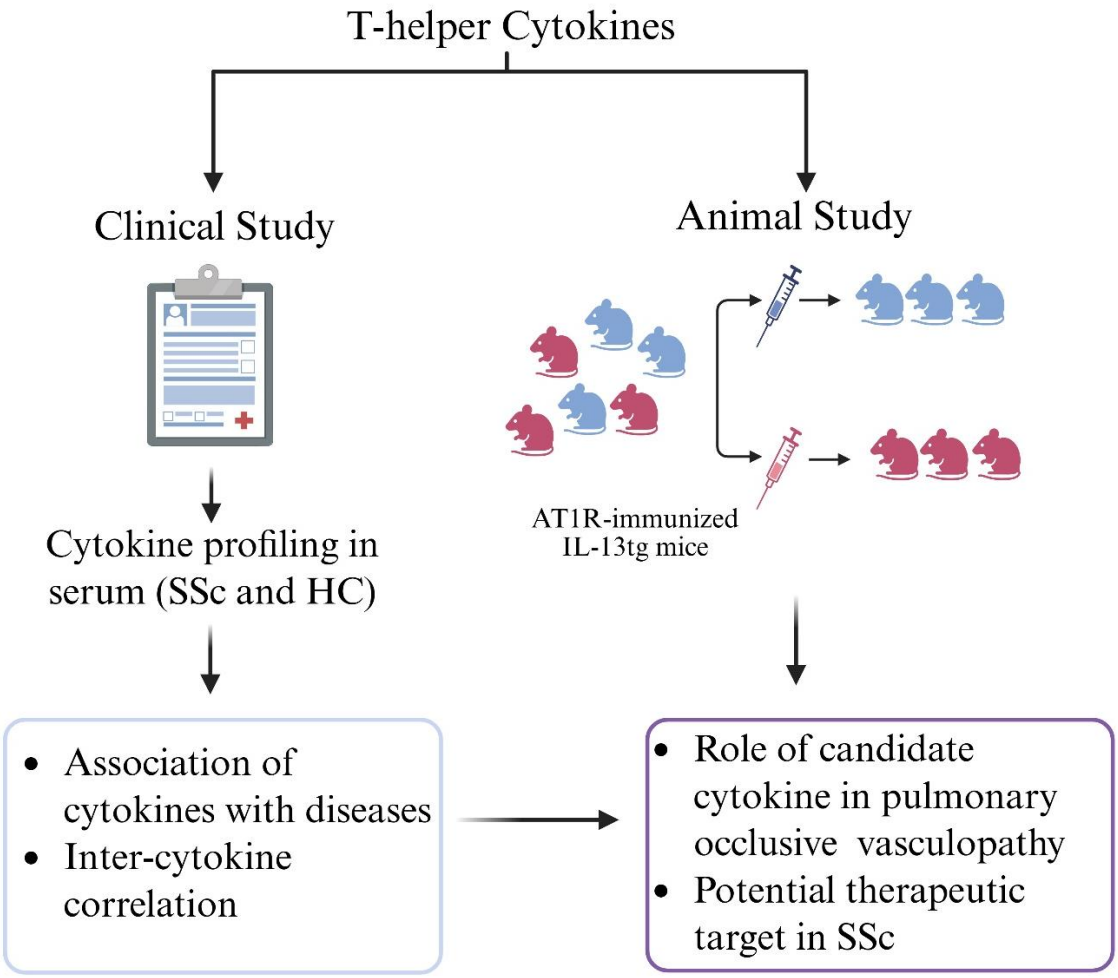

Figure 3. Overview of the study design investigating T helper cytokines in SSc.

The study integrated clinical and preclinical research approaches. In the clinical arm, serum samples from SSc patients and healthy controls were analyzed using multiplex cytokine profiling to compare cytokine expression patterns, examine associations with clinical manifestations, and analyze inter-cytokine correlations. Based on these clinical findings, a candidate cytokine with the strongest link to pulmonary involvement was selected for further investigation in animals. In the experimental arm, the pathogenic role of this cytokine was evaluated using the AT1R-immunized IL-13 transgenic (IL-13tg) mouse model of SSc-associated PAH. This dual approach bridges clinical findings with underlying disease mechanisms and aims to identify potential therapeutic targets for SSc. Figure created using BioRender (https://BioRender.com).

2. Materials and Methods

2.1. Materials

2.1.1. Consumables and equipment

Equipment	**Manufacturer**
96-well filter plate	Biolegend, US
Absorbance reader	TECAN, Switzerland
Balance	Kern & Sohn, Germany
Biosafety bench	Heraeus, Germany
Cells counter	Marienfeld Superior, Germany
Centrifuge	Hettich, Germany
Flow cytometer LSR II	BD, US
Flow cytometer FACSymphony A3	BD, US
Embedding machine	Leica, Thermo Fisher Scientific, USA
Fluid aspiration system	Vacuubrand, Germany
Histological embedding cassette	Simport, Canada
Incubator (5% CO_2)	Heraeus, Germany
Light microscope	Carl Zeiss, Germany
Light microscope with camera	Olympus, Japan
Liquid-blocking PAP pen	Kisker biotech, Germany
Microtome	Leica, Germany
Multichannel pipette	Titertek, Germany

Nanodrop 1000 Spectrophotometer	Thermo Fisher Scientific, USA
Needle	BD, US
PH meter	Knick, Germany
Pipette	Eppendorf, Germany
Repeat dispenser	Eppendorf, Germany
Scissors and forceps	Karl Hammacher, Germany
Varioshaker	GFL/Lauda, Germany
Shaker	IKA, Germany
Slides	R. Langenbrinck, Germany
Serum-separating tube	BD, US
Syring (1 mL)	B. BRAUN, Germany
Syring (50 mL)	BD, US
Vacuum pumps	KNF, Germany
Vortex	Scientific industries, US
Water bath	Grant, UK

2.1.2. Buffers and solutions

Solution	Recipe
BAL fluid solution	1X PBS-D without Ca^{2+}/Mg^{2+}, 0.1mM EDTA
10% BSA	1g BSA + 10 mL PBS
25 × proteinase inhibitor solution	1 × proteinase inhibitor tablet (Sigma-Aldrich, 11697498001) in 2ml PBS
Electrophoresis Buffer (pH=8.6)	Tris: 25 mM (3.04 g), Glycine: 200 mM (14.4g), SDS: 3.5 mM (1g) Add Milli Q water (the amounts are for 1L)
Blotting Buffer (pH=9)	50 mM Boric acid, 20% MeOH (15.46 g boric acid in 4 L Milli Q water, adjust pH to 9, then mix with 1 L of methanol)
PBS-D (pH=7.2)	NaCl: 8 g, KCl: 0.2 g, Na_2HPO_4: 1.15 g, KH_2PO_4: 0.2 g, Milli Q water: 1 L.
PBS-T	500 µL Tween-20 in 1 L PBS-D
RIPA Buffer (pH=7.4)	50 mM Tris-HCl, 150mM NaCl, 1% Triton X-100, 0.5% Na desoxycholate, 0.1% SDS, 0.1 mM EDTA, Add Braun dest

2.1.3. Reagents and chemicals

Products	Manufacturer	Catalog number
0.9% NaCl	B. Braun, Germany	21185012
Ammonium peroxydisulfate (APS)	Carl Roth, Germany	9592.1
AT1R membrane extract	CellTrend GmbH, Germany	(Customized order)
Bovine serum albumin (BSA)	Sigma-Aldrich, US	A4503
Diluent buffer	ZYTOMED, Germany	ZUC025-500
Eosin G solution 1%	Carl Roth, Germany	3137.2
Ethanol	Sigma-Aldrich, US	32205
Fetal calf serum (FCS)	Gibco, US	10270
Freund's Adjuvant, Complete	Sigma-Aldrich, US	F5881-10ML
Freund's Adjuvant, Incomplete	Sigma-Aldrich, US	F5506-10ML
Hematoxylin Gill II solution	Carl Roth, Germany	T864.2
Ketamidor 100mg/ml	WDT, Germany	0320278AE
Live-dead blue fluorescence solution	Invitrogen, US	L34962
L-Glutamine	PAN biotech, Germany	P04-80050
Methanol	Sigma-Aldrich, US	
Mounting medium	Millipore, US	1.07961.0500
Na_2HPO_4	Millipore, US	1.06346.1000
Paraffin	DCS innovative diagnostic system, Germany	PL00352K

PBS 1X (w/o Ca^{2+}/Mg^{2+}), Endotoxin-free Dulbecco's	Merck, Germany	TMS-012-A
PEST (Penicillin/Streptomycin)	PAN Biotech, Germany	P06-07700
Proteinase inhibitor	Roche, Switzerland	11836145001
Rainbow high molecular protein marker	Amersham, UK	RPN756E
RNAlater solution	Invitrogen, US	AM7020
Roti ImmunoBlock	Carl Roth, Germany	T144.1
Rotiphorese Gel 30	Carl Roth, Germany	3029.1
TEMED	Carl Roth, Germany	2367.3
Tris	Carl Roth, Germany	77-86-1
Tween-20	Sigma-Aldrich, US	P1379
Xylazin 20mg/ml	WDT, Germany	00121
Xylene	Walter CMP, Germany	WAL12401

2.1.4. Antibodies

Products	Manufacturer	Catalog Number
Ultra-LEAF purified Rat IgG1-κ Isotype Control, Colon: RTK2071	Biolegend, US	400458
InVivoMAb Rat IgG2b Isotype Control, anti-keyhole limpet hemocyanin, Colon: LTF-2	BioXCell, US	BE0090
InVivoMAb anti-mouse IL-6, Clone: MP5-20F3	BioXCell, US	BE0046
InVivoMAb anti-mouse IL-6R, Clone: 15A7	BioXCell, US	BE0047

2.1.5. Kits

Kits	**Manufacturer**	**Catalog number**
LEGENDplex™ Human Th Cytokine Panel (12-plex)	Biolegend, US	741027
LEGENDplex™ Mouse Th Cytokine Panel (13-plex)	Biolegend, US	740005
High Pure RNA Tissue Kit	Roche, Germany	12033674001
Unrestricted AMADID Release GE 4x44K 60mer, 4x44K features, sold as one 1x3 slide, 4 microarrays per slide	Agilent Technologies, US	G2519F AMADID 026655
LowInput QuickAmp Labeling Kit One-Color	Agilent Technologies, US	5190-2305
RNA Spike In Kit -One Color	Agilent Technologies, US	5188-5282
Pack 5 Backings 4 Arrays per Slide	Agilent Technologies, US	G2534-60011
Gene Expression Hybridization Kit	Agilent Technologies, US	5188-5242

2.2. Methods

2.2.1. Patients and control subjects

SSc patients were recruited from the Department of Rheumatology and Clinical Immunology, University of Lübeck, Lübeck, Germany. All patients fulfilled the 2013 American College of Rheumatology/European League Against Rheumatism (ACR/EULAR) classification criteria for SSc (10). Based on skin involvement, they were subclassified into dcSSc and lcSSc forms. Healthy controls were enrolled at the Research Center Borstel- Leibniz Lung Center, Borstel, Germany. Demographic and clinical characteristics, including age, sex, organ involvement, autoantibody status, and treatment regimens, were obtained from medical records. Written informed consent was obtained from all participants. This study was performed in accordance with the Declaration of Helsinki and approved by the local institutional review board at the University of Lübeck (AZ 16-199).

2.2.2. Mice and immunization

IL-13 transgenic (IL-13tg) mice and wild-type littermate controls were generously provided by Dr. Christoph Hölscher at the Research Center Borstel. The IL-13tg mouse line was originally generated by Emson et al. in 1998 through the injection of a fragment containing the full-length murine IL-13 gene under the control of the human CD2 promoter into fertilized eggs of a CBA × C57BL/6 hybrid background (117). The resulting transgenic line was subsequently backcrossed for four generations onto the C57BL/6 genetic background. All animals were housed under specific pathogen-free (SPF) conditions in the animal facility with a 12-hour light/dark cycle at the Research Centre Borstel. Randomization was used to allocate mice using random numbers. All procedures involving animals were conducted in accordance with institutional and governmental guidelines and were approved by the Animal Research Ethics Board of the Ministry of Energy Transition, Agriculture, Environment, Nature, and Digitalization, Kiel, Germany (105-8/17, 52-9/23).

Cell membrane extract (ME) derived from Chinese Hamster Ovary (CHO) cells overexpressing the human AT1R was kindly provided by CellTrend GmbH (Luchenwalde, Germany). IL-13tg

mice and their wild-type littermate controls, aged 8–12 weeks, were anesthetized via intraperitoneal injection of a narcosis solution containing Xylazine and Ketamine. Following anesthesia, mice were immunized with 0.2 mg of AT1R membrane extract suspended in 50 µl phosphate-buffered saline (PBS) and emulsified with an equal volume of Complete Freund's Adjuvant (CFA). A total of 100 µl of the emulsion was administered via subcutaneous injection into both hind footpads (50 µl per foot). Three weeks later, mice received a booster injection with the same amount of membrane extract emulsified in Incomplete Freund's Adjuvant (IFA), administered in the same manner.

2.2.3. Therapeutic antibody treatment

To evaluate the effects of interleukin-6 (IL-6) signaling blockade, mice were treated with monoclonal antibodies targeting either IL-6 or the IL-6 receptor (IL-6R). For anti-IL-6 therapy, mice received intraperitoneal injections of 150 µg rat anti-mouse IL-6 monoclonal antibody or rat IgG1 kappa isotype control once per week for five consecutive injections over a six-week period, beginning on the third day after the first immunization. For anti- IL-6R therapy, mice received intraperitoneal injections of 200 µg rat anti-mouse -IL-6R monoclonal antibody or rat IgG2b isotype control twice weekly for nine consecutive weeks, beginning on the third day after the first immunization At the end of the experiment period, mice were euthanized under deep anesthesia using overdose of Xylazine (66 mg/kg) and Ketamine (180 mg/kg) in 0.9% NaCl. Peripheral blood, bronchoalveolar lavage (BAL) fluid, lungs, and heart tissues were collected for subsequent analyses.

2.2.4. Serum and bronchoalveolar lavage fluid preparation

Human serum samples were prepared from peripheral blood, while murine sera were prepared from blood drawn directly from the inferior vena cava following euthanasia. Briefly, blood samples were transferred into serum-separating tubes and allowed to clot at room temperature for a minimum of 30 minutes. The samples were then centrifuged at 10,000 x g for 90 seconds at room temperature. The resulting serum was carefully collected, aliquoted into fresh 0.5 ml tubes, and stored at −80 °C until further analysis.

For the preparation of bronchoalveolar lavage (BAL) fluid, mice were euthanized via intraperitoneal injection of a lethal dose of anesthesia. The thoracic area was disinfected with 70% ethanol, and the chest cavity was carefully opened from the diaphragm to expose the lungs. Following blood collection, BAL was performed by flushing the lungs three times with 1 mL of sterile, room temperature 1X PBS-D buffer containing 0.1 mM EDTA. Each lavage was administered using a 1 mL syringe connected to a catheter. The collected lavage fluid was transferred to 2 mL tubes and kept on ice. To separate the supernatant, lavage samples were centrifuged at 250 x g for 10 minutes at 4 °C. Subsequently, the volume of supernatant was measured, and 25x protease inhibitor was added at a final dilution of 1:25. BAL fluid samples were then stored at -80°C for subsequent cytokine array analysis.

2.2.5. Determination of levels of cytokines in serum and BAL fluid

Serum levels of human cytokines were quantified using the LEGENDplex™ HU Th Cytokine Panel (12-plex) Kit (Cat. 741027, BioLegend, San Diego, CA), which simultaneously detects 12 cytokines, including IL-2, IL-4, IL-5, IL-6, IL-9, IL-10, IL-13, IL-17A, IL-17F, IL-22, IFN-γ, and TNF-α. For murine samples, including both serum and BALF, cytokine concentrations were determined using the LEGENDplex™ MU Th Cytokine Panel (13-Plex) Kit (Cat. 741043, BioLegend, San Diego, CA), which simultaneously detects 13 cytokines, including IL-2, IL-4, IL-5, IL-6, IL-9, IL-10, IL-13, IL-17A, IL-17F, IL-21, IL-22, IFN-γ, and TNF-α.

All assays were performed according to the manufacturer's instructions. Briefly, serum and BALF samples were diluted 1:2 in assay buffer and added to 96-well filter plates. Standards and serum samples were run in duplicate. Samples were incubated at room temperature for 2 hours with beads coated with captured antibodies specific to each cytokine. After washing, biotin-labeled detection antibodies were added and incubated for 1 hour at room temperature. This step was followed by a 30-minute incubation with streptavidin-phycoerythrin (PE). Beads were then washed, resuspended with washing buffer, and analyzed using a BD Symphony A3 flow cytometer. Data analysis was conducted using the LEGENDplex™ Data Analysis Software Suite (BioLegend).

2.2.6. Histological assessment

To evaluate pulmonary vasculopathy, the left lung lobe of each mouse was collected and fixed in 4% paraformaldehyde overnight. Following fixation, tissues were dehydrated using an automated tissue processor and embedded in paraffin. Tissue samples were sectioned into 3 μm thick slices for histological analysis. A detailed dehydration and paraffinization protocol is provided in the table below.

Dehydration and paraffinization

Steps	**Solutions**	**Time**
Step 1	4%formalin	60 mins
Step 2	70% ethanol	60 mins
Step 3	80% ethanol	60 mins
Step 4	90% ethanol	60 mins
Step 5	96% ethanol	60 mins
Step 6	100% ethanol	60 mins
Step 7	100% ethanol	60 mins
Step 8	100% ethanol	60 mins
Step 9	Xylene I	60 mins
Step 10	Xylene II	60 mins
Step 11	Paraffin I	90 mins
Step 12	Paraffin II	90 mins

Hematoxylin and eosin (H&E) staining was performed on. In brief, sections were deparaffinized in Xylene and rehydrated through a series of ethanol solutions with gradually decreasing concentrations. Afterward, sections were stained with H&E solution. Subsequently, the stained

sections were dehydrated again through ascending ethanol concentrations, cleared in Xylene, and mounted with a mounting medium. A detailed staining protocol is provided in the table below.

Hematoxylin and eosin staining

Steps	**Reagent**	**Incubation time**
Deparaffinization	Xylene I	5 min
	Xylene II	5 min
	Xylene III	5 min
Re-hydration	100% ethanol I	5 min
	100% ethanol II	5 min
	96% ethanol	5 min
	70% ethanol	5 min
	Tap water	5 min
Staining with Hematoxylin	Gill's II hematoxylin solution	20 min
	Running tap water	10 min
Staining with Eosin	Eosin (1%, acidic) counterstain	3 min
	Tap water	5-10 seconds
Dehydration	70% ethanol	10 seconds
	96% ethanol I	10 seconds
	96% ethanol II	10 seconds
	100% ethanol I	30 seconds
	100% ethanol II	3 min
Transparentize	Xylene I	5 min
	Xylene II	5 min
	Xylene III	5 min
Mounting	Entellan mounting medium	

Histopathological evaluation of H&E-stained sections was conducted by three independent investigators in a double-blinded manner. Small pulmonary arteries exhibiting features of

occlusive vasculopathy were classified as affected vessels. To quantify the severity of vascular pathology, a vasculopathy index was calculated as the percentage of arteries exhibiting occlusive changes relative to the total number of arteries analyzed. The final score was determined by averaging the individual assessments from the three blinded investigators.

2.2.7. RNA extraction

Total RNA was extracted from murine lung tissue using the High Pure RNA Isolation Kit (Roche Diagnostics, Germany) following the manufacturer's instruction. Briefly, lung tissues were immediately preserved in RNAlater™ stabilization solution (Invitrogen, USA) and stored at −80 °C to maintain RNA integrity until extraction. For each sample, approximately one-sixth of the lung tissue, which corresponds to 20–30 mg of tissue, was used for RNA isolation. Tissue was homogenized in lysis buffer containing guanidine thiocyanate, a chaotropic agent that ensures rapid inactivation of RNases and effective cell lysis. The resulting homogenate was filtered to remove debris and combined with ethanol to enable selective RNA binding to the silica membrane of the spin column. After several washing steps to eliminate proteins, salts, and contaminants, total RNA was eluted in 30–50 µL of RNase-free water.

RNA concentration was determined spectrophotometrically using a NanoDrop 2000 (Thermo Fisher Scientific), while RNA quality and Integrity were assessed using the Agilent 2100 Bioanalyzer system (Agilent Biotechnologies) according to the manufacturer's instructions. Only samples with acceptable RNA Integrity Numbers (RINs) and no signs of degradation were included in further analysis.

2.2.8. Transcriptome analysis

To evaluate transcriptomic changes in lung tissue, one-color microarray-based gene expression profiling was conducted using Agilent's platform (One-Color Microarray-Based Gene Expression, Version 6.9.1, Agilent Technologies). Total RNA was extracted from mouse lung tissues as mentioned, and only samples with high RNA integrity and sufficient concentration were selected for downstream processing.

For labeling and amplification, 10–200 ng of total RNA per sample was processed using the Low Input Quick Amp Labeling Kit, One-Color (Agilent Technologies, Cat. No. 5190-2305). To facilitate quality control during downstream hybridization and scanning, each RNA sample was supplemented with the One-Color RNA Spike-In Kit (Agilent Technologies, Cat. No. 5188-5282). RNA was reverse transcribed using a T7 oligo(dT) primer, followed by second-stranded cDNA synthesis and in vitro transcription to produce Cy3-labeled complementary RNA (cRNA). After amplification, labeled cRNA was purified with the RNeasy Mini Kit (Qiagen, Germany) and eluted in RNase-free water. The quantity and dye incorporation (specific activity) of each cRNA sample were assessed via NanoDrop spectrophotometry, and only samples meeting Agilent's yield and specific activity criteria were selected for subsequent hybridization.

For hybridization, 600 ng of Cy3-labeled cRNA per sample was chemically fragmented with a fragmentation buffer and blocking agent at 60 °C for 30 minutes. Subsequently, GEx Hybridization Buffer (Agilent Technologies, Cat. No. 5188-5242) was added to stop the reaction. Samples were then hybridized to Agilent Mouse GE 4x44K v2 microarrays (AMADID 026655), containing ~ 44,000 oligonucleotide probes. After hybridization, arrays were washed according to the manufacturer's instructions and scanned using the Agilent SureScan Microarray Scanner (G4900DA).

Raw microarray data were extracted using Agilent Feature Extraction software and imported into GeneSpring GX for downstream processing. This included background correction, quantile normalization, and $\log_2$ transformation. Low-quality probes were filtered out to ensure robust downstream analysis. Following normalization, differential gene expression was assessed using a moderated t-test with Benjamini-Hochberg correction to control the false discovery rate (FDR). Genes with an FDR-adjusted p-value< 0.05 and an absolute $\log_2$ fold change greater than 1 ($\geq$2-fold change) were considered significantly expressed.

To assess overall transcriptomic variation and sample clustering, multivariate analyses were conducted using ClustVis. Principal component analysis (PCA) was employed to reduce the dimensionality of the gene expression matrix while preserving the variance structure. The PCA plots were generated using the SVD with imputation method in ClustVis, with PC1 and PC2 representing the major axes of variation. Hierarchical clustering was also performed in ClustVis,

using the top differentially expressed genes, yielding a heatmap that visualized expression patterns across experimental groups and highlighted co-regulated gene clusters.

To explore the biological relevance of gene expression changes, pathway enrichment analysis was performed using the curated Reactome database. Differentially expressed genes were mapped to known biological pathways, and statistical overrepresentation was determined using hypergeometric testing. Pathways with p-values less than 0.05 were considered significantly enriched and grouped by functional categories. Upregulated and downregulated pathways were reported separately to distinguish between activated and suppressed biological processes in response to treatment.

2.2.9. Measurement of IL-1RA

The concentration of Interleukin-1 receptor antagonist (IL-1RA) in serum and bronchoalveolar lavage fluid (BALF) samples was determined using the Mouse IL-1ra/IL-1F3 Quantikine® ELISA Kit (R&D Systems, Cat. No. MRA00), following the manufacturer's protocol. This quantitative sandwich enzyme-linked immunosorbent assay (ELISA) is designed for detecting mouse IL-1RA in serum, plasma, and cell culture supernatants.

Briefly, all reagents, standards, controls, and biological samples were equilibrated to room temperature prior to use. A total of 50 µL of Assay Diluent RD1W was added to each well of a 96-well plate, followed by 50 µL of either standard, control, or sample. The plate was sealed with an adhesive strip and incubated for 2 hours at room temperature on a horizontal orbital shaker set to 500 ± 50 rpm. After washing the wells five times with the provided wash buffer, 100 µL of horseradish peroxidase-conjugated anti-mouse IL-1RA antibody was added and incubated for another 2 hours under the same conditions. Following a repeat of the washing steps, 100 µL of substrate solution was added and incubated in the dark for 30 minutes at room temperature. The reaction was stopped by adding 100 µL of stop solution, and absorbance was measured within 30 minutes at 450 nm using a microplate reader, with wavelength correction set at 540 or 570 nm.

Concentrations of IL-1RA in samples were calculated by subtracting background values (zero standard) and interpolating absorbance readings from a standard curve generated from known concentrations of recombinant mouse IL-1RA. All measurements were performed in duplicate for reproducibility. Samples with concentrations exceeding the assay's upper limit were diluted and re-assayed.

2.2.10. Statistical analysis

All statistical analyses were performed using GraphPad Prism (version 10.4.1), with additional multivariate analysis conducted via the ClustVis web tool. For quantitative variables such as cytokine concentrations, vasculopathy indices, and immune cell phenotypes, data distribution was first assessed using the Kolmogorov–Smirnov test to determine normality. Normally distributed data were analyzed using unpaired, two-tailed Student's t-tests for comparisons between two groups, while non-normally distributed data were analyzed using the Mann–Whitney U test. For comparisons involving more than two groups, the One-way ANOVA test was used for normally distributed data, and the Kruskal-Wallis test was applied for non-normally distributed data. All quantitative data are presented as scatter plots, with individual points representing single biological replicates (e.g., animals or patients), and horizontal lines indicating group means with error bars representing the standard error of the mean (SEM). For categorical variables, such as gender distribution and the presence of specific antibodies, either the Chi-square test or Fisher's exact test was used, depending on the sample size. To explore correlations between cytokines in both clinical and experimental samples, Spearman's rank correlation analysis was performed with a two-tailed 95% confidence interval. Correlation strength was interpreted based on Spearman's correlation coefficient (r), and results were visualized as heatmaps using GraphPad Prism software. A P-value of < 0.05 was considered statistically significant.

3. Results

3.1. Association between T helper cytokines and SSc

3.1.1. Demographic and clinical characteristics of patients with SSc

In total, 128 patients with SSc were enrolled in this study, including 97 females and 31 males. In addition, 69 sex-matched healthy subjects (44 females, 25 males) were included as controls. Due to difficulties in recruiting older healthy donors, the control group was significantly younger than the SSc group (42.25 ± 9.8 years vs. 56.66 ± 12.69 years, $p < 0.0001$).

Based on the extent of skin involvement, SSc patients were classified into two subtypes: 48 with dcSSc and 80 with lcSSc. A significant difference in sex distribution was noted between the subtypes: males constituted 47.9% of the dcSSc group and only 10.0% of the lcSSc group ($p < 0.0001$). The prevalence of ANA, ACA, ATA, and anti-RNA-Polymerase III in all SSc patients was 97.6%, 36.7%, 32.03%, and 10.08%, respectively. Significant differences were observed between the subtypes. ACA was more common in lcSSc (51.25% vs. 12.5%, $p < 0.0001$), while ATA was more frequent in dcSSc (50.0% vs. 21.25%, $p = 0.0015$).

Table 4. Clinical characteristics of patients with systemic sclerosis

Characteristics	SSc Patients (Total)	dcSSc	lcSSc	P-value (dcSSc vs lcSSc)
Age (mean± std. dev)	56.66 ± 12.69	55.88 ± 12.83	57.13 ± 12.67	ns
Gender (*n* (%))	97 Female (75.8%)	25 F (52.1%)	72 F (90.0%)	<0.0001
	31 Male (24.2%)	23 M (47.9%)	8 M (10.0%)	
Autoantibodies N/M (%)				
ANA	123/126 (97.6%)	45/47 (95.7%)	78/79 (98.7%)	ns
ACA	47/128 (36.7%)	6/48 (12.5%)	41/80 (51.25%)	<0.0001
ATA	41/128 (32.03%)	24/48 (50,0%)	17/80 (21.25%)	0.0015

anti-RNA-Polymerase III	12/119 (10.08%)	8/47 (17.02%)	4/72 (5.55%)	ns
Organ involvement N (%)				
ILD	47 (36.7%)	27 (56.25%)	20 (25.0%)	0.0004
PAH	19 (14.8%)	11 (22.9%)	8 (10.0%)	ns (0.059)

F. Female; M. Male; ANA. Antinuclear antibodies; ACA. Anticentromere antibodies; ATA. Anti-topoisomerase I antibody. ILD. Interstitial lung disease; PAH. Pulmonary arterial hypertension.

Regarding organ involvement, ILD was diagnosed in 36.7% of SSc patients, with a significantly higher prevalence in dcSSc than in lcSSc (56.25% vs. 25.0%, p = 0.0004). PAH, another common pulmonary involvement, was observed in 14.8% of SSc patients, with a significantly higher prevalence in dcSSc compared to lcSSc (22.9% vs. 10.0%, p = 0.047). A summary of clinical characteristics of SSc patients is presented in Table 4.

3.1.2. Inter-correlation of cytokine expression in SSc patients and healthy controls

Serum levels of 12 Th cytokines were measured in both SSc patients and healthy controls. One of the 12 cytokines, IL-22, was excluded from further analysis due to poor data quality.

To determine differences in Th cytokine profiles, correlation matrices of cytokines were generated separately for SSc patients and healthy donors. As shown in Figure 4, strong inter-cytokine correlations ($r > 0.6$) were frequently observed in patients with SSc. For instance, IL-4 exhibited strong correlations with IL-2 ($r = 0.60$) and IL-9 ($r = 0.67$). Similarly, IL-5, another Th2 cytokine, was correlated with IL-10 ($r = 0.71$), IL-17F ($r = 0.73$), and IL-2 ($r = 0.65$). IL-6 was also strongly correlated with IL-10 ($r = 0.68$). IL-10 further showed correlation with IL-2 ($r = 0.63$), IL-9 ($r = 0.60$) and IL-17F ($r = 0.65$). By contrast, such a strong association was rarely found in healthy controls.

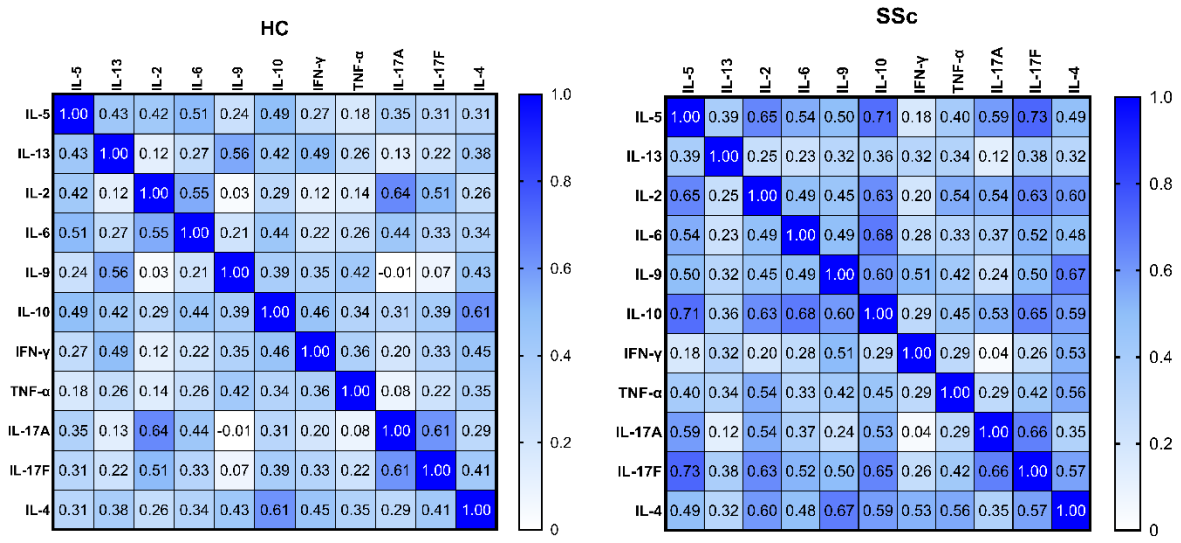

Figure 4. Heatmaps of inter-correlation of Th cytokines in SSc patients and healthy donors.

Spearman correlation coefficients (r) were calculated for 12 cytokines in serum samples from patients with systemic sclerosis (SSc) and healthy control (HC) donors. Each cell in the heatmap represents the correlation between two cytokines, with color intensity indicating the strength of the correlation (see scale bar). Higher values (r closer to 1) indicate stronger positive correlations.

Fisher's r-to-z transformation was used to statistically assess the differences in the strength of inter-correlated cytokine expression between patients and controls. Nine cytokine pairs showed strong correlation ($r > 0.6$) in patients and were significantly more correlated in SSc patients than in healthy controls ($p < 0.05$). These included IL-2/IL-4, IL-2/IL-5, IL-2/IL-10, IL-4/ IL-9, IL-5/IL-10, IL-5/IL-17F, IL-6/IL-10, IL-9/IL-10, and IL-10/IL-17F. These findings suggest an overall enhancement of Th cytokine interactions in SSc.

Table 5. Comparison of inter-correlation between cytokine pairs in SSc patients and healthy controls using Fisher's r-to-z transformation

Cytokine Pair	r (SSc)	r (HC)	z-value	p-value
IL-2 / IL-4	0.60	0.26	2.807	0.003
IL-2 / IL-5	0.65	0.42	2.153	0.016
IL-2 / IL-10	0.63	0.29	2.91	0.002
IL-4 / IL-9	0.68	0.43	2.306	0.011
IL-5 / IL-10	0.71	0.42	2.888	0.002
IL-5 / IL-17F	0.73	0.31	3.997	<0.0001
IL-6 / IL-10	0.68	0.44	2.346	0.01
IL-9 / IL-10	0.60	0.39	1.857	0.032
IL-10 / IL-17F	0.65	0.34	2.768	0.003

3.1.3. Association of T helper cytokines with SSc and its subtypes

To identify cytokines associated with SSc, serum levels of individual cytokines were compared between patients and controls. As shown in Table 6, the comparison showed that 6 out of 12 cytokines were significantly elevated in SSc patients, including IL-2, IL-4, IL-6, IL-10, IFN-γ, and TNF-α. The remaining 6 cytokines showed no significant difference.

Table 6. Levels of Th cytokines in Sera of SSc patients and Healthy controls

Cytokines (pg/ml)	Healthy control (N=69)	SSc patients (N=128)	P values
IL-5	7.33 (6.94–8.11)	7.72 (6.55─8.49)	n.s.
IL-13	6.36 (5.46–8.16)	7.27 (5.46─9.49)	n.s.
IL-2	**8.33 (6.48–9.25)**	**10.17 (7.41─13.80)**	**<0.0001**
IL-6	**27.98 (25.01–31.57)**	**35.05 (28.34─52.27)**	**<0.0001**
IL-9	6.07 (5.11–8.23)	7.02 (5.59–8.47)	n.s.
IL-10	**2.86 (2.39–3.71)**	**3.57 (2.45–5.32)**	**0.0089**
IFN-γ	**15.22 (13.35–18.57)**	**16.63 (14.43─24.67)**	**0.0096**
TNF-α	**21.00 (11.79–31.58)**	**26.95 (21.00─37.42)**	**0.005**
IL-17A	16.58 (14.14–19.84)	18.21 (14.95─21.06)	n.s.
IL-17F	8.58 (7.80–10.57)	9.77 (8.04─11.79)	n.s.
IL-4	**8.62 (7.98–9.28)**	**9.57 (8.62–11.46)**	**<0.0001**

Data were presented as median (Q1-Q3). n.s. not significant.

Subtype analysis revealed higher IL-6 levels in dcSSc compared to lcSSc (42.99 (30.86─69.29) pg/ml vs. 33.33 (26.51─48.32) pg/ml, p = 0.038). No other cytokines showed a significant difference between the two subtypes (Table 7).

Table 7. Comparison of Th cytokines between SSc subtypes

Cytokines (pg/ml)	lcSSc (N=101)	dcSSc (N=56)	P values
IL-5	7.81 (6.16–8.64)	7.33 (6.94–8.49)	n.s.
IL-13	7.27 (5.57–9.93)	7.27 (5.46–9.05)	n.s.
IL-2	10.17 (6.71–14.70)	10.17 (7.64–12.90)	n.s.
IL-6	**33.33 (26.51–48.32)**	**42.99 (30.86–69.29)**	**0.038**
IL-9	7.02 (5.59–8.47)	7.02 (5.59–8.83)	n.s.
IL-10	3.33 (2.15–5.23)	3.68 (2.86–5.46)	n.s.
IFN-γ	17.46 (14.43–25.61)	16.63 (14.43–23.34)	n.s.
TNF-α	28.15 (18.66–37.84)	25.76 (21.00–35.41)	n.s.
IL-17A	16.58 (13.33–19.84)	18.21 (14.95–21.46)	n.s.
IL-17F	9.77 (1.36–13.63)	9.37 (7.60–10.57)	n.s.
IL-4	9.57 (8.62–11.46)	9.57 (8.93–11.10)	n.s.

Data were presented as median (Q1-Q3). n.s. not significant.

3.1.4. Association of Th cytokines with clinical manifestations in SSc

Next, the relationship between Th cytokines and major clinical manifestations, including ILD, PAH, cardiac, and esophageal involvement, was examined. For this purpose, SSc patients were stratified into two subgroups based on the presence of each clinical manifestation.

IL-6 was the only cytokine consistently associated with multiple clinical manifestations in SSc. As shown in Figure 5 and Table 8, serum levels of IL-6 were significantly elevated in SSc patients with ILD (42.3 (27.8–75.5) pg/ml) compared to those without ILD (33.3 (28.3–45.5) pg/ml, $p = 0.044$). Similarly, SSc patients with PAH showed significantly higher serum IL-6 levels (62.1 (28.0–84.3) pg/ml) than those without PAH (34.3 (28.1–49.3) pg/ml, $p = 0.027$).

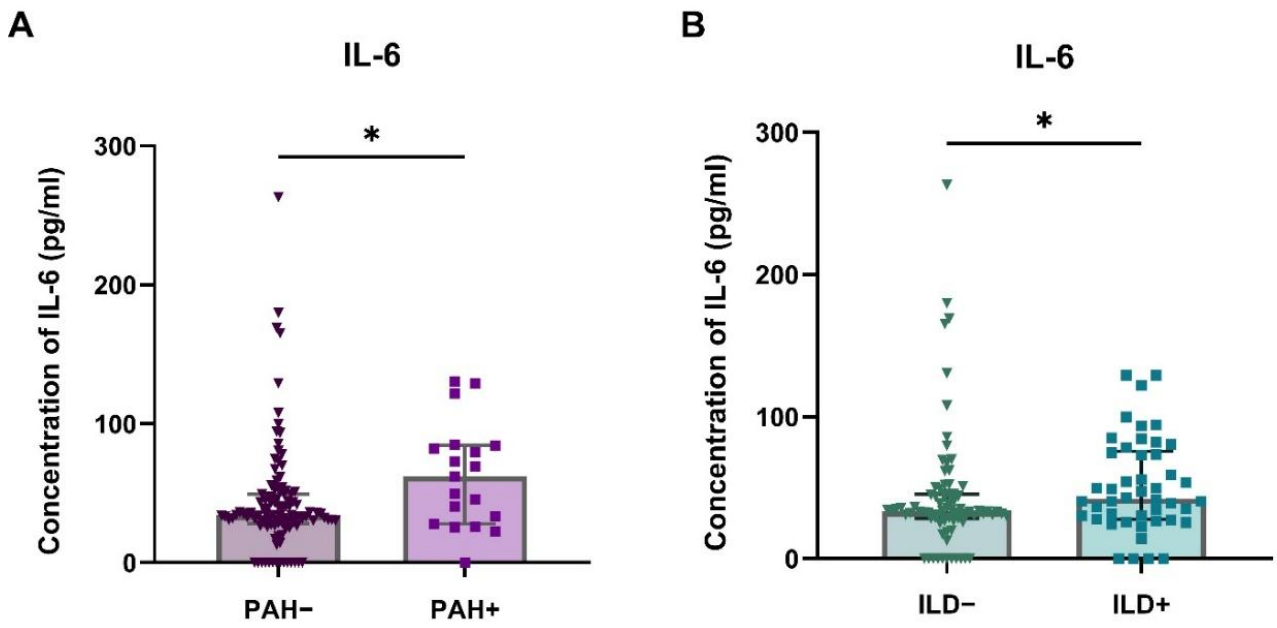

Figure 5. Association between serum IL-6 levels and pulmonary manifestations in SSc

Serum IL-6 concentrations were compared between SSc patients with and without pulmonary complications. (A) IL-6 levels in patients diagnosed with pulmonary arterial hypertension (PAH+) compared to patients without PAH (PAH−). (B) IL-6 levels in patients with ILD (ILD+) compared to those without ILD (ILD−). Data are presented as individual values with median (Q1-Q3). Statistical analysis was conducted with Mann-Whitney test, * $p < 0.05$.

In contrast, levels of IL-17A and TNF-α were significantly reduced in SSc patients with PAH than those without PAH (Table 8).

Table 8. Association of Th cytokines with ILD and PAH in SSc

Cytokines (pg/ml)	ILD−	ILD+	P value	PAH−	PAH+	P value
IL-5	7.91 (6.55−8.69)	7.33 (6.55−8.49)	n.s.	7.72 (6.55−8.49)	7.33 (5.63−8.49)	n.s.
IL-13	7.72 (6.14−9.93)	6.36 (5.00−9.49)	n.s.	7.27 (5.91−9.49)	6.14 (5.00−9.93)	n.s.
IL-2	10.17 (8.3−14.7)	9.25 (7.4−12.9)	n.s.	10.17 (7.41−14.7)	9.25 (0.0−10.17)	n.s.
IL-6	**33.3 (28.3−45.5)**	**42.3 (27.8−75.5)**	**0.044**	**34.4 (28.1−49.3)**	**62.1 (28.0−84.3)**	**0.027**
IL-9	7.02 (5.59−8.47)	6.55 (4.64−8.47)	n.s	7.02 (5.59−8.47)	5.59 (4.64−8.47)	n.s.
IL-10	3.33 (2.62−5.23)	3.8 (2.15−6.06)	n.s.	3.57 (2.62−5.46)	3.09 (0.00−4.99)	n.s.
IFN-γ	17.7 (14.4−25.6)	16.6 (13.9−23.3)	n.s	16.63 (14.4−24.7)	16.6 (12.8−25.6)	n.s.
TNF-α	25.8 (21.0−35.4)	28.1 (21.0−41.5)	n.s.	**28.15 (21.0−37.8)**	**21.0 (0.0−30.56)**	**0.037**
IL-17A	18.2 (14.9−19.8)	18.2 (0.77−21.5)	n.s.	**18.21 (14.9−21.5)**	**14.95 (0.0−18.2)**	**0.040**
IL-17F	9.77 (8.2−12.2)	9.37 (7.4−11.8)	n.s.	9.77 (8.2−12.2)	9.17 (0.0−10.17)	n.s.
IL-4	9.87 (8.9−12.08)	9.25 (8.3−11.14)	n.s.	9.57 (8.93−11.46)	8.93 (0.0−9.88)	n.s.

Data were presented as median (Q1-Q3). n.s. not significant.

Taken together, these findings indicate a central role in SSc pathogenesis, particularly in pulmonary involvement, including ILD and PAH.

3.2. Neutralizing IL-6 signaling in AT1R-immunized IL-13tg mice

3.2.1. Treatment with anti-IL-6 monoclonal antibody in AT1R-immunized IL-13tg mice

Based on my clinical observations, IL-6 emerged as a promising candidate for therapeutic intervention, as elevated serum IL-6 levels were significantly associated with pulmonary complications such as PAH and ILD in SSc patients. In addition, in our previous experimental studies using IL-13tg mice, levels of IL-6 in BALF were markedly increased following AT1R immunization and correlated with the severity of pulmonary vasculopathy. These consistent observations across human and murine models led us to evaluate IL-6 neutralization as a therapeutic strategy in the AT1R-immunized IL-13tg mice.

To evaluate the therapeutic efficacy of IL-6 neutralization, IL-13tg mice were subcutaneously immunized with 0.2 mg AT1R membrane extract emulsified in CFA on day 0 and boosted with AT1R in IFA on day 21. As outlined in Figure 6, these mice were divided into two groups: anti-IL-6 neutralizing monoclonal antibody-treated (n = 20) and IgG1κ isotype control (n = 20). Antibodies were administered intraperitoneally five times, beginning on day 3 after the first immunization. Serum, BAL, and lung tissues were collected at the end of the study for further evaluation.

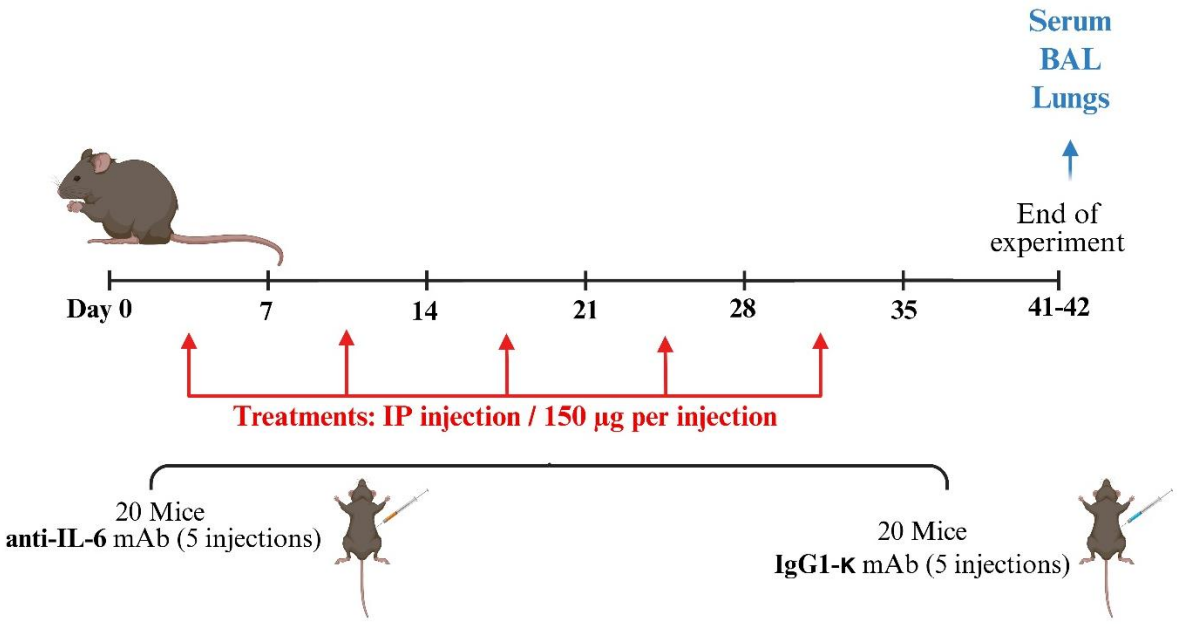

Figure 6. Experimental design for IL-6 neutralization in AT1R-immunized IL-13 transgenic mice.

A total of 45 IL-13tg mice were immunized subcutaneously with 0.2 mg of AT1R membrane extract (ME) emulsified in Complete Freund's Adjuvant (CFA) on day 0, followed by a booster injection with AT1R ME emulsified in Incomplete Freund's Adjuvant (IFA) on day 21. The mice were divided into two groups: 20 mice were treated intraperitoneally with anti-IL-6 monoclonal antibody, and 20 mice received IgG1κ isotype control antibody. Treatments were administered five times throughout the experiment, starting on day 3 post-immunization. Figure created using BioRender (https://BioRender.com).

3.2.1.1. Serum cytokine levels in mice following anti-IL-6 treatment

Serum levels of 13 Th cytokines were quantified using a multiplex bead-based immunoassay. As expected, IL-6 concentrations were significantly reduced in the anti-IL-6-treated group compared to isotype controls (p = 0.0003), confirming effective systemic neutralization. However, no significant differences were observed between treatment groups for other Th cytokines analyzed, including IL-2, IL-4, IL-5, IL-10, IL-13, IFN-γ, TNF-α, IL-9, IL-17A, IL-17F, and IL-22 (Table 9).

Table 9. Cytokine levels in serum of IL-13tg mice with anti-IL-6 or Isotype treatments

Cytokines (pg/ml)	IL-13tg mice (N=20) Isotype treatment	IL-13tg mice (N=20) Anti-IL-6 treatment	P values
IL-5	0.00 (0.00-0.00)	0.00 (0.00-3.34)	n.s.
IL-13	0.00 (0.00-0.00)	0.00 (0.00-0.00)	n.s.
IL-2	0.00 (0.00-0.00)	0.00 (0.00-0.00)	n.s.
IL-6	**3.66 (0.00-24.35)**	**0.00 (0.00-0.00)**	**<0.0001**
IL-9	0.00 (0.00-0.00)	0.00 (0.00-0.00)	n.s.
IL-10	0.00 (0.00-0.00)	0.00 (0.00-0.00)	n.s.
IFN-γ	47.73 (24.52-74.86)	47.74 (22.72-95-61)	n.s.
TNF-α	5.21 (0.00-15.03)	5.21 (0.00-15.85)	n.s.
IL-17A	0.00 (0.00-0.00)	0.00 (0.00-0.00)	n.s.
IL-17F	0.00 (0.00-0.00)	0.00 (0.00-0.00)	n.s.
IL-4	0.00 (0.00-1.40)	1.07 (0.00-1.72)	n.s.
IL-22	0.00 (0.00-0.00)	0.00 (0.00-0.00)	n.s.

Data were presented as median (Q1-Q3). n.s. not significant.

3.2.1.2. Histopathological assessment of pulmonary vasculopathy in AT1R-immunized IL-13tg mice following IL-6 neutralization

Pulmonary vasculopathy was assessed on paraffin-embedded sections of the lung by H&E staining. Blind histological analysis quantified the proportion of affected pulmonary arteries. As shown in Figure 7, although not significant, a trend toward increased severity of vasculopathy was observed in the anti-IL-6-treated group compared to the isotype group (8.93 ± 3.52% *vs.* 2.68 ± 1.42%, $p = 0.59$). These findings suggest that anti-IL-6 neutralizing antibody mitigates AT1R-induced pulmonary vasculopathy in IL-13tg mice.

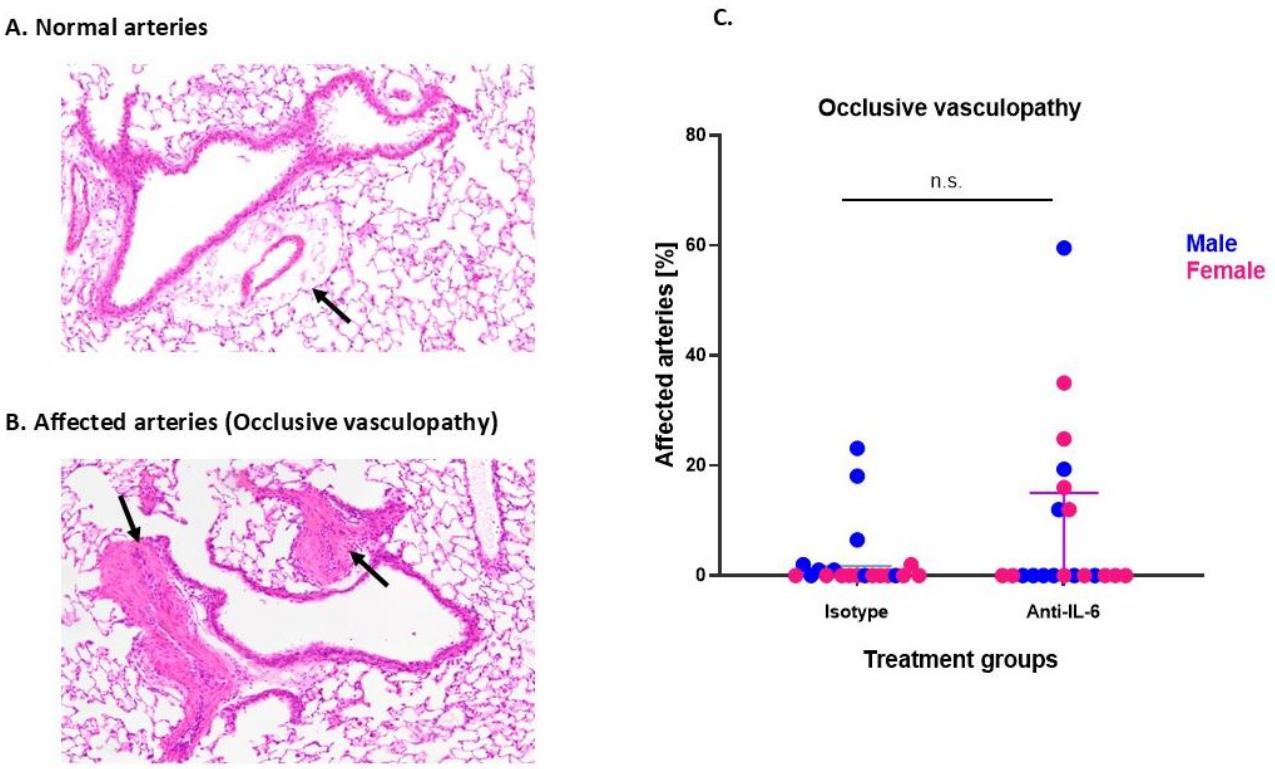

Figure 7. Histopathological evaluation of pulmonary vasculopathy in AT1R-immunized IL-13 transgenic mice.

AT1R-immunized IL-13tg mice were either treated with anti-IL-6 monoclonal antibody or treated with rat IgG1κ isotype control. Lung sections were stained with hematoxylin and eosin (H&E) and assessed for pulmonary vasculopathy. Representative micrographs show (A) unaffected and (B) affected pulmonary arteries. Arrows indicate pulmonary arteries. Scale bars = 50 μm. (C) Quantitative analysis of the proportion of affected arteries among total pulmonary arteries assessed in each group. Data are shown as individual values for female (pink) and male (blue) mice, with median (Q1-Q3). Statistical analysis was conducted using the Mann-Whitney test. n.s. not significant.

3.2.1.3. BALF levels of cytokines in mice following IL-6 neutralization

Given that anti-IL-6 treatment inhibited IL-6 at the systemic level, I next determined whether it also inhibits local IL-6 production. For this purpose, cytokine levels in BAL fluid were measured to assess local pulmonary immune responses in treatment groups. Despite effective systemic IL-6 neutralization, BALF levels of IL-6 in anti-IL-6-treated mice were similar to those in isotype control IgG-treated mice (5.33 pg/ml vs. 4.15 pg/ml, $p = 0.28$). Similarly, levels of other Th cytokines showed no significant difference between the two treatment groups (Table 10). This suggests that anti-IL-6 therapy may not adequately suppress pulmonary IL-6 signaling.

Table 10. Cytokine levels in BAL fluid of IL-13tg mice with anti-IL-6 or Isotype treatments

Cytokines (pg/ml)	IL-13tg mice (N=20) Isotype treatment	IL-13tg mice (N=20) Anti-IL-6 treatment	P values
IL-5	0.00 (0.00-0.00)	0.00 (0.00-0.590)	n.s.
IL-13	0.00 (0.00-0.00)	0.00 (0.00-0.00)	n.s.
IL-2	1.205 (0.00-3.530)	2.620 (0.00-3.130)	n.s.
IL-6	4.145 (1.218-9.453)	5.330 (1.868-14.15)	n.s.
IL-9	0.00 (0.00-0.00)	0.00 (0.00-0.00)	n.s.
IL-10	0.00 (0.00-0.00)	0.00 (0.00-0.00)	n.s.
IFN-γ	2.380 (0.00-10.81)	2.380 (0.00-25.76)	n.s.
TNF-α	0.00 (0.00-0.00)	0.00 (0.00-0.00)	n.s.
IL-17A	0.00 (0.00-0.00)	0.00 (0.00-0.00)	n.s.
IL-17F	0.00 (0.00-0.00)	0.00 (0.00-0.00)	n.s.
IL-4	0.00 (0.00-1.400)	1.070 (0.00-1.720)	n.s.
IL-22	0.00 (0.00-0.00)	0.00 (0.00-0.00)	n.s.

Data were presented as median (Q1-Q3). n.s. not significant.

3.2.2. Treatment with anti-IL-6R monoclonal antibody in AT1R-immunized IL-13tg mice

Given the limited efficacy of IL-6 neutralization, I next explored whether blocking IL-6 receptor (IL-6R), thereby inhibiting both classical and trans-signaling pathways, might yield improved outcomes. IL-13tg mice were immunized with AT1R as before and treated intraperitoneally twice weekly with either anti-IL-6R monoclonal antibody (n=15) or an IgG2b isotype control (n=14), starting on day 3 post-immunization (Figure 8).

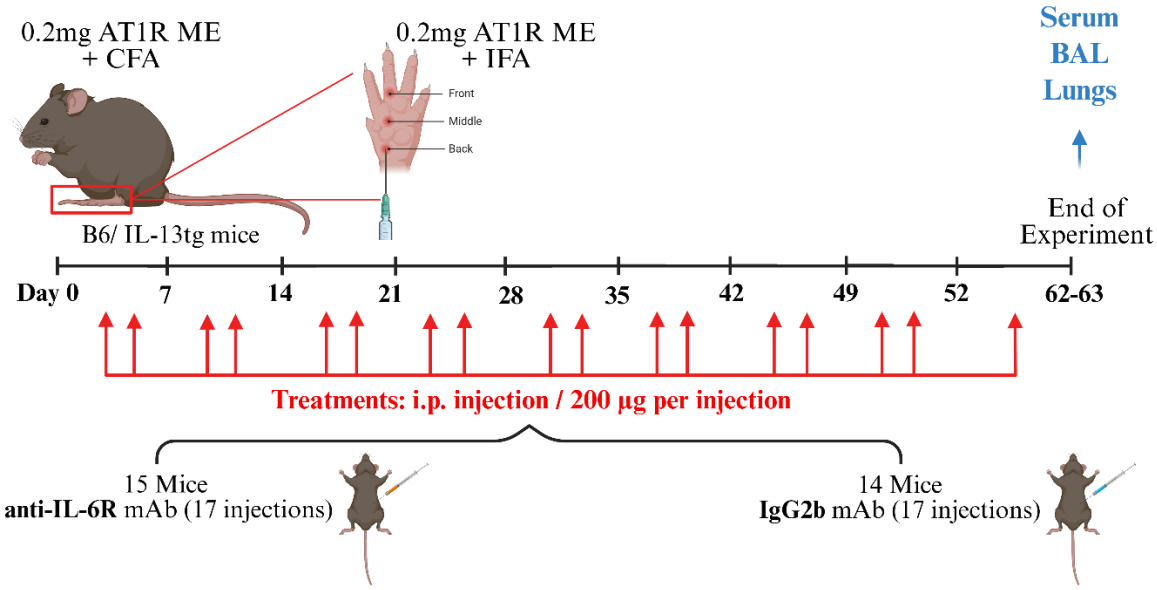

Figure 8. Experimental design for IL-6R blockade in AT1R-immunized IL-13 transgenic mice.

A total of 29 IL-13tg mice were immunized subcutaneously with 0.2 mg of AT1R membrane extract (ME) emulsified in Complete Freund's Adjuvant (CFA) on day 0, followed by a booster injection with AT1R ME emulsified in Incomplete Freund's Adjuvant (IFA) at day 21. Starting on day 3 after the first immunization, 15 mice received intraperitoneal injections of anti-IL-6R monoclonal antibody twice per week, while 14 mice received IgG2b isotype control. Figure created using BioRender (https://BioRender.com).

3.2.2.1. Serum cytokine profiling in mice following anti-IL-6R treatment

To explore serum Th cytokine profiling, serum cytokine levels were quantified using a multiplex bead-based immunoassay. Notably, IL-13 levels were significantly elevated in anti-IL-6R-treated group compared to isotype control group (6,85 pg/ml vs. 2.34 pg/ml, $p = 0.0051$). Levels of other Th cytokines, including IL-2, IL-4, IL-5, IL-6, TNF-α, IFN-γ, IL-9, IL-10, IL-17A, IL-17F, and IL-22, did not show significant differences between the two groups (Table 11).

Table 11. Serum cytokine levels in AT1R-immunized IL-13tg mice treated with anti-IL-6R monoclonal antibody or isotype control

Cytokines (pg/ml)	IL-13tg mice (N=14) Isotype treatment	IL-13tg mice (N=15) Anti-IL-6R treatment	P values
IL-5	0.00 (0.00-6.965)	0.00 (0.00-7.210)	n.s.
IL-13	**2.335 (0.00-5.210)**	**6.850 (3.300-8.280)**	**0.0051**
IL-2	0.00 (0.00-0.00)	0.00 (0.00-0.00)	n.s.
IL-6	0.00 (0.00-5.413)	0.00 (0.00-7.930)	n.s.
IL-9	0.00 (0.00-0.00)	0.00 (0.00-0.00)	n.s.
IL-10	166.4 (0.00-1774)	1216 (256.7-1649)	n.s.
IFN-γ	18.12 (14.95-29.83)	21.32 (13.78-31.69)	n.s.
TNF-α	19.06 (16.25-27.12)	22.24 (0.00-27.29)	n.s.
IL-17A	1.290 (0.975-1.565)	0.660 (0.00-1.280)	n.s.
IL-17F	0.00 (0.00-0.00)	0.00 (0.00-0.00)	n.s.
IL-4	0.00 (0.00-0.00)	0.00 (0.00-0.00)	n.s.
IL-22	0.00 (0.00-7.865)	5.435 (0.00-11.11)	n.s.

Data were presented as median (Q1-Q3). n.s. not significant.

3.2.2.2. BAL cytokine profiling in mice following anti-IL-6R treatment

BALF cytokine analysis was conducted to evaluate the local pulmonary immune response following IL-6R neutralization. As summarized in Table 12, there was no significant difference in IL-6 and other Th cytokines between the anti-IL-6R and isotype-treated groups. This suggests that IL-6R blockade did not modulate pulmonary cytokine expression in AT1R-immunized IL-13tg mice.

Table 12. BALF cytokine levels in AT1R-immunized IL-13tg mice treated with anti-IL-6R monoclonal antibody or isotype control

Cytokines (pg/ml)	IL-13tg mice (N=14) Isotype treatment	IL-13tg mice (N=15) Anti-IL-6R treatment	P values
IL-5	0.00 (0.00-0.00)	0.00 (0.00-0.00)	n.s.
IL-13	0.00 (0.00-0.00)	0.00 (0.00-0.370)	n.s.
IL-2	0.135 (0.007-1.098)	0.310 (0.00-0.40)	n.s.
IL-6	0.230 (0.00-2.660)	1.290 (0.190-23.15)	n.s.
IL-9	0.00 (0.00-2.310)	0.00 (0.00-0.00)	n.s.
IL-10	0.00 (0.00-1.922)	0.00 (0.00-9.047)	n.s.
IFN-γ	0.335 (0.00-1.543)	0.500 (0.120-4.100)	n.s.
TNF-α	0.450 (0.00-1.045)	0.00 (0.00-2.480)	n.s.
IL-17A	0.00 (0.00-0.00)	0.00 (0.00-0.00)	n.s.
IL-17F	0.00 (0.00-0.00)	0.00 (0.00-0.00)	n.s.
IL-4	0.00 (0.00-0.00)	0.00 (0.00-0.00)	n.s.
IL-22	0.00 (0.00-0.00)	0.00 (0.00-0.00)	n.s.

Data were presented as median (Q1-Q3). n.s. not significant.

3.2.3. Elevated proportion of pulmonary vasculopathy in AT1R-immunized IL-13tg mice treated with anti-IL-6R

Next, H&E-stained murine lung sections were examined to assess pulmonary vasculopathy. Although statistical analysis did not show a significant difference between the two groups (Figure 9), a notable trend toward increased occlusive vasculopathy was observed in the anti-IL-6R-treated group compared to isotype controls (16.28 ± 4.33% vs 10.29 ± 3.65%, $p = 0.227$). These histopathological changes are consistent with those observed in IL-13tg mice treated with anti-IL-6 neutralizing antibody, raising concerns about potential disease exacerbation through IL-6 pathway inhibition.

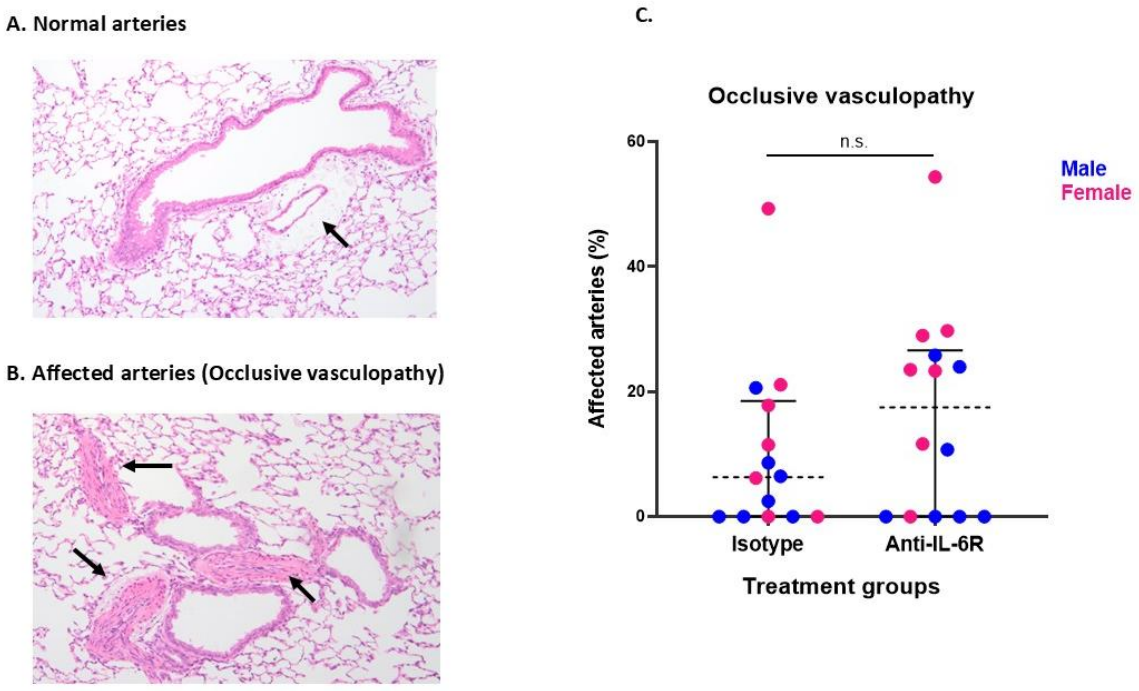

Figure 9. Assessment of pulmonary vasculopathy in AT1R-immunized IL-13 transgenic mice treated with anti-IL-6R monoclonal antibody.

AT1R-immunized IL-13tg mice were treated with anti-IL-6R monoclonal antibody, rat IgG2b isotype control. Lung sections were stained with hematoxylin and eosin (H&E) and assessed for pulmonary vasculopathy. Representative micrographs show (A) unaffected and (B) affected pulmonary arteries. Arrows indicate pulmonary arteries. Scale bars = 50 μm. (C) Quantitative analysis of the proportion of affected arteries among total pulmonary arteries assessed in each group. Data are presented as median (Q1-Q3). Statistical analysis was performed using the Mann-Whitney test. n.s. not significant.

3.3. Neutralizing IL-6 signaling in unimmunized IL-13tg mice

Given the observation that IL-6 and IL-6R blockade tended to increase the severity of pulmonary vasculopathy in AT1R-immunized IL-13tg mice, I hypothesized that IL-6 signaling may exert a protective role in maintaining pulmonary vascular integrity. To test whether IL-6 neutralization alone is sufficient to promote the development of pulmonary vasculopathy, I investigated its effect in the absence of immunization-induced inflammation. Unimmunized IL-13tg mice were treated intraperitoneally with either anti-IL-6 monoclonal antibody or IgG1κ isotype control, as illustrated in the experimental design (Figure 10). Mice received five weekly injections of the respective antibodies. At the end of the experiment, serum, BAL fluid, and lung tissues were collected for subsequent cytokine profiling and histopathological evaluation.

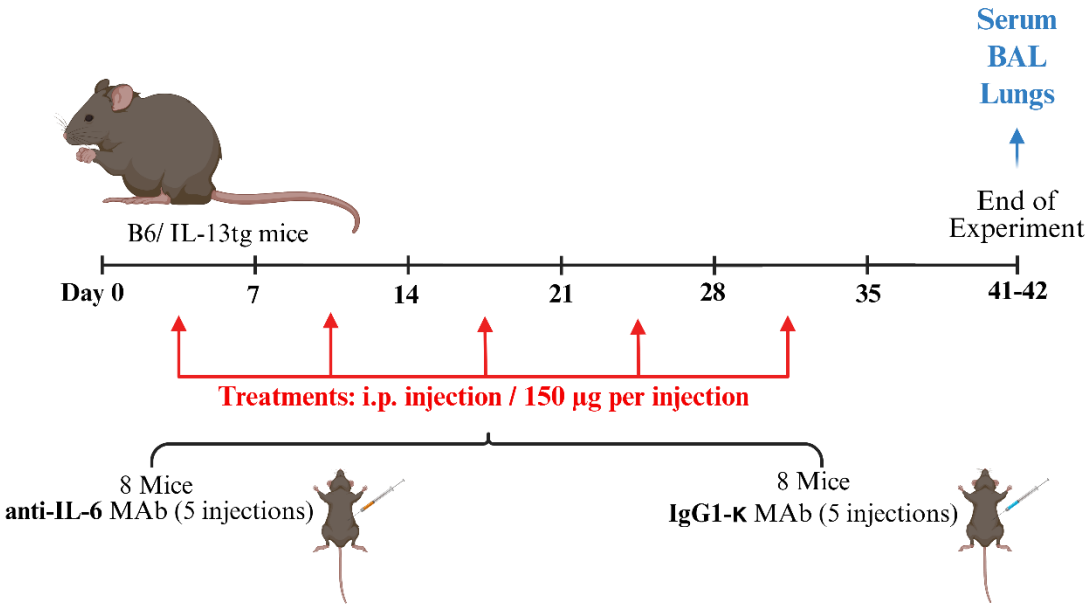

Figure 10. Experimental design for anti-IL-6 treatment in unimmunized IL-13 transgenic mice.

Unimmunized IL-13tg mice were treated weekly with either anti-IL-6 monoclonal antibody or IgG1κ isotype control via intraperitoneal injection (150 µg per injection). Treatments were administered five times during the experiment. At the end of the experiment, samples were harvested for downstream histological and molecular analyses. Figure created using BioRender (https://BioRender.com).

3.3.1. Induction of pulmonary occlusive vasculopathy via anti-IL-6 treatment in unimmunized IL-13tg mice

Histopathological examination of H&E-stained lung sections was performed to assess pulmonary vasculopathy in IL-13tg mice treated with either anti-IL-6 monoclonal antibody or IgG1κ isotype control. As expected, none of the eight IL-13tg mice receiving IgG1κ isotype control developed occlusive vasculopathy. In contrast, 5 out of 8 IL-13tg mice receiving anti-IL-6 monoclonal antibody exhibited histological evidence of occlusive vasculopathy. Quantitative assessment demonstrated a significantly increased proportion of affected pulmonary arteries in the anti-IL-6-treated group compared to the isotype control group (7.21% vs. 0.00%, $p = 0.0256$) (Figure 11). These results indicate that systemic blockade of IL-6 signaling, even in the absence of antigenic stimulation, is sufficient to trigger pulmonary vascular remodeling and occlusion in the IL-13tg background.

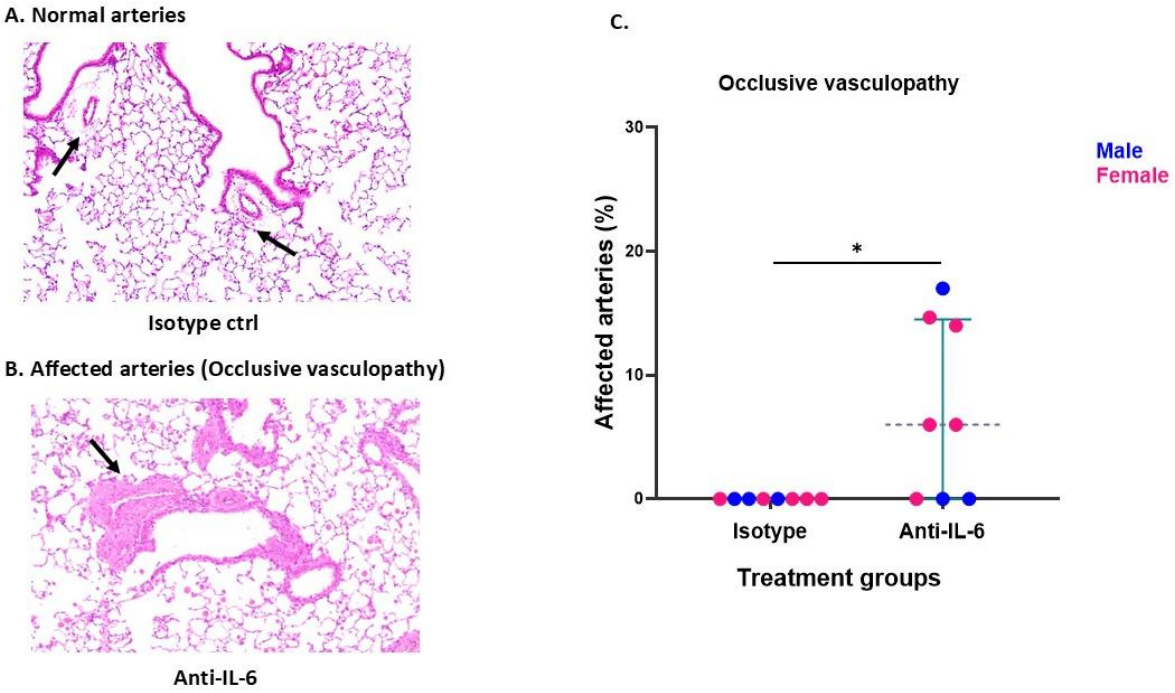

Figure 11. Induction of pulmonary occlusive vasculopathy in unimmunized IL-13tg mice following anti-IL-6 treatment.

Unimmunized IL-13tg mice were treated with either anti-IL-6 monoclonal antibody or IgG1κ isotype control. Lung sections were stained with hematoxylin and eosin (H&E) and assessed for pulmonary vasculopathy. Representative micrographs show (A) unaffected and (B) affected pulmonary arteries. Arrows indicate pulmonary arteries. Scale bars = 50 μm. (C) Quantitative analysis of the proportion of affected arteries among total pulmonary arteries assessed in each group. The data represent the percentage of affected pulmonary arteries per animal. Individual data points are shown for female (pink) and male (blue) mice. Bars indicate median (Q1-Q3). Statistical analysis was conducted using the Mann-Whitney test, * $p < 0.05$.

3.3.2. Serum and BALF cytokine profiles in unimmunized IL-13tg mice treated with anti-IL-6 monoclonal antibody

Serum and BALF cytokine analysis were performed to evaluate the local pulmonary immune response following IL-6 neutralization. As shown in Table 13, there were no significant differences in serum levels of IL-6 or other Th cytokines between the anti-IL-6 and isotype control groups. In BALF, only IL-4 levels were significantly elevated in anti-IL-6-treated group compared to isotype control group (1.235 pg/ml vs. 0.00 pg/ml, $p = 0.035$) (Table 14).

Table 13. Serum cytokine levels in unimmunized IL-13tg mice treated with anti-IL-6 monoclonal antibody or isotype control

Cytokines (pg/ml)	IL-13tg mice (N=8) Isotype treatment	IL-13tg mice (N=8) Anti-IL-6 mAb treatment	P values
IL-5	0.00 (0.00-8.108)	0.00 (0.00-2.168)	n.s.
IL-13	0.00 (0.00-0.00)	0.00 (0.00-0.370)	n.s.
IL-2	0.00 (0.00-0.00)	0.00 (0.00-84.07)	n.s.
IL-6	0.00 (0.00-0.00)	0.00 (0.00-0.00)	n.s.
IL-9	0.00 (0.00-0.00)	0.00 (0.00-0.00)	n.s.
IL-10	0.00 (0.00-0.00)	289.8 (0.00-1665)	n.s.
IFN-γ	0.00 (0.00-0.00)	0.00 (0.00-0.00)	n.s.
TNF-α	0.00 (0.00-0.00)	0.00 (0.00-0.00)	n.s.
IL-17A	0.00 (0.00-0.00)	0.00 (0.00-0.00)	n.s.
IL-17F	0.00 (0.00-0.00)	0.00 (0.00-0.00)	n.s.
IL-4	0.00 (0.00-0.00)	0.00 (0.00-0.00)	n.s.
IL-22	0.00 (0.00-0.00)	0.00 (0.00-0.00)	n.s.

Data were presented as Median (Q1-Q3). n.s. not significant.

Table 14. BALF cytokine levels in unimmunized IL-13tg mice treated with anti-IL-6 monoclonal antibody or isotype control

Cytokines (pg/ml)	IL-13tg mice (N=8) Isotype treatment	IL-13tg mice (N=8) Anti-IL-6 mAb treatment	P values
IL-5	0.00 (0.00-0.00)	0.00 (0.00-0.240)	n.s.
IL-13	0.00 (0.00-0.00)	0.00 (0.00-0.370)	n.s.
IL-2	3.230 (2.410-3.915)	0.00 (0.00-0.00)	n.s.
IL-6	0.00 (0.00-1.05)	0.00 (0.00-0.95)	n.s.
IL-9	0.00 (0.00-2.783)	0.00 (0.00-0.00)	n.s.
IL-10	0.00 (0.00-6.090)	0.00 (0.00-18.22)	n.s.
IFN-γ	0.00 (0.00-0.00)	0.00 (0.00-0.00)	n.s.
TNF-α	0.00 (0.00-0.00)	0.00 (0.00-0.00)	n.s.
IL-17A	0.00 (0.00-0.00)	0.00 (0.00-0.502)	n.s.
IL-17F	0.00 (0.00-0.00)	0.00 (0.00-0.00)	n.s.
IL-4	**0.00 (0.00-0.00)**	**1.235 (0.267-1.960)**	**0.035**
IL-22	0.00 (0.00-0.00)	0.00 (0.00-0.00)	n.s.

Data were presented as Median (Q1-Q3). n.s. not significant.

3.3.3. Lung transcriptomic profile in the unimmunized IL-13tg mice treated with anti-IL-6 monoclonal antibody

To explore the molecular mechanism underlying the impact of IL-6 signaling neutralization in IL-13tg mice, transcriptomic profiling of lung tissue was performed in unimmunized IL-13tg mice treated with anti-IL-6 monoclonal antibody or IgG1κ isotype control. Total RNA was extracted from whole lung tissue, and genome-wide gene expression was assessed using a microarray platform. Following data quality control, background correction, and normalization, transcriptomes from 3 mice in the anti-IL-6 group and 6 mice in the isotype control group were included in the analysis.

Principal component analysis (PCA) revealed a clear separation between treatment groups, with samples clustering distinctly along the first principal component (PC1), which accounted for 79.4% of the total variance, and the second principal component (PC2), explaining 6.4% of the total variance (Figure 12). This separation indicates substantial transcriptomic divergence in response to IL-6 neutralization.

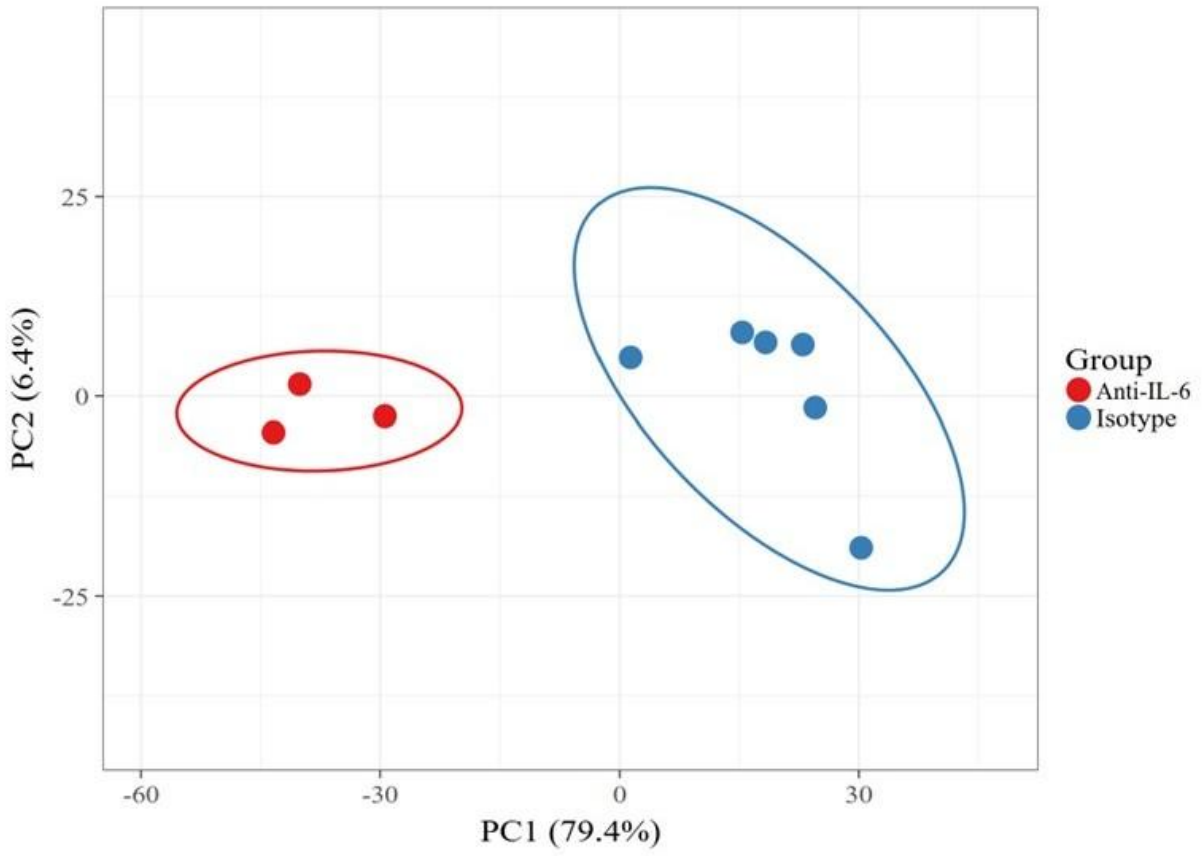

Figure 12. Principal component analysis (PCA) of lung transcriptomes from unimmunized IL-13tg mice treated with anti-IL-6 monoclonal antibody or IgG isotype control.

PCA was performed using whole-transcriptome expression profiles derived from lung tissues of unimmunized IL-13tg mice treated with either anti-IL-6 monoclonal antibody (green, n=3) or IgG1κ isotype control (orange, n=6). Gene expression data were subjected to background correction, normalization, and filtering prior to analysis. Each data point represents an individual mouse, and ellipses indicate the 95% confidence interval for each treatment group, illustrating distinct clustering based on treatment.

Differentially expressed genes (DEGs) were identified using a fold change threshold of > 2 and an adjusted *p*-value of < 0.05 (Benjamini–Hochberg correction). A total of 673 DEGs were found, including 449 upregulated and 224 downregulated genes in the anti-IL-6-treated group compared to the isotype control group. Heatmap-based hierarchical clustering further supported this divergence, revealing two distinct gene expression clusters distinguishing between the treatment groups (Figure 15).

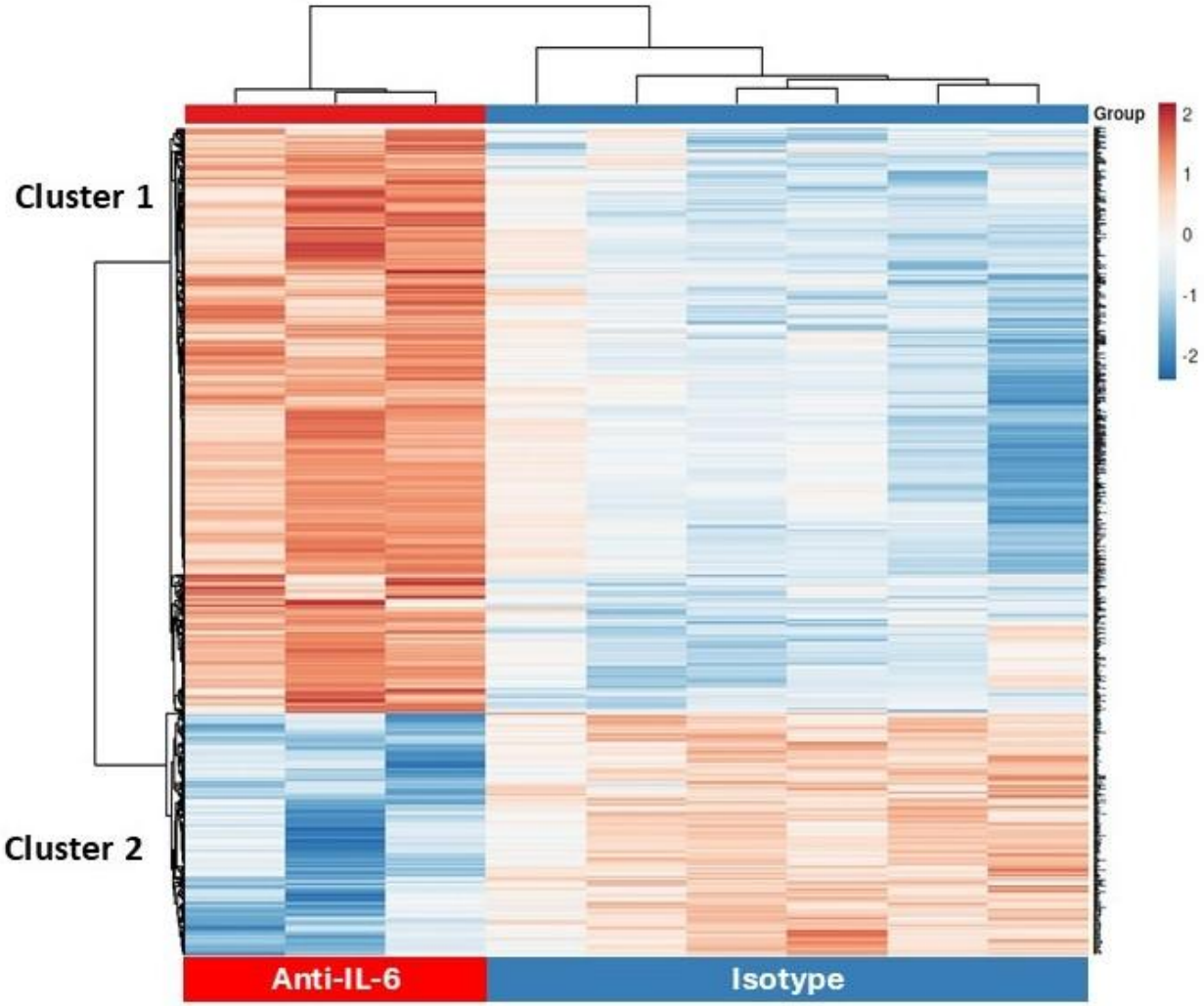

Figure 13. Heatmap of differentially expressed genes in lung tissue from anti-IL-6- and isotype-treated unimmunized IL-13tg mice.

The heatmap displays hierarchical clustering of the top differentially expressed genes according to treatment group. Each column represents an individual mouse, and each row represents a single gene. Gene expression values are shown as a color scale corresponding to the log2 fold change (red: upregulation, blue: downregulation relative to the mean expression). Two major gene clusters (Cluster 1 and Cluster 2) were identified, clearly distinguishing anti-IL-6-treated mice from isotype controls. Differentially expressed genes were identified based on a log2 fold change > 1 or < -1 and an adjusted p-value < 0.05 (Benjamini–Hochberg method).

Table 15 presents the top 10 upregulated and top 10 downregulated genes. Notably, several neural genes, such as *Gabbr2* and *Gabra2*, were among the most highly upregulated genes. In contrast, a number of immune-related genes, including *Igkv6-14*, *Igkv4-91*, *Ccr3*, *Igkv10-96*, and *Igkv1-131,* were significantly downregulated in response to IL-6 blockade.

Table 15. Top 10 upregulated and top 10 downregulated genes in response to IL-6 blockade

Upregulated genes (anti-IL-6 vs Isotype)	Log FC	Downregulated genes (anti-IL-6 vs Isotype)	Log FC
Gabbr2	3.27278	*Igkv6-14*	–3.3285685
Gabra2	3.2556574	*Igkv4-91*	–2.948515
Cts7	3.2050967	*Ccr3*	–2.8563104
Rabgap1	3.1762767	*Igkv10-96*	–2.7619553
Cmya5	3.16846	*Igkv1-131*	–2.6965952
Skint1	3.1408849	*Igkv13-85*	–2.6095116
Cd300lf	3.1370833	*Igkv4-80*	–2.5665069
Ccdc172	3.1210685	*Igkv15-103*	–2.522625
Ncoa7	3.052787	*Igkv3-2*	–2.4693675
Olfr1097	3.042223	*Igkv4-90*	–2.4341683

Gabbr2. gamma-aminobutyric acid (GABA) B receptor 2; *Gabra2*. Gamma-aminobutyric acid (GABA) A receptor-subunit alpha 2; *Cts7*. Cathepsin 7; *Rabgap1*. RAB GTPase activating protein 1; *Cmya5*. Cardiomyopathy associated 5; *Skint1*. Selection and upkeep of intraepithelial T cells 1; *Cd300lf*. CD300 molecule-like family member F; *Ccdc172*. Coiled-coil domain containing 172; *Ncoa*. Nuclear receptor coactivator 7; *Olfr1097*. Olfactory receptor 1097; *Igkv*. Immunoglobulin kappa variable; *Ccr3*. Chemokine (C-C motif) receptor 3.

To gain functional insights into these gene expression changes, gene set enrichment analysis (GSEA) was performed using the Reactome pathway database. Among the 776 significantly upregulated genes, eight pathways were significantly enriched (FDR $q < 0.05$), predominantly related to neurodevelopmental and structural processes. These included ‘development biology’, ‘neuronal system’, ‘neurexins and neuroligins’, ‘protein-protein interactions at synapses’, ‘transmission across chemical synapses’, and ‘sensory perception’. Additionally, upregulated genes were enriched in pathways involving ‘extracellular matrix organization’ and ‘post-translational protein modification’ (Table 15).

In contrast, 321 genes were downregulated following anti-IL-6 treatment. Enrichment analysis identified 50 significantly enriched pathways (FDR $q < 0.05$), many of which were associated with immune regulation, including 'neutrophil degranulation', 'innate immune system', 'adaptive immune system', 'cytokine signaling', and 'complement cascade activation'. Notably, several pathways related to Fc receptor signaling, such as 'FCGR activation', 'FCGR3A-mediated IL-10 synthesis', and 'FCERI-mediated NF-κB activation', were also suppressed, indicating broad attenuation of effector immune functions (Table 16).

Correctively, these transcriptomic and enrichment analyses suggest that IL-6 neutralization profoundly alters lung gene expression in IL-13tg mice, affecting both immune and non-immune pathways.

Table 16. Reactome pathway enrichment analysis of upregulated and downregulated genes

Pathways (Gene Set Name)	**Regulation**	**# Genes in Overlap (k)**	**p-value**
Adaptive immune system	Downregulated	21	3.63E-09
Antigen activates B Cell Receptor (BCR) leading to generation of second messengers	Downregulated	4	1.12E-03
Anti-inflammatory response favouring Leishmania parasite infection	Downregulated	6	7.98E-05
Assembly of collagen fibrils and other multimeric structures	Downregulated	4	3.04E-04
Binding and uptake of ligands by scavenger receptors	Downregulated	5	1.73E-04
Cargo concentration in the ER	Downregulated	3	6.91E-04
CD22 mediated BCR regulation	Downregulated	4	3.04E-04
Cell cycle	Downregulated	11	1.16E-03
Cell surface interactions at the vascular wall	Downregulated	7	7.96E-05
Cell-Cell communication	Downregulated	7	1.91E-05
Class A/1 (Rhodopsin-like receptors)	Downregulated	9	7.00E-05
Complement cascade	Downregulated	5	3.64E-04
Creation of C4 and C2 activators	Downregulated	4	5.43E-04
Cytokine Signaling in immune system	Downregulated	13	3.13E-04
Defective CSF2RB causes SMDP5	Downregulated	2	7.51E-04
Developmental biology	Upregulated	36	1.79E-6
Disorders of transmembrane transporters	Downregulated	6	3.62E-04
Extracellular matrix organization	Upregulated	12	9.5E-5
FCERI mediated Ca+2 mobilization	Downregulated	4	1.12E-03
FCERI mediated MAPK activation	Downregulated	4	1.17E-03
FCERI mediated NF-kB activation	Downregulated	5	7.81E-04

Fcgamma receptor (FCGR) dependent phagocytosis	Downregulated	5	9.79E-04
FCGR activation	Downregulated	5	3.24E-05
FCGR3A-mediated IL10 synthesis	Downregulated	5	1.50E-04
G alpha (q) signaling events	Downregulated	6	1.05E-03
GPCR ligand binding	Downregulated	11	3.87E-05
Hemostasis	Downregulated	19	4.15E-09
Immunoregulatory interactions between a lymphoid and a non-lymphoid cell	Downregulated	11	6.50E-09
Infectious disease	Downregulated	16	1.07E-04
Initial triggering of complement	Downregulated	4	8.52E-04
Innate immune system	Downregulated	34	2.00E-16
Leishmania infection	Downregulated	6	1.10E-03
Linoleic acid (LA) metabolism	Downregulated	2	7.51E-04
Metabolism of amino acids and derivatives	Downregulated	10	3.20E-05
Metabolism of ingested SeMet, Sec, MeSec into H2Se	Downregulated	2	7.51E-04
Metabolism of lipids	Downregulated	13	1.76E-04
Neurexins and neuroligins	Upregulated	6	2.77E-5
Neuronal system	Upregulated	19	1.06E-7
Neutrophil degranulation	Downregulated	24	1.22E-16
Peptide ligand-binding receptors	Downregulated	6	6.53E-04
Phase 3 - rapid repolarization	Downregulated	2	9.62E-04
Post-translational protein modification	Upregulated	32	1.14E-4
Protein-protein interactions at synapses	Upregulated	8	4.06E-6
Role of LAT2/NTAL/LAB on calcium mobilization	Downregulated	4	5.43E-04
Role of phospholipids in phagocytosis	Downregulated	5	7.45E-05
SARS-CoV Infections	Downregulated	11	4.43E-05
SARS-CoV-2 Infection	Downregulated	7	1.08E-03
Scavenging of heme from plasma	Downregulated	5	3.24E-05
Sensory perception	Upregulated	20	1.78E-5
Signal regulatory protein family interactions	Downregulated	3	7.57E-05
Signaling by GPCR	Downregulated	12	3.75E-04
Signaling by interleukins	Downregulated	10	2.23E-04
Sulfur amino acid metabolism	Downregulated	3	4.23E-04
Surfactant metabolism	Downregulated	3	5.20E-04
Transmission across chemical synapses	Upregulated	11	1.57E-4
Transport of small molecules	Downregulated	14	3.40E-05
Vesicle-mediated transport	Downregulated	14	3.30E-05
Viral infection pathways	Downregulated	14	1.31E-04

3.3.4. IL-1RA concentrations in serum and BALF of unimmunized IL-13tg mice

Given that the anti-inflammatory effect of IL-6 has been associated with increased levels of IL-1 receptor antagonist (IL-1RA) (118), I next determined IL-RA concentrations in both serum and bronchoalveolar lavage fluid (BALF) samples from unimmunized IL-13tg mice treated with either IgG1κ isotype control or anti-IL-6 monoclonal antibody. In serum, the median IL-1RA concentration in the isotype group was 71.10 pg/ml, which was comparable to the level observed in the anti-IL-6-treated group (68.44 pg/ml). In contrast, BALF samples from the anti-IL-6 group showed significantly higher IL-1RA levels compared to the isotype control group (71.59 pg/ml vs 41.31 pg/ml, $p < 0.05$) (Figure 14).

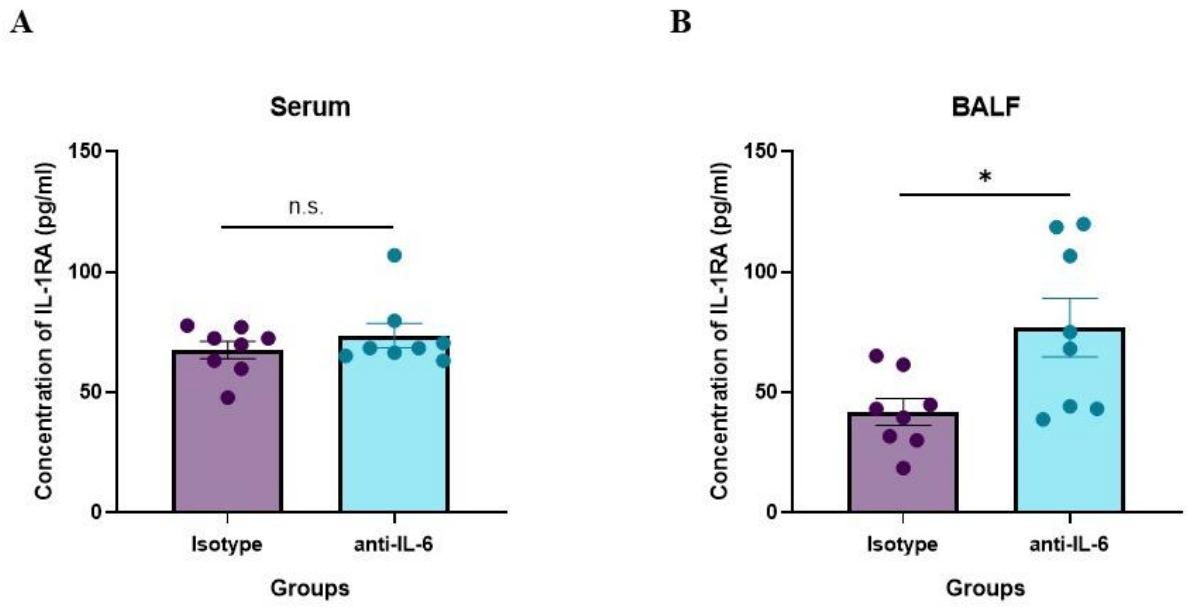

Figure 14. IL-1RA concentrations in unimmunized IL-13tg mice.

Unimmunized IL-13tg mice were treated with either an IgG1κ isotype control or an anti-IL-6 monoclonal antibody. Concentrations of IL-1RA in serum (A) and BALF (B) are shown. Data are presented as median with interquartile range (Q1–Q3). -Statistical analysis was conducted using the Mann–Whitney test; * $p<0.05$, n.s. not significant.

4. Discussion

SSc is a rare and multifaceted autoimmune disorder with the highest mortality among rheumatic diseases. Pulmonary complications, particularly ILD and PAH, are recognized as the leading causes of death in SSc patients (1). Early identification of immunopathogenic mechanisms driving these manifestations may facilitate the development of more precise and effective therapeutic interventions. In the present study, I employed a combined clinical and experimental approach to investigate the role of Th cytokines in SSc and to evaluate the therapeutic potential of cytokine-targeting strategies to alleviate disease manifestations.

The clinical arm of the study involved a comprehensive profiling of Th cytokines in serum samples from SSc patients and healthy controls. Compared to healthy individuals, patients with SSc exhibited significantly elevated serum levels of several cytokines, including IL-2, IL-4, IL-6, IL-10, IFN-γ, and TNF-α. Notably, correlation analysis revealed stronger inter-correlation among cytokines in SSc patients than in healthy individuals, indicating a systemic dysregulation of cytokines network. Importantly, serum levels of IL-6 were significantly elevated in patients with pulmonary complications, including both ILD and PAH, supporting the hypothesis that IL-6 contributes to the development of SSc-related lung disease.

In subsequent animal studies, I evaluated the therapeutic efficacy of IL-6 signaling blockade in a preclinical model of SSc-associated PAH. This model involved immunization with AT1R-associated PAH in IL-13tg mice, which overexpress IL-13 in activated T cells (111,117). Unexpectedly, neither anti-IL-6 nor anti-IL-6R monoclonal antibodies prevented the development of pulmonary occlusive vasculopathy in AT1R-immunized IL-13 mice. In fact, a trend toward increased disease severity was observed in antibody-treated mice compared to isotype controls. Further investigations revealed that treatment with anti-IL-6 monoclonal antibody alone was sufficient to induce occlusive vasculopathy in unimmunized IL-13tg mice, suggesting a previously unrecognized protective role of IL-6 in certain immunopathologic contexts.

4.1. Dysregulated cytokine profiles and their association with pulmonary manifestations

SSc is characterized by profound immune dysregulation involving a wide array of cytokines that contribute to inflammation, fibrosis, and vascular damage (119). Inter-correlation analysis among cytokines in the current study revealed a highly interconnected cytokine environment in SSc patients, indicating that normal immunoregulatory mechanisms are compromised. These altered cytokine interactions likely facilitate the development of chronic inflammation, tissue fibrosis, and vascular changes that define the disease (120,121). For example, a strong correlation between IL-6 and IL-10, two cytokines with divergent functional roles, suggests concurrent activation of both pro-inflammatory and regulatory immune responses. Moreover, IL-5 exhibited significantly stronger correlations with IL-2, IL-10, and IL-17F in SSc patients compared to healthy controls. Stronger correlations between IL-4, another Th2 cytokine, and IL-2 and IL-9 were also observed in SSc patients. These findings support the notion of a Th2-skewed immune network in SSc (122).

Consistent with previous reports, the present study found that multiple Th cytokines, including IL-2, IL-4, IL-6, IL-10, IFN-γ, and TNF-α, were significantly elevated in SSc patients relative to healthy individuals (100). Dantas et al. similarly demonstrated increased levels of IL-2, IL-6, IL-10, and TNF in the supernatants from unstimulated PBMCs of SSc patients (99), while another study has confirmed elevated circulating levels of IL-6, TNFα, and IFN-γ in the plasma of SSc patients (123).

Recent literature underscores the role of Th2 cytokines in fibrosis development. Kuzumi et al. demonstrated elevated levels of IL-31, a cytokine promoting Th2 polarization, in SSc patients, implicating this Th2 cytokine in fibrotic progression (120). Similarly, Pellicano et al. highlighted the central role of IL-4, IL-13, and IL-31 in the pathogenesis of SSc-associated ILD (122). Although IL-31 was not evaluated in the present study, the elevated levels of IL-4 in the total cohort and Th2 cytokines enhanced network connectivity, reinforcing the hypothesis of a Th2-skewed immune environment driving fibrosis and vascular remodeling in SSc.

Among all Th cytokines examined, IL-6 was uniquely associated with both ILD and PAH in SSc. Elevated IL-6 levels in these patient subgroups support its central role in pulmonary disease

pathogenesis. This finding aligns with previous observations: Ibrahim-Achi et al. demonstrated IL-6 as a predictive biomarker for pulmonary and cardiovascular complications in SSc (124). Gourh et al. reported elevated IL-6 and IL-13 levels in SSc-PAH patients (123), and Kolstad et al. identified IL-6 as a key molecule distinguishing SSc patients at risk for PAH from those without vascular involvement (121). Additionally, Baraut et al. linked elevated IL-6 levels to worse prognosis and increased mortality in SSc patients (100). Collectively, these studies, along with findings in the present study, strongly support the critical role of IL-6 in the development and progression of pulmonary involvement in SSc.

Overall, the clinical data presented herein demonstrate significant dysregulation of Th cytokine networks in SSc, with IL-6 emerging as a critical molecule associated with ILD and PAH. These results, supported by prior research, suggest a model in which IL-6 and Th2 cytokines coordinate essential pathogenic processes in SSc.

4.2. IL-13 as a second hit for the development of pulmonary involvement

The increased levels of IL-6 in SSc patients and their association with pulmonary complications prompted the investigation of the role of IL-6 and its underlying mechanisms, with the aim of identifying potential therapeutic targets. For this purpose, I employed the AT1R-immunized IL-13tg mouse model, expanding upon our earlier in vivo system in which immunization with hAT1R induces inflammation in the skin and lungs, along with dermal fibrotic changes in C57BL/6 mice (111). Although the model recapitulates several features of SSc, such as autoantibody production and tissue inflammation, it does not fully capture the hallmark pulmonary manifestations of SSc, namely PAH and interstitial lung fibrosis (111). To address these limitations, our laboratory established a combined model by introducing an IL-13 transgenic background to AT1R-immunized mice, thereby sustaining a chronic type 2 cytokine milieu that favors fibrosis and vascular remodeling. IL-13, a key Th2 cytokine, is known to regulate endothelial cells' migration, activate fibroblasts, and contribute to endothelial dysfunction (125,126). Notably, levels of IL-13 are elevated in both serum and tissue samples from SSc patients with interstitial lung fibrosis (122).

The AT1R-immunized IL-13tg model represents a significant advancement over earlier models by more closely reproducing immune-mediated pulmonary vasculopathy observed in human SSc. Unlike bleomycin-induced models, which are driven by acute chemical injury and lack autoimmune features, this model integrates both antigen-driven autoimmunity and sustained Th2-mediated inflammation (101,127). Furthermore, in contrast to TSK-1 or sclerodermatous graft-versus-host disease models, which primarily mirror skin fibrosis (45), the AT1R-IL-13tg model exhibits prominent pulmonary vascular pathology, a key determinant of mortality in SSc. Additionally, although human PBMC-graft induced models in immunodeficient mice effectively replicate patient-specific autoimmunity and are translationally relevant (110,128), their technical complexity and limited pulmonary involvement constrain their utility for therapeutic studies. By contrast, the AT1R-IL-13tg model enables investigation into both immune activation and vascular injury mechanisms.

However, limitations of the AT1R-IL-13tg model should be acknowledged. While it effectively captures immune-mediated pulmonary vasculopathy, it does not fully represent the multi-organ fibrotic spectrum or heterogeneity of autoantibody profiles observed in human SSc. Moreover, the constant overexpression of IL-13 in all activated T cells does not reflect the dynamic regulation of IL-13 observed in patients. Despite these limitations, the model remains a robust and immunologically relevant tool for exploring underlying molecular mechanisms and testing therapeutic strategies.

Importantly, this novel model demonstrates that the interaction between AT1R-driven autoimmunity and continuous IL-13 expression results in SSc-PAH-like pulmonary vasculopathy, characterized by smooth muscle hyperplasia and remodeling of small pulmonary arteries. These findings support the “Second-hit” hypothesis: AT1R immunization acts as the first hit, triggering immune activation and pulmonary inflammation; IL-13 overexpression in infiltrated T cells constitutes the second hit, driving occlusive vasculopathy.

Taken together, AT1R immunization and IL-13 overexpression represent upstream and downstream effectors in the pathogenic cascade leading to vascular damage. Yet, many additional molecular players likely modulate this pathway, warranting further investigation.

4.3. IL-6 does not promote pulmonary vasculopathy in experimental SSc

Cytokine profiling in AT1R-immunized IL-13tg model revealed that among 13 Th cytokines analyzed in the BAL fluid, only IL-6 was significantly elevated compared to the control group. This selective elevation mirrors clinical observations in SSc patients and suggests IL-6 as a potential contributor to pulmonary vascular pathology. Based on this, I hypothesized that IL-6 mediates chronic inflammation in the lung and promotes occlusive vasculopathy. Specifically, IL-6 may promote the production of chemoattractants and thus mediates the recruitment of immune cells, including IL-13-expressing T cells, to the lung, resulting in endothelial damage and vascular remodeling. This hypothesis is supported by previous studies. For instance, Savale et al. reported that IL-6-deficient mice are resistant to hypoxia-induced lung inflammation and pulmonary vascular remodeling (129). Similarly, Hashimoto-Kataoka et al. found that IL-6R blockade mitigates disease in hypoxia-induced pulmonary hypertension, but only when applied early, before extensive vascular damage occurs (130). In addition, transgenic IL-6 overexpression induces occlusive vasculopathy in mice (131). Clinical data further support this link: elevated IL-6 is associated with SSc-PAH progression and poor prognosis (121,124).

To test the hypothesis, I evaluated the therapeutic impact of IL-6 signaling blockade in AT1R-immunized IL-13tg mice. Surprisingly, both anti-IL-6 and anti-IL-6R treatments failed to prevent occlusive vasculopathy. This aligns with findings from the TRANSFORM-UK trial, in which tocilizumab (anti-IL-6R) reduced systemic inflammation in PAH patients without improving pulmonary vascular resistance or exercise capacity. Genetic analyses also failed to support a protective effect of IL-6R blockade against PAH development (132,133).

Even more strikingly, a trend toward worsened vascular pathology was observed in anti-IL-6- and anti-IL-6R-treated AT1R-immunized IL-13tg mice. This suggests a possible protective role of IL-6 in the context of IL-13-driven vascular pathology. To examine this further, I administered anti-IL-6 monoclonal antibody to unimmunized IL-13tg mice, thus isolating the effect of IL-6 blockade in a type 2 cytokine-rich environment, independent of AT1R-directed autoimmunity. Remarkably, these mice developed pulmonary vasculopathy ranging from mild to moderate, while control IL-13tg mice treated with isotype IgG did not exhibit such changes. This finding challenges the original hypothesis that IL-6 acts as a pathogenic driver and instead suggests that IL-6 may play context-dependent protective roles.

Therefore, these results underscore the complex and context-dependent biology of IL-6 in SSc, particularly in relation to pulmonary vascular pathology. While IL-6 is broadly recognized as a pro-inflammatory and pro-fibrotic cytokine in autoimmune conditions, emerging evidence suggests that it may also exert protective regulatory functions, depending on the immune environment and disease phase (134,135). It has been demonstrated that IL-6 influences a variety of immune cell populations, including Th17 cells and macrophages, in ways that are highly dependent on temporal and tissue-specific cues (130). This dual nature of IL-6 is further exemplified by studies demonstrating that it can promote both pathogenic and anti-inflammatory processes. On one hand, IL-6 facilitates inflammatory cytokines, fibroblast activation, and chronic inflammation. On the other hand, it may support endothelial survival, promote tissue regeneration, and stimulate the induction of regulatory T cells under specific conditions (136). These divergent effects are mediated through classical and trans-signaling mechanisms (136,137). Classical signaling, via membrane-bound IL-6R and membrane glycoprotein gp130, is typically associated with homeostatic and anti-inflammatory effects, such as immune regulation and tissue repair. Anti-inflammatory and regenerative functions. In contrast, trans-signaling, mediated through the soluble IL-6R, allows IL-6 to act on cells lacking membrane-bound IL-6R and is considered primarily pro-inflammatory, driving leukocyte recruitment, fibroblast activation, and vascular remodeling (Figure 15) (136,137). This signaling balance is tightly regulated by soluble gp130 (sgp130), which selectively neutralizes IL-6/sIL-6R complexes and thereby restricts pathological trans-signaling.

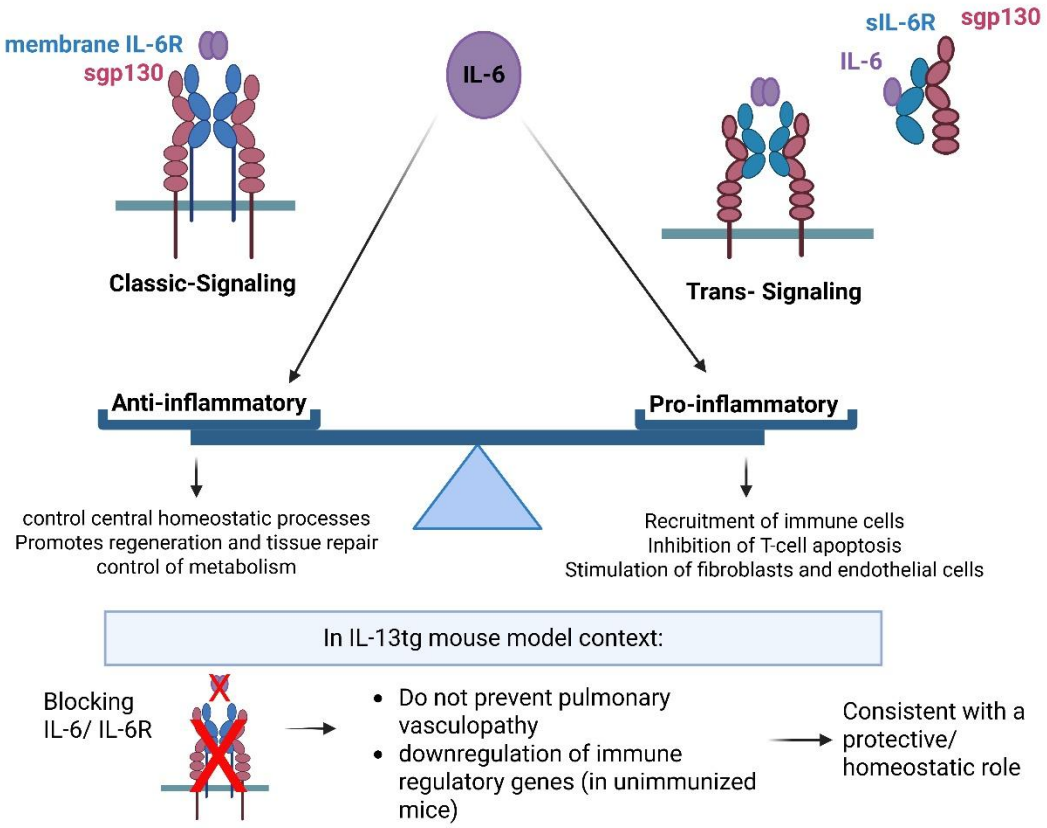

Figure 15. Dual roles of IL-6 signaling in immune regulation and its context-dependent function in the IL-13tg mouse model.

IL-6 exerts its pleiotropic effects through two distinct pathways. In classical signaling (left), IL-6 binds to membrane-bound IL-6R and gp130, promoting anti-inflammatory, regenerative, and homeostatic functions, including tissue repair, metabolic regulation, and immune tolerance. In trans-signaling (right), IL-6 binds to soluble IL-6R (sIL-6R), allowing IL-6 to act on cells lacking membrane-bound IL-6R. This mechanism drives pro-inflammatory responses, including chronic inflammation, leukocyte recruitment, fibroblast activation, and vascular remodeling. The balance between these pathways is regulated by soluble gp130 (sgp130), which neutralizes IL-6/sIL-6R complexes and restricts trans-signaling. In the IL-13tg mouse model, blockade of IL-6 or IL-6R failed to prevent pulmonary vasculopathy and was associated with downregulation of immune-regulatory genes, suggesting that IL-6 may exert a protective, homeostatic role in pulmonary vascular pathology within this context. Figure created using BioRender (https://BioRender.com).

Together, these observations highlight the context-specific and phase-dependent function of IL-6 in SSc-associated pulmonary disease, particularly in PAH.

Potential mechanisms underlying the protective effect of IL-6 on pulmonary vascular pathology. The protective role of IL-6 in disease development has also been demonstrated in other autoimmune models, including experimental epidermolysis bullosa acquisita (EBA). In a study by Samavedam et al., IL-6 blockade significantly exacerbated disease severity, while treatment

with recombinant IL-6 ameliorated disease manifestations, suggesting a protective effect of IL-6 in EBA (118). Mechanistically, treatment with sgp130Fc, a specific inhibitor of IL-6 trans-signaling, had no effect on disease progression, indicating that the beneficial effect of IL-6 is mediated via classical signaling and is independent of the trans-signaling pathway. Moreover, the induction of EBA in mice resulted in an IL-6-dependent increase in interleukin-1 receptor antagonist (IL-1RA) in both skin and serum, and exogenous IL-1RA administration significantly impaired disease induction. These results suggest that IL-6 exerts its protective role, at least in part, by promoting IL-1RA production (118).

In the present study, *IL-1ra* mRNA expression in the lungs of anti-IL-6–treated IL-13tg mice was reduced compared to isotype IgG controls. However, this difference was reflected at the protein level in serum. In contrast, levels of IL-1RA in the BALF were elevated in the anti-IL-6-treated group compared to the isotype control group. These findings suggest that IL-6 signaling blockade elevates IL-1RA expression at the protein level and therefore, the IL-6/IL-1RA axis is unlikely to mediate the protective effect of IL-6 in pulmonary occlusive vasculopathy observed in IL-13tg mice. This interpretation is also consistent with the pathomechanism of the SSc-PAH model, in which infiltrating IL-13 overexpressing T cells are the primary drivers of the disease. Since IL-1RA mainly modulates innate immune responses, its influence on T cell recruitment and activation is likely limited in this setting.

Notably, the transcriptomic analysis of lung tissue in unimmunized IL-13tg mice treated with anti-IL-6 antibodies revealed a significant downregulation of immune-related gene expression. These included pathways related to cytokine signaling, innate and adaptive immunity, neutrophil degranulation, complement activation, and Fc receptor–mediated responses. This observation is consistent with previous reports demonstrating IL-6's role in regulating immune gene expression. For example, in IL-6 knockout mice, Luckett et al. reported marked alterations in skin transcriptomic profiles, including downregulation of genes involved in epithelial integrity, chemokine signaling, and inflammatory responses (138). Furthermore, IL-6 deficiency altered skin microbiota composition, indicating that IL-6 is crucial for maintaining immune–microbial homeostasis at barrier sites (138). Although the lung microenvironment differs from that of skin, findings in the present study similarly demonstrate reduced immune activation signatures in response to IL-6 neutralization.

Interestingly, the downregulation of immune-related genes in the lung upon IL-6 neutralization was not accompanied by compensatory alterations in other inflammatory cytokines in serum or BALF. This suggests that the transcriptional changes resulted directly from IL-6 neutralization rather than from broader cytokine network remodeling. The downregulated genes are involved in key immune processes, including cytokine receptor engagement, intracellular signaling cascades, and antigen-driven responses. These results suggest that IL-6 plays a key role in maintaining immune homeostasis in the lung by regulating both innate and adaptive immune functions. This notion is supported by the previous observation that IL-6 is essentially involved in the activation and differentiation of autoreactive T cells (118,139).

Based on these findings, I propose a hypothetical model for the protective role of IL-6 in pulmonary vascular pathology in IL-13tg mice. In this model, basal IL-6 levels are essential for maintaining immune homeostasis in naïve IL-13tg mice. Systemic IL-6 neutralization disrupts this balance, leading to immune dysregulation. This dysregulation facilitates aberrant T cell recruitment to the lung, where IL-13 released by these infiltrating cells induces hyperproliferation of pulmonary arterial smooth muscle cells (PASMCs), ultimately resulting in the development of occlusive vasculopathy (Figure 16). However, this hypothetical model remains to be experimentally validated in future studies.

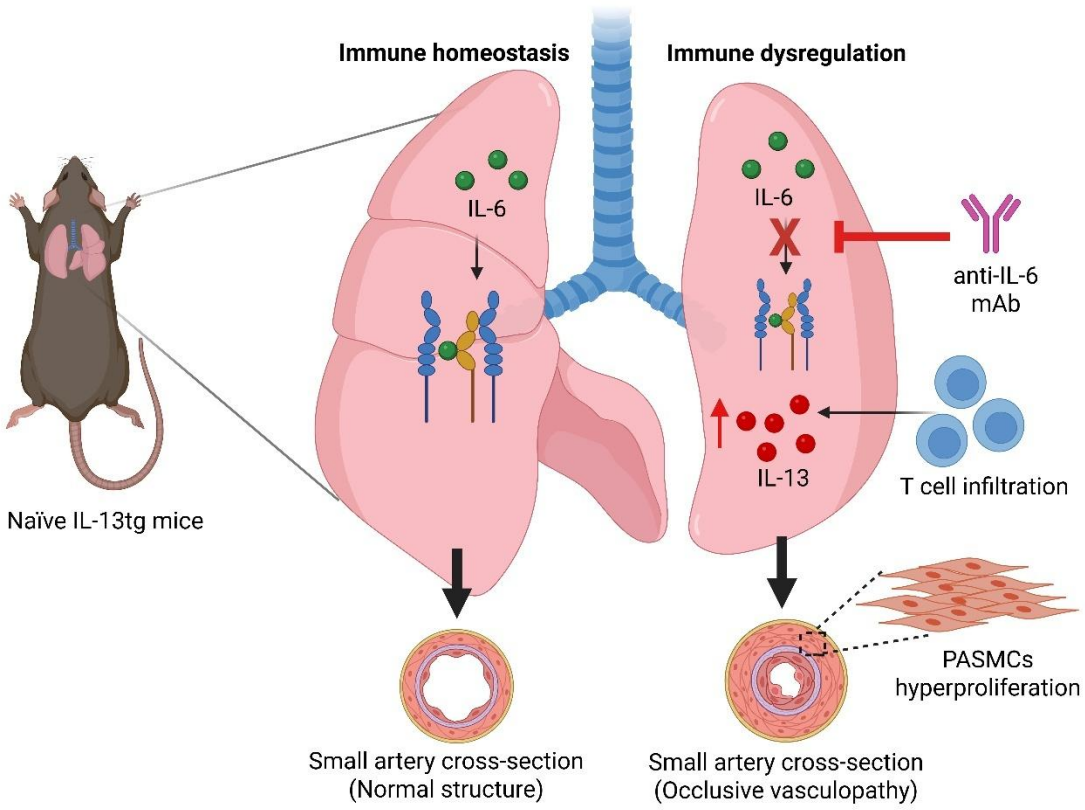

Figure 16. Hypothetical model of IL-6's protective role in pulmonary vascular homeostasis in IL-13tg mice.

In naïve IL-13 transgenic (IL-13tg) mice, basal IL-6 signaling contributes to immune homeostasis in the lung. Systemic IL-6 neutralization with monoclonal antibodies (anti-IL-6 mAb) disrupts this regulatory pathway, leading to immune dysregulation characterized by T cell infiltration and increased IL-13 expression. The elevated IL-13 drives hyperproliferation of pulmonary artery smooth muscle cells (PASMCs), ultimately resulting in occlusive vasculopathy.

4.4. Clinical implications of targeting IL-6 in systemic sclerosis

The clinical and experimental findings of this study carry significant implications, particularly regarding the therapeutic targeting of IL-6 in pulmonary complications associated with SSc. Elevated serum levels of IL-6 in patients with SSc were associated with ILD and PAH, confirming previous reports that identify IL-6 as a biomarker of disease activity and poor outcome (124,140). The observation of elevated IL-6 levels in BAL fluid from IL-13tg in our SSc-PAH model further supports IL-6's involvement in pulmonary pathology. Additionally, high circulating IL-6 concentrations have been linked to worsened clinical outcomes, including reduced survival rates, worse hemodynamics, and accelerated lung fibrosis progression (123).

For instance, De Lauretis et al. demonstrated a significant association between IL-6 levels in serum and both disease progression and mortality in a large, well-characterized SSc-ILD cohort with long-term follow-up (140). These findings collectively suggest that IL-6 neutralization could represent a potential therapeutic strategy for SSc-related pulmonary disease.

Tocilizumab, a humanized monoclonal antibody targeting the IL-6 receptor (IL-6R), has been employed in the treatment of several autoimmune diseases, including SSc (141). However, clinical trials investigating its efficacy in SSc have yielded mixed results. In the "focuSSced" phase 3 trial, tocilizumab demonstrated some benefit in preserving lung function in patients with SSc-ILD, although it did not meet its primary endpoint of improving the modified Rodnan Skin Score (mRSS) (43,44). Preclinical studies further support a pathogenic role for IL-6 in pulmonary fibrosis. For instance, IL-6–deficient mice are less susceptible to bleomycin-induced fibrosis and inflammation (142)**,** and selective blockade of IL-6 trans-signaling using recombinant sgp130Fc attenuates pulmonary fibrosis in similar models (130). In addition to lung fibrosis, cardiac fibrosis also appears to benefit from IL-6 signaling inhibition in mice (136).

The therapeutic efficacy of IL-6 blockade in PAH is far more limited. In the aforementioned phase 3 clinical trials, no beneficial effect was observed for pulmonary vascular changes in SSc patients (43,44). In the TRANSFORM-UK trial, tocilizumab reduced systemic inflammation but failed to improve pulmonary vascular resistance, despite reducing systemic inflammation (132). Genetic studies also found no causal association between IL-6 signaling and PAH risk (133). These clinical outcomes align with the experimental findings in the present study. In the AT1R-immunized IL-13tg mice, treatment with monoclonal antibodies against IL-6 or IL-6R failed to attenuate the disease, and instead trended toward disease exacerbation.

Strikingly, in unimmunized IL-13tg mice, IL-6 neutralization alone was sufficient to trigger pulmonary vascular pathology, clearly demonstrating a protective role for IL-6 in this context. This unexpected result urges caution in the use of systemic IL-6 blockade, as it may induce or exacerbate pulmonary occlusive vasculopathy under specific immunological conditions in SSc. This concern is echoed by a clinical observation during the open-label extension phase of the focuSSced trial (44), where a patient receiving continuous tocilizumab developed severe PAH shortly before death. The event was considered treatment-related by the investigator, raising further safety concerns for IL-6R inhibition in patients with vascular complications (44).

In addition to PAH, other pulmonary adverse events have been reported with IL-6 blockade. Several case studies describe the development of ILD, organizing pneumonia, or worsening pulmonary symptoms during tocilizumab treatment in patients with autoimmune conditions. These include a case of acute interstitial pneumonitis in an elderly woman with rheumatoid arthritis, and a case of organizing pneumonia in an SSc-ILD patient, both of whom improved following drug discontinuation and corticosteroid administration (143,144). Similar pulmonary toxicities have been reported in patients with juvenile idiopathic arthritis and in other rheumatoid contexts (145,146). Although these are isolated cases, they collectively suggest that prolonged or poorly timed IL-6 blockade may disrupt the immune homeostasis in the lung and trigger harmful remodeling.

Taken together, the results in the present study suggest several key clinical implications:

First, although IL-6 remains a promising therapeutic target for autoimmune conditions, its systemic inhibition should be pursued with caution in SSc. The ineffectiveness in reversing vascular pathology, along with clinical reports of ILD and organizing pneumonia during tocilizumab treatment in autoimmune patients, raises concern about unintended pulmonary complications (143–146). IL-6 inhibition may be particularly risky in patients with existing vasculopathy or prominent infiltration of Th2 cells, especially IL-13-producing T cells.

Second, these findings support a precision medicine strategy for IL-6-targeted therapies in SSc. IL-6 inhibition may be beneficial during early, inflammatory phases of ILD, but potentially ineffective or even detrimental in advanced disease stages or among those with vascular involvement. Incorporating cytokine profiling into clinical practice may help identify patients likely to benefit from IL-6 inhibition, while avoiding treatment in those at risk for adverse outcomes.

Third, these findings highlight the importance of transitioning from global IL-6 blockade to more selective approaches. Preclinical data indicate that inhibition of IL-6 trans-signaling, while preserving classical signaling, can attenuate fibrosis more effectively and safely than total IL-6 blockade (147,148). Such targeted approaches may offer a more balanced and context-specific means of modulating IL-6 activity in SSc.

In summary, IL-6 plays a complex, dual role in SSc pathogenesis. While its elevation is clearly associated with disease activity and pulmonary complications, therapeutic inhibition must be carefully timed and contextually informed. IL-6 may function as both a potential driver and regulator of disease, and indiscriminate blockade may carry risks. Future therapeutic strategies must therefore be carefully designed to account for disease stage, the dominant IL-6 signaling pathway, and the underlying immune context, to avoid unintended consequences while preserving potential beneficial effects.

4.5. Limitations

While this study provides novel insights into the multifaceted role of IL-6 in SSc-associated PAH, several limitations should be acknowledged.

First, the clinical data was based on cross-sectional measurements of serum cytokine levels. Although informative, such measurements may not accurately reflect the dynamic and spatially localized cytokine signaling occurring within affected tissues. In diseases like ILD and PAH, cytokine concentrations in the systemic circulation can differ markedly from those in the local lung microenvironment, where inflammation and fibrosis are often compartmentalized (129,140,149).

Second, the relatively limited sample size and high heterogeneity of the SSc patient cohort, including variability in disease subtype, treatment status, and comorbidities, may have introduced confounding variables affecting cytokine levels and correlation network analysis.

Third, the IL-13tg mouse model was employed due to its ability to recapitulate key histopathological features of SSc-associated PAH. p. However, this model does not capture the full complexity of human disease. In the transgenic mice, IL-13 is constitutively overexpressed in activated T cells, creating a sustained Th2-skewed immune environment that does not mimic the temporal and spatial heterogeneity of cytokine expression observed in patients (117). Moreover, the model lacks multiorgan fibrosis and may oversimplify the autoimmune mechanisms driving systemic pathology.

Fourth, while this study reveals a harmful effect of systemic IL-6 blockade in the IL-13tg model, the clinical relevance of this finding must be interpreted cautiously. Species-specific differences in IL-6 biology, including distinctions in downstream signaling cascades and the balance between classical and trans-signaling, may limit translational applicability (150,151).

Finally, the therapeutic strategy employed in this study, systemic neutralization of anti-IL-6 or anti-IL-6R using monoclonal antibodies, has its own intrinsic limitations. This strategy does not distinguish between classical signaling, which is typically associated with anti-inflammatory or homeostatic functions, and trans-signaling, which is more often linked to pathological inflammation. Selective targeting of specific IL-6 signaling modes could produce divergent outcomes. This highlights the need for future drug development to consider approaches that differentially inhibit these pathways (147,152). Furthermore, treatment duration, dosage, and pharmacodynamics in the mouse models may not accurately reflect human clinical scenarios, and the long-term effects of prolonged IL-6 inhibition remain unclear.

Despite these limitations, the study offers valuable mechanistic insights into the complex, context-dependent roles of IL-6 in SSc-related pulmonary vasculopathy.

4.6. Future perspectives

The findings of this study underscore the complexity of IL-6 biology in SSc, particularly in the context of pulmonary vascular remodeling and immune regulation. Although IL-6 is frequently involved in SSc pathogenesis, our results suggest that its function may be context-dependent, potentially including regulatory or even protective role, particularly under chronic Th2-dominant conditions.

These findings warrant a critical re-evaluation of IL-6-targeted therapies in SSc. While global IL-6 inhibition with tocilizumab has demonstrated efficacy in certain clinical contexts, it may be unsuitable for all disease stages or organ systems. Selective inhibition of the IL-6 trans-signaling, such as with sgp130Fc, could provide a more refined therapeutic approach by preserving classical signaling, which supports tissue repair and homeostasis (137,147,148). Preclinical studies comparing global IL-6 blockade and selective trans-signaling inhibition, focusing on

vascular remodeling, endothelial integrity, and immune balance, will be essential to determine the optimal therapeutic strategy.

Mechanistically, further investigation is needed to elucidate how IL-6 exerts its protective effect in the IL-13tg model. The transcriptomic analysis performed in this study was based on bulk lung tissue, precluding resolution of cell type-specific gene expression. Given IL-6's divergent roles across cell populations, such as promoting inflammation in immune cells while supporting survival or barrier function in endothelial cells, future studies employing single-cell RNA sequencing and spatial transcriptomics are warranted. These approaches will allow a more granular understanding of IL-6's impacts on specific cellular niches, particularly the pulmonary endothelium in the context of chronic Th2 inflammation.

Finally, refinement of the animal model is essential for enhancing translational relevance. While the IL-13tg model mirrors certain aspects of Th2-driven pulmonary vasculopathy, it represents only a subset of the clinical spectrum of SSc. Future studies should validate findings in complementary models that incorporate broader immune dysregulation and multi-organ involvement to better capture the heterogeneity of human disease.

4.7. Conclusion

In summary, this study demonstrated that IL-6 is significantly elevated in patients with SSc, particularly those with ILD or PAH. In preclinical models, therapeutic blockade of IL-6 or IL-6R did not prevent the development of pulmonary vasculopathy in immunized IL-13tg mice and was even associated with exacerbation of disease features. Notably, IL-6 neutralization alone was sufficient to induce pulmonary occlusive vasculopathy in unimmunized IL-13tg mice, even in the absence of an external immunologic trigger. Together, these clinical and experimental findings challenge the prevailing view of IL-6 as solely pathogenic in SSc, instead suggesting a nuanced, context-dependent role for this cytokine. IL-6 may be required to maintain immune homeostasis within the lung, and its inhibition may impair protective pathways, leading to vascular injury.

This study provides novel insight into the immunopathogenesis of SSc, particularly in relation to its PAH component, which remains a leading cause of mortality in affected patients. These data suggest that IL-6 plays a key role in maintaining immune homeostasis within the lung. The potential regulatory and protective role of IL-6 highlights the need for precision in cytokine-targeted therapy design, taking into account the tissue-specific and context-dependent role of IL-6. In particular, they call for caution in the indiscriminate application of IL-6 inhibition strategies and support the exploration of more selective therapeutic approaches.

5. Reference

1. Volkmann ER, Andréasson K, Smith V. Systemic sclerosis. The Lancet. 2023 Jan;401(10373):304–18.

2. Rubio-Rivas M, Royo C, Simeón CP, Corbella X, Fonollosa V. Mortality and survival in systemic sclerosis: Systematic review and meta-analysis. Semin Arthritis Rheum. 2014 Oct;44(2):208–19.

3. Zhang Y, Maskan Bermudez N, Sa B, Maderal AD, Jimenez JJ. Epigenetic mechanisms driving the pathogenesis of systemic lupus erythematosus, systemic sclerosis and dermatomyositis. Exp Dermatol. 2024 Jan;33(1):e14986.

4. Namas R, Elarabi M, Khan S, Mubashir A, Memisoglu E, El-Kaissi M, et al. Comprehensive description of the prevalence, serological and clinical characteristics, and visceral involvement of systemic sclerosis (scleroderma) in a large cohort from the United Arab Emirates Systemic Sclerosis Registry. J Scleroderma Relat Disord. 2023 Jun;8(2):137–50.

5. Potera J, Manadan AM. Reasons for hospitalization and in-hospital mortality in adults with systemic sclerosis: Analysis of the National Inpatient Sample. J Scleroderma Relat Disord. 2022 Oct;7(3):189–96.

6. Lee SG, Moon KW. Epidemiology and Treatment of Systemic Sclerosis in Korea. J Rheum Dis. 2022 Oct 1;29(4):200–14.

7. Kong W, Wang Y, Wang H, Zhou Q, Chen J, Han F. Systemic sclerosis complicated with renal thrombotic microangiopathy: a case report and literature review. BMC Nephrol. 2022 Dec;23(1):22.

8. Masi AT, Subcommittee For Scleroderma Criteria of the American Rheumatism Association Diagnostic and Therapeutic Criteria Committee. Preliminary criteria for the classification of systemic sclerosis (scleroderma). Arthritis Rheum. 1980 May;23(5):581–90.

9. LeRoy EC, Medsger TA. Criteria for the classification of early systemic sclerosis. J Rheumatol. 2001 Jul;28(7):1573–6.

10. Van Den Hoogen F, Khanna D, Fransen J, Johnson SR, Baron M, Tyndall A, et al. 2013 classification criteria for systemic sclerosis: an American college of rheumatology/European league against rheumatism collaborative initiative. Ann Rheum Dis. 2013 Nov;72(11):1747–55.

11. Lescoat A, Huang S, Carreira PE, Siegert E, De Vries-Bouwstra J, Distler JHW, et al. Cutaneous Manifestations, Clinical Characteristics, and Prognosis of Patients With Systemic Sclerosis Sine Scleroderma: Data From the International EUSTAR Database. JAMA Dermatol. 2023 Aug 1;159(8):837.

12. Di Maggio G, Confalonieri P, Salton F, Trotta L, Ruggero L, Kodric M, et al. Biomarkers in Systemic Sclerosis: An Overview. Curr Issues Mol Biol. 2023 Sep 25;45(10):7775–802.

13. Varma S, Yun JH, Kim JS, Podolanczuk AJ, Patel NM, Bernstein EJ. Clinical characteristics associated with small airways disease in systemic sclerosis. J Scleroderma Relat Disord. 2022 Jun;7(2):128–34.

14. Yang C, Tang S, Zhu D, Ding Y, Qiao J. Classical Disease-Specific Autoantibodies in Systemic Sclerosis: Clinical Features, Gene Susceptibility, and Disease Stratification. Front Med. 2020 Nov 19;7:587773.

15. Jandali B, Salazar GA, Hudson M, Fritzler MJ, Lyons MA, Estrada-Y-Martin RM, et al. The Effect of ANTI-SCL -70 Antibody Determination Method on Its Predictive Significance for Interstitial Lung Disease Progression in Systemic Sclerosis. ACR Open Rheumatol. 2022 Apr;4(4):345–51.

16. Allanore Y, Simms R, Distler O, Trojanowska M, Pope J, Denton CP, et al. Systemic sclerosis. Nat Rev Dis Primer. 2015 Apr 23;1(1):15002.

17. Sobanski V, Giovannelli J, Allanore Y, Riemekasten G, Airò P, Vettori S, et al. Phenotypes Determined by Cluster Analysis and Their Survival in the Prospective European Scleroderma Trials and Research Cohort of Patients With Systemic Sclerosis. Arthritis Rheumatol. 2019 Sep;71(9):1553–70.

18. Kumánovics G, Péntek M, Bae S, Opris D, Khanna D, Furst DE, et al. Assessment of skin involvement in systemic sclerosis. Rheumatology. 2017 Sep 1;56(suppl_5):v53–66.

19. Lemmers JM, Van Caam AP, Kersten B, Van Den Ende CH, Knaapen H, Van Dijk AP, et al. Nailfold capillaroscopy and candidate-biomarker levels in systemic sclerosis-associated pulmonary hypertension: A cross-sectional study. J Scleroderma Relat Disord. 2023 Oct;8(3):221–30.

20. Wigger GW, Zafar MA, Elwing JM. Improving adherence to pulmonary hypertension screening in patients with systemic sclerosis: Overcoming the provider-level barriers. J Scleroderma Relat Disord. 2020 Oct;5(3):219–23.

21. Moinzadeh P, Bonella F, Oberste M, Weliwitage J, Blank N, Riemekasten G, et al. Impact of Systemic Sclerosis-Associated Interstitial Lung Disease With and Without Pulmonary Hypertension on Survival. CHEST. 2024 Jan;165(1):132–45.

22. Hoffmann-Vold AM, Allanore Y, Alves M, Brunborg C, Airó P, Ananieva LP, et al. Progressive interstitial lung disease in patients with systemic sclerosis-associated interstitial lung disease in the EUSTAR database. Ann Rheum Dis. 2021 Feb;80(2):219–27.

23. Denton CP, Khanna D. Systemic sclerosis. The Lancet. 2017 Oct;390(10103):1685–99.

24. Chung L, Domsic RT, Lingala B, Alkassab F, Bolster M, Csuka ME, et al. Survival and Predictors of Mortality in Systemic Sclerosis-Associated Pulmonary Arterial Hypertension: Outcomes From the Pulmonary Hypertension Assessment and Recognition of Outcomes in Scleroderma Registry. Arthritis Care Res. 2014 Mar;66(3):489–95.

25. Lai YC, Potoka KC, Champion HC, Mora AL, Gladwin MT. Pulmonary Arterial Hypertension: The Clinical Syndrome. Circ Res. 2014 Jun 20;115(1):115–30.

26. Shreiner AB, Murray C, Denton C, Khanna D. Gastrointestinal manifestations of systemic sclerosis. J Scleroderma Relat Disord. 2016 Sep;1(3):247–56.

27. Jones XM, Bottini N, Boin F, Marbán E. Cardiac involvement in systemic sclerosis: A critical review of knowledge gaps and opportunities. J Scleroderma Relat Disord. 2025 Jan 20;23971983241313096.

28. Scheen M, Dominati A, Olivier V, Nasr S, De Seigneux S, Mekinian A, et al. Renal involvement in systemic sclerosis. Autoimmun Rev. 2023 Jun;22(6):103330.

29. Morrisroe KB, Nikpour M, Proudman SM. Musculoskeletal Manifestations of Systemic Sclerosis. Rheum Dis Clin N Am. 2015 Aug;41(3):507–18.

30. Lepri G, Catalano M, Bellando-Randone S, Pillozzi S, Giommoni E, Giorgione R, et al. Systemic Sclerosis Association with Malignancy. Clin Rev Allergy Immunol. 2022 Sep 19;63(3):398–416.

31. Bukiri H, Volkmann ER. Current advances in the treatment of systemic sclerosis. Curr Opin Pharmacol. 2022 Jun;64:102211.

32. Fernández-Lázaro D, Iglesias-Lázaro M, Garrosa E, Rodríguez-García S, Jerves Donoso D, Gutiérrez-Abejón E, et al. Impact of Innovative Treatment Using Biological Drugs for the Modulation of Diffuse Cutaneous Systemic Sclerosis: A Systematic Review. Medicina (Mex). 2023 Jan 27;59(2):247.

33. Namas R, Tashkin DP, Furst DE, Wilhalme H, Tseng C, Roth MD, et al. Efficacy of Mycophenolate Mofetil and Oral Cyclophosphamide on Skin Thickness: Post Hoc Analyses From Two Randomized Placebo-Controlled Trials. Arthritis Care Res. 2018 Mar;70(3):439–44.

34. Volkmann ER, Tashkin DP, Li N, Roth MD, Khanna D, Hoffmann-Vold A, et al. Mycophenolate Mofetil Versus Placebo for Systemic Sclerosis–Related Interstitial Lung Disease: An Analysis of Scleroderma Lung Studies I and II. Arthritis Rheumatol. 2017 Jul;69(7):1451–60.

35. Emadi A, Jones RJ, Brodsky RA. Cyclophosphamide and cancer: golden anniversary. Nat Rev Clin Oncol. 2009 Nov;6(11):638–47.

36. Di Luigi L, Sgrò P, Duranti G, Sabatini S, Caporossi D, Del Galdo F, et al. Sildenafil Reduces Expression and Release of IL-6 and IL-8 Induced by Reactive Oxygen Species in Systemic Sclerosis Fibroblasts. Int J Mol Sci. 2020 Apr 30;21(9):3161.

37. Galiè N, Barberà JA, Frost AE, Ghofrani HA, Hoeper MM, McLaughlin VV, et al. Initial Use of Ambrisentan plus Tadalafil in Pulmonary Arterial Hypertension. N Engl J Med. 2015 Aug 27;373(9):834–44.

38. Galiè N, Brundage BH, Ghofrani HA, Oudiz RJ, Simonneau G, Safdar Z, et al. Tadalafil Therapy for Pulmonary Arterial Hypertension. Circulation. 2009 Jun 9;119(22):2894–903.

39. Zanatta E, Polito P, Favaro M, Larosa M, Marson P, Cozzi F, et al. Therapy of scleroderma renal crisis: State of the art. Autoimmun Rev. 2018 Sep;17(9):882–9.

40. Wind S, Schmid U, Freiwald M, Marzin K, Lotz R, Ebner T, et al. Clinical Pharmacokinetics and Pharmacodynamics of Nintedanib. Clin Pharmacokinet. 2019 Sep;58(9):1131–47.

41. Papadimitriou TI, Van Caam A, Van Der Kraan PM, Thurlings RM. Therapeutic Options for Systemic Sclerosis: Current and Future Perspectives in Tackling Immune-Mediated Fibrosis. Biomedicines. 2022 Jan 29;10(2):316.

42. Allanore Y, Wung P, Soubrane C, Esperet C, Marrache F, Bejuit R, et al. A randomised, double-blind, placebo-controlled, 24-week, phase II, proof-of-concept study of romilkimab (SAR156597) in early diffuse cutaneous systemic sclerosis. Ann Rheum Dis. 2020 Dec;79(12):1600–7.

43. Khanna D, Lin CJF, Furst DE, Goldin J, Kim G, Kuwana M, et al. Tocilizumab in systemic sclerosis: a randomised, double-blind, placebo-controlled, phase 3 trial. Lancet Respir Med. 2020 Oct;8(10):963–74.

44. Khanna D, Lin CJF, Furst DE, Wagner B, Zucchetto M, Raghu G, et al. Long-Term Safety and Efficacy of Tocilizumab in Early Systemic Sclerosis–Interstitial Lung Disease: Open-Label Extension of a Phase 3 Randomized Controlled Trial. Am J Respir Crit Care Med. 2022 Mar 15;205(6):674–84.

45. Cardoneanu A, Burlui AM, Macovei LA, Bratoiu I, Richter P, Rezus E. Targeting Systemic Sclerosis from Pathogenic Mechanisms to Clinical Manifestations: Why IL-6? Biomedicines. 2022 Jan 29;10(2):318.

46. Goswami RP, Ray A, Chatterjee M, Mukherjee A, Sircar G, Ghosh P. Rituximab in the treatment of systemic sclerosis–related interstitial lung disease: a systematic review and meta-analysis. Rheumatology. 2021 Feb 1;60(2):557–67.

47. Ebata S, Yoshizaki A, Oba K, Kashiwabara K, Ueda K, Uemura Y, et al. Safety and efficacy of rituximab in systemic sclerosis (DESIRES): a double-blind, investigator-initiated, randomised, placebo-controlled trial. Lancet Rheumatol. 2021 Jul;3(7):e489–97.

48. Bergmann C, Müller F, Distler JHW, Györfi AH, Völkl S, Aigner M, et al. Treatment of a patient with severe systemic sclerosis (SSc) using CD19-targeted CAR T cells. Ann Rheum Dis. 2023 Aug;82(8):1117–20.

49. Auth J, Müller F, Völkl S, Bayerl N, Distler JHW, Tur C, et al. CD19-targeting CAR T-cell therapy in patients with diffuse systemic sclerosis: a case series. Lancet Rheumatol. 2025 Feb;7(2):e83–93.

50. Farge D, Loisel S, Resche-Rigon M, Lansiaux P, Colmegna I, Langlais D, et al. Safety and preliminary efficacy of allogeneic bone marrow-derived multipotent mesenchymal stromal cells for systemic sclerosis: a single-centre, open-label, dose-escalation, proof-of-concept, phase 1/2 study. Lancet Rheumatol. 2022 Feb;4(2):e91–104.

51. Gasteiger G, D'Osualdo A, Schubert DA, Weber A, Bruscia EM, Hartl D. Cellular Innate Immunity: An Old Game with New Players. J Innate Immun. 2017;9(2):111–25.

52. Murphy K, Weaver C. Janeway's immunobiology. 9th edition. New York, NY: Garland Science/Taylor & Francis Group, LLC; 2016. 904 p.

53. Netea MG, Joosten LAB, Latz E, Mills KHG, Natoli G, Stunnenberg HG, et al. Trained immunity: A program of innate immune memory in health and disease. Science. 2016 Apr 22;352(6284):aaf1098.

54. Perez-Lopez A, Behnsen J, Nuccio SP, Raffatellu M. Mucosal immunity to pathogenic intestinal bacteria. Nat Rev Immunol. 2016 Mar;16(3):135–48.

55. Merle NS, Noe R, Halbwachs-Mecarelli L, Fremeaux-Bacchi V, Roumenina LT. Complement System Part II: Role in Immunity. Front Immunol [Internet]. 2015 May 26 [cited 2025 Apr 24];6. Available from: http://www.frontiersin.org/Molecular_Innate_Immunity/10.3389/fimmu.2015.00257/abstract

56. Sarma JV, Ward PA. The complement system. Cell Tissue Res. 2011 Jan;343(1):227–35.

57. Jouault T, Sarazin A, Martinez-Esparza M, Fradin C, Sendid B, Poulain D. Host responses to a versatile commensal: PAMPs and PRRs interplay leading to tolerance or infection by *Candida albicans*. Cell Microbiol. 2009 Jul;11(7):1007–15.

58. Bonilla FA, Oettgen HC. Adaptive immunity. J Allergy Clin Immunol. 2010 Feb;125(2):S33–40.

59. Nagata T, Koide Y. Induction of Specific $CD8^+$ T Cells against Intracellular Bacteria by $CD8^+$ T-Cell-Oriented Immunization Approaches. J Biomed Biotechnol. 2010;2010:1–11.

60. Raskov H, Orhan A, Christensen JP, Gögenur I. Cytotoxic CD8+ T cells in cancer and cancer immunotherapy. Br J Cancer. 2021 Jan 19;124(2):359–67.

61. Fang D, Chen B, Lescoat A, Khanna D, Mu R. Immune cell dysregulation as a mediator of fibrosis in systemic sclerosis. Nat Rev Rheumatol. 2022 Dec;18(12):683–93.

62. Zhu X, Zhu J. CD4 T Helper Cell Subsets and Related Human Immunological Disorders. Int J Mol Sci. 2020 Oct 28;21(21):8011.

63. Yasmeen F, Pirzada RH, Ahmad B, Choi B, Choi S. Understanding Autoimmunity: Mechanisms, Predisposing Factors, and Cytokine Therapies. Int J Mol Sci. 2024 Jul 12;25(14):7666.

64. Wang L, Wang F, Gershwin ME. Human autoimmune diseases: a comprehensive update. J Intern Med. 2015 Oct;278(4):369–95.

65. Silverstein AM. Autoimmunity versus horror autotoxicus: The struggle for recognition. Nat Immunol. 2001 Apr;2(4):279–81.

66. Kamradt T, Mitchison NA. Tolerance and Autoimmunity. Mackay IR, Rosen FS, editors. N Engl J Med. 2001 Mar;344(9):655–64.

67. Pelanda R, Torres RM. Receptor editing for better or for worse. Curr Opin Immunol. 2006 Apr;18(2):184–90.

68. Klein L, Kyewski B, Allen PM, Hogquist KA. Positive and negative selection of the T cell repertoire: what thymocytes see (and don't see). Nat Rev Immunol. 2014 Jun;14(6):377–91.

69. Takada K, Takahama Y. Positive-Selection-Inducing Self-Peptides Displayed by Cortical Thymic Epithelial Cells. In: Advances in Immunology [Internet]. Elsevier; 2015 [cited 2025 Apr 24]. p. 87–110. Available from: https://linkinghub.elsevier.com/retrieve/pii/S0065277614000042

70. Lo WL, Huseby ES. The partitioning of TCR repertoires by thymic selection. J Exp Med. 2024 Oct 7;221(10):e20230897.

71. Kondo K, Ohigashi I, Takahama Y. Thymus machinery for T-cell selection. Int Immunol. 2019 Mar 5;31(3):119–25.

72. Meng X, Layhadi JA, Keane ST, Cartwright NJK, Durham SR, Shamji MH. Immunological mechanisms of tolerance: Central, peripheral and the role of T and B cells. Asia Pac Allergy. 2023 Dec;13(4):175–86.

73. Powell JD. The induction and maintenance of T cell anergy. Clin Immunol. 2006 Sep;120(3):239–46.

74. Ferrara JLM. Cytokines and the regulation of tolerance. J Clin Invest. 2000 Apr 15;105(8):1043–4.

75. Cherwinski HM, Schumacher JH, Brown KD, Mosmann TR. Two types of mouse helper T cell clone. III. Further differences in lymphokine synthesis between Th1 and Th2 clones revealed by RNA hybridization, functionally monospecific bioassays, and monoclonal antibodies. J Exp Med. 1987 Nov 1;166(5):1229–44.

76. Ramponi G, Brunetta E, Folci M. Role of Th1 and Th2 in autoimmunity. In: Translational Autoimmunity [Internet]. Elsevier; 2022 [cited 2025 Apr 7]. p. 61–92. Available from: https://linkinghub.elsevier.com/retrieve/pii/B9780128225646000203

77. Kumar S, Jeong Y, Ashraf MU, Bae YS. Dendritic Cell-Mediated Th2 Immunity and Immune Disorders. Int J Mol Sci. 2019 May 1;20(9):2159.

78. Sun L, Su Y, Jiao A, Wang X, Zhang B. T cells in health and disease. Signal Transduct Target Ther. 2023 Jun 19;8(1):235.

79. Dupuis S, Döffinger R, Picard C, Fieschi C, Altare F, Jouanguy E, et al. Human interferon-g-mediated immunity is a genetically controlled continuous trait that determines the outcome of mycobacterial invasion. Immunol Rev. 2000 Dec;178(1):129–37.

80. Sun Y, Subudhi SK, Fu YX. Co-stimulation agonists as a new immunotherapy for autoimmune diseases. Trends Mol Med. 2003 Nov;9(11):483–9.

81. Kokubo K, Onodera A, Kiuchi M, Tsuji K, Hirahara K, Nakayama T. Conventional and pathogenic Th2 cells in inflammation, tissue repair, and fibrosis. Front Immunol. 2022 Aug 9;13:945063.

82. Hammad H, Lambrecht BN. Barrier Epithelial Cells and the Control of Type 2 Immunity. Immunity. 2015 Jul;43(1):29–40.

83. Maizels RM, Gause WC. Targeting helminths: The expanding world of type 2 immune effector mechanisms. J Exp Med. 2023 Oct 2;220(10):e20221381.

84. Lee GR. The Balance of Th17 versus Treg Cells in Autoimmunity. Int J Mol Sci. 2018 Mar 3;19(3):730.

85. Jin W, Zheng Y, Zhu P. T cell abnormalities in systemic sclerosis. Autoimmun Rev. 2022 Nov;21(11):103185.

86. Truchetet ME, Brembilla NC, Chizzolini C. Current Concepts on the Pathogenesis of Systemic Sclerosis. Clin Rev Allergy Immunol. 2021 Sep 6;64(3):262–83.

87. Manno R, Boin F. Immunotherapy of systemic sclerosis. Immunotherapy. 2010 Nov;2(6):863–78.

88. Gasparini G, Cozzani E, Parodi A. Interleukin-4 and interleukin-13 as possible therapeutic targets in systemic sclerosis. Cytokine. 2020 Jan;125:154799.

89. Muraille E, Leo O, Moser M. Th1/Th2 Paradigm Extended: Macrophage Polarization as an Unappreciated Pathogen-Driven Escape Mechanism? Front Immunol [Internet]. 2014 Nov 26 [cited 2025 Apr 8];5. Available from: http://journal.frontiersin.org/article/10.3389/fimmu.2014.00603/abstract

90. Faffe DS, Flynt L, Bourgeois K, Panettieri RA, Shore SA. Interleukin-13 and Interleukin-4 Induce Vascular Endothelial Growth Factor Release from Airway Smooth Muscle Cells: Role of Vascular Endothelial Growth Factor Genotype. Am J Respir Cell Mol Biol. 2006 Feb;34(2):213–8.

91. Patnaik E, Lyons M, Tran K, Pattanaik D. Endothelial Dysfunction in Systemic Sclerosis. Int J Mol Sci. 2023 Sep 21;24(18):14385.

92. Kibet M, Abebayehu D. Crosstalk between T cells and fibroblasts in biomaterial-mediated fibrosis. Matrix Biol Plus. 2025 Jun;26:100172.

93. Yang X, Yang J, Xing X, Wan L, Li M. Increased frequency of Th17 cells in systemic sclerosis is related to disease activity and collagen overproduction. Arthritis Res Ther. 2014 Jan 7;16(1):R4.

94. Frantz C, Auffray C, Avouac J, Allanore Y. Regulatory T Cells in Systemic Sclerosis. Front Immunol. 2018 Oct 15;9:2356.

95. Fenoglio D, Battaglia F, Parodi A, Stringara S, Negrini S, Panico N, et al. Alteration of Th17 and Treg cell subpopulations co-exist in patients affected with systemic sclerosis. Clin Immunol. 2011 Jun;139(3):249–57.

96. Chizzolini C, Dufour AM, Brembilla NC. Is there a role for IL-17 in the pathogenesis of systemic sclerosis? Immunol Lett. 2018 Mar;195:61–7.

97. Kobayashi S, Nagafuchi Y, Shoda H, Fujio K. The Pathophysiological Roles of Regulatory T Cells in the Early Phase of Systemic Sclerosis. Front Immunol. 2022 May 24;13:900638.

98. Sekiguchi A, Shimokawa C, Kato T, Uchiyama A, Yokoyama Y, Ogino S, et al. Inhibition of skin fibrosis via regulation of Th17/Treg imbalance in systemic sclerosis. Sci Rep. 2025 Jan 9;15(1):1423.

99. Dantas AT, Almeida ARD, Sampaio MCPD, Cordeiro MF, Oliveira PSSD, Mariz HDA, et al. Different profile of cytokine production in patients with systemic sclerosis and association with clinical manifestations. Immunol Lett. 2018 Jun;198:12–6.

100. Baraut J, Michel L, Verrecchia F, Farge D. Relationship between cytokine profiles and clinical outcomes in patients with systemic sclerosis. Autoimmun Rev. 2010 Dec;10(2):65–73.

101. Yue X, Yu X, Petersen F, Riemekasten G. Recent advances in mouse models for systemic sclerosis. Autoimmun Rev. 2018 Dec;17(12):1225–34.

102. Maurer B, Distler JHW, Distler O. The Fra-2 transgenic mouse model of systemic sclerosis. Vascul Pharmacol. 2013 Mar;58(3):194–201.

103. Yu X, Petersen F. A methodological review of induced animal models of autoimmune diseases. Autoimmun Rev. 2018 May;17(5):473–9.

104. Shultz LD, Brehm MA, Garcia-Martinez JV, Greiner DL. Humanized mice for immune system investigation: progress, promise and challenges. Nat Rev Immunol. 2012 Nov;12(11):786–98.

105. Noda S, Asano Y, Nishimura S, Taniguchi T, Fujiu K, Manabe I, et al. Simultaneous downregulation of KLF5 and Fli1 is a key feature underlying systemic sclerosis. Nat Commun. 2014 Dec 12;5(1):5797.

106. Yamamoto T, Takagawa S, Katayama I, Yamazaki K, Hamazaki Y, Shinkai H, et al. Animal Model of Sclerotic Skin. I: Local Injections of Bleomycin Induce Sclerotic Skin Mimicking Scleroderma. J Invest Dermatol. 1999 Apr;112(4):456–62.

107. Luchetti MM, Moroncini G, Jose Escamez M, Svegliati Baroni S, Spadoni T, Grieco A, et al. Induction of Scleroderma Fibrosis in Skin-Humanized Mice by Administration of Anti−Platelet-Derived Growth Factor Receptor Agonistic Autoantibodies. Arthritis Rheumatol. 2016 Sep;68(9):2263–73.

108. Ross RL, Corinaldesi C, Migneco G, Carr IM, Antanaviciute A, Wasson CW, et al. Targeting human plasmacytoid dendritic cells through BDCA2 prevents skin inflammation and fibrosis in a novel xenotransplant mouse model of scleroderma. Ann Rheum Dis. 2021 Jul;80(7):920–9.

109. Odell ID, Agrawal K, Sefik E, Odell AV, Caves E, Kirkiles-Smith NC, et al. IL-6 trans-signaling in a humanized mouse model of scleroderma. Proc Natl Acad Sci. 2023 Sep 12;120(37):e2306965120.

110. Yue X, Petersen F, Shu Y, Kasper B, Magatsin JDT, Ahmadi M, et al. Transfer of PBMC From SSc Patients Induces Autoantibodies and Systemic Inflammation in Rag2-/-/IL2rg-/- Mice. Front Immunol. 2021 Jun 23;12:677970.

111. Yue X, Yin J, Wang X, Heidecke H, Hackel AM, Dong X, et al. Induced antibodies directed to the angiotensin receptor type 1 provoke skin and lung inflammation, dermal fibrosis and act species overarching. Ann Rheum Dis. 2022 Sep;81(9):1281–9.

112. Riemekasten G, Philippe A, Näther M, Slowinski T, Müller DN, Heidecke H, et al. Involvement of functional autoantibodies against vascular receptors in systemic sclerosis. Ann Rheum Dis. 2011 Mar;70(3):530–6.

113. Tóth AD, Turu G, Hunyady L, Balla A. Novel mechanisms of G-protein-coupled receptors functions: AT1 angiotensin receptor acts as a signaling hub and focal point of receptor cross-talk. Best Pract Res Clin Endocrinol Metab. 2018 Apr;32(2):69–82.

114. Li H, Kem DC, Zhang L, Huang B, Liles C, Benbrook A, et al. Novel Retro-Inverso Peptide Inhibitor Reverses Angiotensin Receptor Autoantibody–Induced Hypertension in the Rabbit. Hypertension. 2015 Apr;65(4):793–9.

115. Varga J, Abraham D. Systemic sclerosis: a prototypic multisystem fibrotic disorder. J Clin Invest. 2007 Mar 1;117(3):557–67.

116. O'Reilly S, Ciechomska M, Fullard N, Przyborski S, Van Laar JM. IL-13 mediates collagen deposition via STAT6 and microRNA-135b: a role for epigenetics. Sci Rep. 2016 Apr 26;6(1):25066.

117. Emson CL, Bell SE, Jones A, Wisden W, McKenzie ANJ. Interleukin (IL)-4–independent Induction of Immunoglobulin (Ig)E, and Perturbation of T Cell Development in Transgenic Mice Expressing IL-13. J Exp Med. 1998 Jul 20;188(2):399–404.

118. Samavedam UKSRL, Kalies K, Scheller J, Sadeghi H, Gupta Y, Jonkman MF, et al. Recombinant IL-6 treatment protects mice from organ specific autoimmune disease by IL-6 classical signalling-dependent IL-1ra induction. J Autoimmun. 2013 Feb;40:74–85.

119. Brown M, O'Reilly S. The immunopathogenesis of fibrosis in systemic sclerosis. Clin Exp Immunol. 2019 Feb 18;195(3):310–21.

120. Kuzumi A, Yoshizaki A, Matsuda KM, Kotani H, Norimatsu Y, Fukayama M, et al. Interleukin-31 promotes fibrosis and T helper 2 polarization in systemic sclerosis. Nat Commun. 2021 Oct 12;12(1):5947.

121. Kolstad KD, Khatri A, Donato M, Chang SE, Li S, Steen VD, et al. Cytokine signatures differentiate systemic sclerosis patients at high versus low risk for pulmonary arterial hypertension. Arthritis Res Ther. 2022 Dec;24(1):39.

122. Pellicano C, Vantaggio L, Colalillo A, Pocino K, Basile V, Marino M, et al. Type 2 cytokines and scleroderma interstitial lung disease. Clin Exp Med. 2023 Jul 1;23(7):3517–25.

123. Gourh P, Arnett FC, Assassi S, Tan FK, Huang M, Diekman L, et al. Plasma cytokine profiles in systemic sclerosis: associations with autoantibody subsets and clinical manifestations. Arthritis Res Ther. 2009;11(5):R147.

124. Ibrahim-Achi Z, De Vera-González A, González-Delgado A, López-Mejías R, González-Gay MÁ, Ferraz-Amaro I. Interleukin-6 serum levels are associated with disease features and cardiovascular risk in patients with systemic sclerosis. Clin Exp Rheumatol [Internet]. 2023 Jul 27 [cited 2025 May 14]; Available from: https://www.clinexprheumatol.org/abstract.asp?a=20198

125. Firszt R, Francisco D, Church TD, Thomas JM, Ingram JL, Kraft M. Interleukin-13 induces collagen type-1 expression through matrix metalloproteinase-2 and transforming growth factor-β1 in airway fibroblasts in asthma. Eur Respir J. 2014 Feb;43(2):464–73.

126. Corne J, Chupp G, Lee CG, Homer RJ, Zhu Z, Chen Q, et al. IL-13 stimulates vascular endothelial cell growth factor and protects against hyperoxic acute lung injury. J Clin Invest. 2000 Sep 15;106(6):783–91.

127. Artlett C. Animal models of systemic sclerosis: their utility and limitations. Open Access Rheumatol Res Rev. 2014 Jul;65.

128. Park MJ, Park Y, Choi JW, Baek JA, Jeong HY, Na HS, et al. Establishment of a humanized animal model of systemic sclerosis in which T helper-17 cells from patients with systemic sclerosis infiltrate and cause fibrosis in the lungs and skin. Exp Mol Med. 2022 Sep 29;54(9):1577–85.

129. Savale L, Tu L, Rideau D, Izziki M, Maitre B, Adnot S, et al. Impact of interleukin-6 on hypoxia-induced pulmonary hypertension and lung inflammation in mice. Respir Res. 2009 Dec;10(1):6.

130. Hashimoto-Kataoka T, Hosen N, Sonobe T, Arita Y, Yasui T, Masaki T, et al. Interleukin-6/interleukin-21 signaling axis is critical in the pathogenesis of pulmonary arterial hypertension. Proc Natl Acad Sci [Internet]. 2015 May 19 [cited 2025 May 19];112(20). Available from: https://pnas.org/doi/full/10.1073/pnas.1424774112

131. Steiner MK, Syrkina OL, Kolliputi N, Mark EJ, Hales CA, Waxman AB. Interleukin-6 overexpression induces pulmonary hypertension. Circ Res. 2009 Jan 30;104(2):236–44, 28p following 244.

132. Hernández-Sánchez J, Harlow L, Church C, Gaine S, Knightbridge E, Bunclark K, et al. Clinical trial protocol for TRANSFORM-UK: A therapeutic open-label study of tocilizumab in the treatment of pulmonary arterial hypertension. Pulm Circ. 2018 Jan;8(1):1–8.

133. Toshner M, Church C, Harbaum L, Rhodes C, Villar Moreschi SS, Liley J, et al. Mendelian randomisation and experimental medicine approaches to interleukin-6 as a drug target in pulmonary arterial hypertension. Eur Respir J. 2022 Mar;59(3):2002463.

134. Hunter CA, Jones SA. IL-6 as a keystone cytokine in health and disease. Nat Immunol. 2015 May;16(5):448–57.

135. Jin JO, Han X, Yu Q. Interleukin-6 induces the generation of IL-10-producing Tr1 cells and suppresses autoimmune tissue inflammation. J Autoimmun. 2013 Feb;40:28–44.

136. Scheller J, Chalaris A, Schmidt-Arras D, Rose-John S. The pro- and anti-inflammatory properties of the cytokine interleukin-6. Biochim Biophys Acta BBA - Mol Cell Res. 2011 May;1813(5):878–88.

137. Villar-Fincheira P, Sanhueza-Olivares F, Norambuena-Soto I, Cancino-Arenas N, Hernandez-Vargas F, Troncoso R, et al. Role of Interleukin-6 in Vascular Health and Disease. Front Mol Biosci [Internet]. 2021 Mar 16 [cited 2025 May 23];8. Available from: https://www.frontiersin.org/articles/10.3389/fmolb.2021.641734/full

138. Luckett-Chastain LR, King CJ, McShan WM, Gipson JR, Gillaspy AF, Gallucci RM. Loss of Interleukin-6 Influences Transcriptional Immune Signatures and Alters Bacterial Colonization in the Skin. Front Microbiol. 2021 Jul 6;12:658980.

139. Samoilova EB, Horton JL, Hilliard B, Liu TST, Chen Y. IL-6-Deficient Mice Are Resistant to Experimental Autoimmune Encephalomyelitis: Roles of IL-6 in the Activation and Differentiation of Autoreactive T Cells. J Immunol. 1998 Dec 15;161(12):6480–6.

140. De Lauretis A, Sestini P, Pantelidis P, Hoyles R, Hansell DM, Goh NSL, et al. Serum Interleukin 6 Is Predictive of Early Functional Decline and Mortality in Interstitial Lung Disease Associated with Systemic Sclerosis. J Rheumatol. 2013 Apr;40(4):435–46.

141. Rubbert-Roth A, Furst DE, Nebesky JM, Jin A, Berber E. A Review of Recent Advances Using Tocilizumab in the Treatment of Rheumatic Diseases. Rheumatol Ther. 2018 Jun;5(1):21–42.

142. Saito F, Tasaka S, Inoue KI, Miyamoto K, Nakano Y, Ogawa Y, et al. Role of interleukin-6 in bleomycin-induced lung inflammatory changes in mice. Am J Respir Cell Mol Biol. 2008 May;38(5):566–71.

143. Silva S, Amarasena R, Moorcroft J, Rajakulenthiran T, Singh R. Tocilizumab-induced pulmonary fibrosis in a patient with rheumatoid arthritis. Clin Med. 2020 Mar;20(2):s57.

144. Kuzumi A, Yoshizaki A, Mitsuo S, Miyake T, Sato S. Tocilizumab-induced organizing pneumonia in a patient with systemic sclerosis–associated interstitial lung disease. Rheumatology. 2023 Feb 6;62(SI):SI143–4.

145. Ikegawa K, Hanaoka M, Ushiki A, Yamamoto H, Kubo K. A Case of Organizing Pneumonia Induced by Tocilizumab. Intern Med. 2011;50(19):2191–3.

146. Sugihara K, Wakiya R, Shimada H, Kato M, Kameda T, Nakashima S, et al. Interstitial lung disease occurring shortly after tocilizumab infusion in a patient with polyarticular juvenile idiopathic arthritis: a case report. Allergy Asthma Clin Immunol [Internet]. 2021 Dec [cited 2025 May 23];17(1). Available from: https://aacijournal.biomedcentral.com/articles/10.1186/s13223-021-00594-7

147. Le TTT, Karmouty-Quintana H, Melicoff E, Le TTT, Weng T, Chen NY, et al. Blockade of IL-6 *Trans* Signaling Attenuates Pulmonary Fibrosis. J Immunol. 2014 Oct 1;193(7):3755–68.

148. George MJ, Jasmin NH, Cummings VT, Richard-Loendt A, Launchbury F, Woollard K, et al. Selective Interleukin-6 Trans-Signaling Blockade Is More Effective Than Panantagonism in Reperfused Myocardial Infarction. JACC Basic Transl Sci. 2021 May;6(5):431–43.

149. Zheng B, Keen KJ, Fritzler MJ, Ryerson CJ, Wilcox P, Whalen BA, et al. Circulating cytokine levels in systemic sclerosis related interstitial lung disease and idiopathic pulmonary fibrosis. Sci Rep. 2023 Apr 24;13(1):6647.

150. Lacroix M, Rousseau F, Guilhot F, Malinge P, Magistrelli G, Herren S, et al. Novel Insights into Interleukin 6 (IL-6) Cis- and Trans-signaling Pathways by Differentially Manipulating the Assembly of the IL-6 Signaling Complex. J Biol Chem. 2015 Nov;290(45):26943–53.

151. Lokau J, Kleinegger F, Garbers Y, Waetzig GH, Grötzinger J, Rose-John S, et al. Tocilizumab does not block interleukin-6 (IL-6) signaling in murine cells. Spencer JV, editor. PLOS ONE. 2020 May 4;15(5):e0232612.

152. Avci AB, Feist E, Burmester GR. Targeting IL-6 or IL-6 Receptor in Rheumatoid Arthritis: What Have We Learned? BioDrugs. 2024 Jan;38(1):61–71.

Scientific achievements

Publications

- Ohmes J*, **Mehrpouyan A***, Wimmer-Groß J*, Ahmed AR, Amber KT, Biswas S, Christiano A, Emtenani S, Goletz S, Hundt JE, Kirchhoff L, Kridin K, Lasselin J, Laudes M, Lee WY, Ludwig RJ, Murthy S, Mousavi S, Nemeth T, Neumann M, Popken I, Saurabh R, Sbaraglia AM, Schanzenbacher J, Schmidt C, Schmidt-Jimènez LF, Scheiner CW, Schlotfeldt M, Schoell N, Bahreini F*, Stenger S*. Meeting Report on Autoimmune Pre-Disease, JID Innovations, 2024, DOI: 10.1016/j.xjidi.2024.100342. *, These authors contributed equally to this work.

Participation in scientific conferences

- **Jul 2025 – Poster Presentation:** "T helper Cytokines in Systemic Sclerosis: Clinical and Experimental Perspectives on Pulmonary Involvement"; DGFI Translational Immunology School 2025, Potsdam, Germany.

- **Jun 2025 – Poster Presentation:** "Treatment with IL-6 neutralizing antibody promotes the development of pulmonary occlusive vasculopathy in IL-13 transgenic mice"; DZL annual meeting 2025, Heidelberg, Germany.

- **Sep 2024 – Oral Presentation:** "Unexpected impacts of IL-6 on the development of pulmonary occlusive vasculopathy in an experimental mouse model for SSc"; International Congress on Autoimmune Pre-Disease, University of Lübeck, **Lübeck, Germany.**

- **Mar 2024 – Oral Presentation**: "OC25: Unraveling the unexpected impacts of IL-6 on pulmonary vasculopathy and cytokine dysregulation in experimental systemic sclerosis"; 8th Systemic Sclerosis World Congress, **Prague, Czech Republic.**

- **Nov 2024 – Oral Presentation**: "Evaluation of Th Cytokines in Systemic Sclerosis Patients and its Correlation with Clinical Manifestations"; NDI3, Borstel, Germany.

- **Oct 2023 – Poster Presentation**: "P30: Investigation of the role of IL-6 in the development of pulmonary occlusive vasculopathy in IL-13tg mice"; German Society for Immunology (DGFI), 14th Autumn School "Current Concepts in Immunology", **Merseburg, Germany.**

- **Nov 2023 – Poster Presentation**: “Investigation of the role of IL-6 in the development of pulmonary occlusive vasculopathy in IL 13tg mice”; NDI3, Borstel, Germany.

Acknowledgement

The research presented in this thesis was conducted at the Research Centre Borstel, Germany, with financial support from the Deutsche Forschungsgemeinschaft (DFG) and the Research Training Group RTG2633, from April 2025 to August 2025. This work was carried out while I was registered as a candidate for the Dr. rer. nat. degree at the University of Lübeck. Throughout this journey, I have received invaluable guidance, help, and encouragement from many people, to whom I am deeply grateful.

First and foremost, I would like to express my sincere gratitude to my supervisors, Dr. Xinhua Yu and Dr. Frank Petersen, for their continuous support, guidance, and motivation throughout this work. Their expertise, insightful feedback, and patience have been essential in shaping my scientific thinking and professional development.

I would like to express my gratitude to the Research Center Borstel and the Research Training Group RTG2633 for providing an excellent environment for research and scientific growth. My sincere thanks go to Dr. Ralf Ludwig and Dr. Jennifer Hundt, whose efforts created a great platform for discussing science, exchanging ideas, building friendships, and presenting our work to receive valuable feedback.

I would also like to thank all members of our research group, Jacqueline Wax, Christine Engellenner, Cindy Jensen, Carola Schneider, Diana Heinrich, Liang Zhang, Adeela Sana, Jianrui Zheng, Karin Böhm, and Madleen Reddig, for their help, friendship, and support throughout my time in the lab, which made my work life much easier and brighter.

My deepest gratitude goes to my family, my parents and my sisters, for their endless love, support, and encouragement from afar. Although they are in Iran and I am in Germany, their belief in me has always been my greatest strength and motivation to pursue my dreams.

I am also deeply grateful to Shadi and Shahab, who were my family in Germany. Their kindness and support made my time here warmer and much easier, and I am truly grateful for their presence in my life.

And to my beloved husband, Mahdi. Thank you for being my partner in both life and science. As an immunologist, your insights were invaluable, but your patience and trust in me meant even more. You constantly encouraged me to stay strong and confident, and tolerated my mouse tragedies and thesis-writing moods like a true hero!

Last but not least, I want to thank myself for believing in myself, for working hard, for never giving up, and for being a fighter through every challenge along the way.

I would like to end this journey with a verse that reflects my belief in the pursuit of knowledge and the guidance it offers in life:

به دانش گرای و بدو شو بلند چو خواهی که از بد نیابی گزند

“Seek wisdom, and rise through its grace

If you wish to be safe from harm’s embrace” — Ferdowsi

“The more a person grows in knowledge and wisdom, the stronger and wiser they become in facing life’s challenges and choosing the right path.”

October 2025

Hamburg, Germany

Declaration

I hereby declare that this thesis has been written independently and without the assistance of others, and that no sources or aids other than those stated have been used. Furthermore, I confirm that I have not participated in any other doctoral procedure, that no other application for admission has been submitted, and that this thesis has not been presented elsewhere.